

Ligand Displacement Reactions of *fac*-(η^2 -C₆₀)(η^2 -phen)M(CO)₃ (M = Mo, Cr, and W)

By
Griseida Galloza-Rivera

A thesis submitted in partial fulfillment of the requirements for the degree of

Master in Science
in
Chemistry

University of Puerto Rico
Mayagüez Campus
2009

Approved by:

José E. Cortés-Figueroa, PhD
President, Graduate Committee

Date

Nairmen Mina, PhD
Member, Graduate Committee

Date

Jorge Ríos-Steiner, PhD
Member, Graduate Committee

Date

Jaime E. Ramirez-Vick
Graduate Studies Representative

Date

Francis Patrón, PhD
Director, Chemistry Department

Date

Abstract

A mechanistic description of the ligand exchange reactions of $fac-(^2-C_{60})(^2-phen)M(CO)_3$ ($M = Cr, W$ and Mo); phen = 1,10-phenanthroline) will be presented in this work.

The Lewis bases (L) piperidine (pip), triphenyl phosphine (PPh_3) and tricyclohexyl phosphine ($P(Cy)_3$) displace [60]fullerene (C_{60}) from $fac-(^2-C_{60})(^2-phen)M(CO)_3$ to produce $fac-(^2-phen)(^1-L)M(CO)_3$ and $fac-(^1-L)_3M(CO)_3$, depending on M . The progress of the reactions were followed by observing the change of absorbance values at various wavelengths, depending on M and entering ligand (L). The reactions were also monitored by observing the stretching carbonyl region from 1700 to 2100cm^{-1} to establish the nature of non-steady-state intermediate species and products.

The reactions of $fac-(^2-phen)(^2-C_{60})W(CO)_3$ produced $fac-(^2-phen)(^1-L)W(CO)_3$ as the only product. For $M = Mo$, the formation of $fac-(^2-phen)(^1-L)Mo(CO)_3$ was followed by thermal decomposition. For, $M = Cr$, the formation of $fac-(^2-phen)(^1-L)Cr(CO)_3$ was followed displacement of phen producing $fac-(^1-L)_3Cr(CO)_3$.

The reactions of $fac-(^2-phen)(^2-C_{60})Cr(CO)_3$ were biphasic depending on L. For example, plots of absorbance vs. time were biexponential for reactions under conditions where $[L] \gg [fac-(^2-C_{60})(^2-phen)Cr(CO)_3]$. The plots of absorbance vs. time consisted of two consecutive segments. The first segment (increasing) of the plot was assigned to step-wise additions of piperidine to uncoordinated C_{60} . The second segment (decreasing) was ascribed to solvent-assisted displacement of C_{60} from $fac-(^2-C_{60})(^2-phen)Cr(CO)_3$. The observation of an experimentally-accessible isokinetic temperature suggests that the seemingly different mechanistic path for the systems investigated is actually limiting cases of the general mechanism that will be presented.

Resumen

En este trabajo se presentará una descripción mecanística de las reacciones de intercambio de ligando en $fac-(^2-C_{60})(^2-phen)M(CO)_3$ ($M = Cr, W$ and Mo); phen = 1,10-fenantrolina). Las bases de Lewis (L) piperidina (pip), trifenil fosfina (PPh_3) y Triciclohexil fosfina ($P(Cy)_3$) desplazan a [60] fullereno (C_{60}) de $fac-(^2-C_{60})(^2-phen)M(CO)_3$ produciendo: $fac-(^2-phen)(^1-L)M(CO)_3$ and $fac-(^1-L)_3M(CO)_3$, dependiendo del metal.

Los progresos de reacción fueron monitoreado observando el cambio en los valores de absorbancia en varios longitudes de onda, dependiendo del metal y del ligando (L) entrante. Para establecer la naturaleza del estado no estacionario de la especie intermediaria y de los productos, las reacciones fueron monitoreadas observando la región carbonílica desde 1700 a 2100 cm^{-1} . Las reacciones de $fac-(^2-phen)(^2-C_{60})W(CO)_3$ producen $fac-(^2-phen)(^1-L)W(CO)_3$ como único producto. Para $M = Mo$, la formación de $fac-(^2-phen)(^1-L)Mo(CO)_3$ fue seguida por descomposición térmica. Para, $M = Cr$, la formación de $fac-(^2-phen)(^1-L)Cr(CO)_3$ fue seguido por el desplazamiento de fenantrolina, siendo el producto de reacción $fac-(^1-L)_3Cr(CO)_3$. Por ejemplo, las graficas de absorbancia vs tiempo fueron biexponencial bajo condiciones en donde $[pip] \gg [fac-(^2-C_{60})(^2-Phen)Cr(CO)_3]$. Las graficas de absorbancia vs tiempo consisten de dos segmentos consecutivos. El primer segmento (aumento) de la grafica se asignó a la reacción de piperidina con el fullereno (C_{60}) que se encuentra sin coordinar. El segundo segmento (la disminución) se atribuye al desplazamiento asistido por el disolvente de C_{60} de $fac-(^2-C_{60})(^2-phen)Cr(CO)_3$. La observación de una temperatura isocinética, experimentalmente accesible, sugiere que el mecanismo de reacción para los sistemas investigados son en realidad casos limites del mecanismo general que se presentará.

Acknowledgements

There are several people that love, help, and support me. These people were the source of my inspiration throughout my life, but more importantly during the past years when I was acquiring my master's degree. First of all, my family: my father: Héctor E. Galloza; my mother: Rosa N. Rivera; my sisters: Suhein D. Galloza-Rivera, Briseida Galloza-Rivera and my brother: Héctor E. Galloza-Rivera.

I would like to express my gratitude toward my laboratory partners and friends who were there whenever I needed. Specials thanks to: Yahaira López, Marissa Morales and Cynthia Capella, for the great time we spent together and also to Carlos A. Rivera-Rivera for all the support and quality time he gave me during all these years.

Acknowledgement is made to Dr. José E. Cortés-Figueroa, the experimental assistance of Elvin Igartúa-Nieves are acknowledged and last but not least thank you to the member of my committee: Dr. Nairmen Mina and Dr. Jorge Ríos-Steiner for their collaboration.

© 2009 Griseida Galloza-Rivera

to my Family

Table of Contents

Contents	Page
Abstract	ii
Resumen	iii
Acknowledgements	vi
Table list	ix
Figure List	x
Chapter 1: Introduction	1
1.1- Objectives	3
Chapter II: Previous Work	4
Chapter III: Displacement of C ₆₀ from <i>fac</i> -(² -C ₆₀)(² -phen)Cr(CO) ₃	7
3.1: Materials and Methodology	7
3.1.1- General	7
3.1.2- Preparation of the starting material (² -phen)Cr(CO) ₄	8
3.1.3- Preparation of <i>fac</i> -(² -C ₆₀)(² -phen)Cr(CO) ₃	11
3.1.4- Preparation of the product (¹ -pip) ₃ Cr(CO) ₃ using (² -phen)Cr(CO) ₄	14
3.1.5- Preparation of the product (¹ -pip) ₃ Cr(CO) ₃ using <i>fac</i> -(² -C ₆₀)(² -phen)Cr(CO) ₃	16
3.2: Kinetic Studies of <i>fac</i> -(² -pip)(² -phen)Cr(CO) ₃	17
3.2.1- Kinetic of <i>fac</i> -(² -C ₆₀)(² -phen)Cr(CO) ₃ with Piperidine in chlorobenzene	17
3.2.2- Kinetic of <i>fac</i> -(² -C ₆₀)(² -phen)Cr(CO) ₃ with triphenylphosphine in chlorobenzene	17
3.2.3- Kinetic of <i>fac</i> -(² -C ₆₀)(² -phen)Cr(CO) ₃ with tricyclohexylphosphine in toluene	17
3.2.4- Kinetic of <i>fac</i> -(² -C ₆₀)(² -phen)Cr(CO) ₃ with triphenylphosphine in benzene	17

3.3: Data Analysis	18
3.3.1- Kinetic data for the displacement of C ₆₀ from <i>fac</i> -(² -C ₆₀)(² -phen)Cr(CO) ₃ by PPh ₃	18
3.3.2- Kinetic data for the displacement of C ₆₀ from <i>fac</i> -(² -C ₆₀)(² -phen)Cr(CO) ₃ by piperidine	19
3.3.3- Eyring Plots	20
3.4: Results	21
3.4.1- Displacement of C ₆₀ from <i>fac</i> -(² -C ₆₀)(² -phen)Cr(CO) ₃ by piperidine	21
3.4.2- Displacements of C ₆₀ from <i>fac</i> -(² -C ₆₀)(² -phen)Cr(CO) ₃ by PPh ₃ and P(Cy) ₃	26
3.5: Discussion	33
Chapter IV: Ligand displacement reactions of <i>fac</i> -(² -C ₆₀)(² -phen)M(CO) ₃ (M = W, Mo and Cr)	37
4.1 - Materials and Methodology	37
4.1.1- General	37
4.1.2- Preparation of <i>fac</i> -(² -C ₆₀)(² -phen)Mo(CO) ₃	41
4.1.3- Preparation of <i>fac</i> -(² -C ₆₀)(² -phen)W(CO) ₃	42
4.2- Data Analysis	43
4.3- Results	45
4.4- Discussion	48
Chapter V: Conclusion and future works	51
5.1- Conclusion	51
5.2- Future works	53
Reference	54
Appendix	57

Table List

Table	Page
3.1 Average rate constant values of k_{obsd1} and k_{obsd2} for C_{60} displacement from <i>fac</i> -($^{2}\text{-C}_{60}$)($^{2}\text{phen}$)Cr(CO) $_3$ by Piperidine (pip) in chlorbenzene	23
3.2 Activation parameter values for the dissociation of C_{60} from <i>fac</i> -($^{2}\text{-C}_{60}$)($^{2}\text{phen}$)Cr(CO) $_3$ by Piperidine (pip) in chlorbenzene	25
3.3 Average rate constant values of k_{obsd} for C_{60} displacement from <i>fac</i> -($^{2}\text{-C}_{60}$)($^{2}\text{phen}$)Cr(CO) $_3$ by tri-phenylphosphine (PPh $_3$) in chlorbenzene	28
3.4 Rate constant values of k_{obsd} for the displacement of C_{60} from <i>fac</i> -($^{2}\text{-C}_{60}$)($^{2}\text{phen}$)Cr(CO) $_3$ by triphenylphosphine and tricyclohexylphosphine in chlorobenzene at various [L] and [C_{60}]/[L]	29
3.5 Activation Parameters for the dissociation of C_{60} from <i>fac</i> -($^{2}\text{-C}_{60}$)($^{2}\text{-phen}$)Cr(CO) $_3$ by PPh $_3$ in chlorobenzene, benzene and toluene.	32
4.1 Half-wave potentials ($E_{1/2}$) of the <i>fac</i> -($^{2}\text{-C}_{60}$)M(CO) $_3$ complexes (M = Cr, Mo, W) and C_{60} in dichloromethane at room temperature*.	47

Figure List

Figure	Page
2.1 Schematic representation for reactions of C ₆₀ with piperidine to produce tetra(pip)-fullerene epoxide.	4
2.2 Schematic representation for reactions of C ₆₀ from Cr(CO) ₅ (C ₆₀) by piperidine.	5
2.3 Proposed mechanisms for C ₆₀ displacement from <i>fac</i> -(² -C ₆₀)(² -phen)W(CO) ₃ . Path A describes a solvent-assisted displacement of C ₆₀ , whereas path B describes a dissociative displacement. I _A and I _B are steady-state intermediates. TS ₁ and TS ₂ are plausible transition states.	6
3.1 Schematic Representation of the equipment used for the thermal preparation of (² -phen)Cr(CO) ₄	9
3.2 Infrared Spectrum in the carboxylic region of Cr(CO) ₆ in toluene	10
3.3 Infrared Spectrum in the carbonyl region of (² -phen)Cr(CO) ₄ in toluene	10
3.4 Schematic Representation of the photochemical preparation of <i>fac</i> -(² -C ₆₀)(² -phen) ₃ Cr(CO) ₃	12
3.5 Infrared Spectrum in the Carbonyl region of <i>fac</i> -(² -C ₆₀)(² -phen)Cr(CO) ₃ in toluene	13
3.6 Infrared Spectrum in the Carbonyl region of the intermediate <i>fac</i> -(¹ -pip)(² -phen)Cr(CO) ₃ in toluene	14
3.7 Infrared Spectrum in the Carbonyl region of the product (¹ -pip) ₃ Cr(CO) ₃ in toluene	15
3.8 Infrared Spectrum in the Carbonyl region of the product (¹ -pip) ₃ Cr(CO) ₃ in toluene	16
3.9 Schematic representation of the displacement of C ₆₀ from <i>fac</i> -(² -C ₆₀)(² -phen)Cr(CO) ₃ by piperidine.	21
3.10 Plot of Absorbance (407 nm) vs. time (s) for C ₆₀ displacement from <i>fac</i> -(² -C ₆₀)(² -phen)Cr(CO) ₃ by piperidine in chlorobenzene to form (¹ -pip) ₃ Cr(CO) ₃ at 313.2 K under flooding conditions.	22
3.11 Plot of k _{obsd2} versus [pip] for the reaction of <i>fac</i> -(² -C ₆₀)(² -phen)Cr(CO) ₃ with piperidine in chlorobenzene at 313.2 K	24
3.12 Eyring plot of ln(k _{obsd} /T) vs. 1/T for C ₆₀ displacement from (² -C ₆₀)(² -phen)Cr(CO) ₃ by piperidine in chlorobenzene.	24
3.13 Plot of Absorbance (500 nm) vs. time (s) for C ₆₀ displacement from (² -C ₆₀)(² -phen)Cr(CO) ₃ by P(Cy) ₃ in chlorobenzene at 313.2K	27
3.14 Plot of k _{obsd} versus Ratio of [C ₆₀]/[PPh ₃] (mol/L) for the reaction of <i>fac</i> -(² -C ₆₀)(² -phen)Cr(CO) ₃ with [C ₆₀]/[PPh ₃] at 313.2 K and 500nm	27

- 3.15** Plot of k_{obsd} versus Ratio of $[C_{60}]/[P(\text{Cy})_3]$ (mol/L) for the reaction of $fac\text{-}(^2\text{-}C_{60})(^2\text{-phen})Cr(\text{CO})_3$ with $[C_{60}]/[P(\text{Cy})_3]$ at 313.2 K and 500nm 30
- 3.16** Eyring plot of $\ln(k_{\text{obsd2}}/T)$ vs. $1/T$ for C_{60} displacement from $fac\text{-}(^2\text{-}C_{60})(^2\text{-phen})Cr(\text{CO})_3$ by piperidine in chlorobenzene. The k_{obsd2} values were obtained under flooding conditions where $[\text{pip}] \gg [fac\text{-}(^2\text{-}C_{60})(^2\text{-phen})Cr(\text{CO})_3]$. 30
- 3.17** Eyring plot of $\ln(k_{\text{obsd}}/T)$ vs. $1/T$ for C_{60} dissociation from $fac\text{-}(^2\text{-}C_{60})(^2\text{-phen})Cr(\text{CO})_3$ in chlorobenzene by tri-phenylphosphine. The k_{obsd} values were obtained under flooding conditions where $[\text{PPh}_3] \gg [fac\text{-}(^2\text{-}C_{60})(^2\text{-phen})Cr(\text{CO})_3]$. 31
- 3.18** Eyring plot of $\ln(k_{\text{obsd}}/T)$ vs. $1/T$ for C_{60} dissociation from $fac\text{-}(^2\text{-}C_{60})(^2\text{-phen})Cr(\text{CO})_3$ in benzene by tri-phenylphosphine. The k_{obsd} values were obtained under flooding conditions where $[\text{PPh}_3] \gg [fac\text{-}(^2\text{-}C_{60})(^2\text{-phen})Cr(\text{CO})_3]$. 31
- 3.19** Eyring plot of $\ln(k_{\text{obsd}}/T)$ vs. $1/T$ for C_{60} dissociation from $fac\text{-}(^2\text{-}C_{60})(^2\text{-phen})Cr(\text{CO})_3$ in toluene by tri-phenylphosphine. The k_{obsd} values were obtained under flooding conditions where $[\text{PPh}_3] \gg [fac\text{-}(^2\text{-}C_{60})(^2\text{-phen})Cr(\text{CO})_3]$. 32
- 3.20** Proposed mechanisms for C_{60} displacement from $fac\text{-}(^2\text{-}C_{60})(^2\text{-phen})Cr(\text{CO})_3$. The mechanism describes a solvent assisted displacement of C_{60} . I_A and I_B are steady-state intermediates. TS_A and TS_B are plausible transition states. 34
- 3.21** Eyring plots of $\ln(k_{\text{obsd}}/T)$ vs. $1/T$ for C_{60} dissociation from $fac\text{-}(^2\text{-}C_{60})(^2\text{-phen})Cr(\text{CO})_3$ in chlorobenzene, benzene and toluene by tri-phenylphosphine. 36
- 4.1** Schematic representation of the vacuum line used to transfer and mix reagents in electrochemical runs. 39
- 4.2** Schematic representation of the Electrochemical cell with a three-electrode configuration used for electrochemical runs. 40
- 4.3** Cyclic voltammetric responses recorded at a glassy carbon working electrode on dichloromethane solution containing, 0.1 M TBPF6, $fac\text{-}(^2\text{-}C_{60})(^2\text{-phen})Cr(\text{CO})_3$ (saturated solution), and traces of decamethylferrocene (Fc) scan rate 100 mV/s. 43
- 4.4** Cyclic voltammetric responses recorded at a glassy carbon working electrode on dichloromethane solution containing, 0.1 M TBPF6, $fac\text{-}(^2\text{-}C_{60})(^2\text{-phen})Cr(\text{CO})_3$ (saturated solution), and traces 46

- of decamethylferrocene (Fc) scan rate 100 mV/s.
- 4.5** Cyclic voltammetric responses recorded at a glassy carbon working electrode on dichloromethane solution containing, 0.1 M TBPF6, *fac*-(η^5 -C₆₀)(η^2 -phen)Mo(CO)₃ (saturated solution), and traces of decamethylferrocene (Fc) scan rate 100 mV/s. 46
- 4.6** Cyclic voltammetric responses recorded at a glassy carbon working electrode on dichloromethane solution containing, 0.1 M TBPF6, *fac*-(η^5 -C₆₀)(η^2 -phen)W(CO)₃ (saturated solution), and traces of decamethylferrocene (Fc) scan rate 100 mV/s. 47
- 4.7** Plots of ln(k/T) vs. 1/T showing the isokinetic region for the solvent-assisted C₆₀ displacement from *fac*-(η^5 -C₆₀)(η^2 -phen)Mo(CO)₃ in chlorobenzene 49
- 4.8** Plots of ln(k_{obsd}/T) versus 1/T in Toluene, Benzene and Chlorobenzene for the complexes *fac*-(η^5 -C₆₀)(η^2 -phen)M(CO)₃ (were M = Cr, W and Mo) 50

Chapter I

Introduction

In 1985, Harold Kroto, James R. Heath, Sean O'Brien, Robert Curl, and Richard Smalley, discovered C_{60} ; shortly thereafter, they discovered the fullerenes, the third allotropic form of carbon¹. Fullerenes are spherical molecules containing an arrangement of five- and six-member carbon atom rings¹. The most common fullerenes contain an array of 60 or 70 carbon atoms. Some of the fullerenes properties include high cohesive force, high hydrophobicity, high compressibility, hardness, heat resistance and superconductivity, photo-activity, ability to accept and release electrons, and relatively high reactivity that allows structural modifications.^{1,5}

Fullerenes are slightly soluble in many solvents. [60] Fullerene (C_{60}) is the only known allotrope of carbon that can be dissolved in common solvents at room temperature.⁶ Toluene, benzene, carbon disulfide, ethanol, and 1-chloronaphthalene are the most common solvents used. For example, C_{60} solubility at room temperature ranges from 0.001 mg / mL in ethanol and up to 51 mg / mL in 1-chloronaphthalene.⁶

The solubilization of fullerenes in water has been investigated extensively, since their applicability was limited due to the poor solubility in polar solvents.⁷ C_{60} has been solubilized in water combined with α -cyclodextrin, β -cyclodextrin, polyvinylpyrrolidone, and fluoroalkyl oligomer. [60] Fullerene can also solubilize in water by connecting it with functional chargeable groups such as carboxylic acids or amines, or by adding polarizable phenyl groups to C_{60} to stabilize its anion⁸.

Over the past few years, several studies showed that [60] fullerene derivatives can be used as biologically active compounds in medicinal chemistry⁹. They have attracted much attention for their unique cage-like shape and biological activities such as HIV-1 protease inhibition. Fullerenes

were under study for potential medicinal use, such as binding specific antibiotics to its structure and even target certain cancer cells⁵. Likewise, studies of [60] fullerenes as light-activated antimicrobial agents⁵ and as free-radical sponges¹¹ have been reported. These properties have made C₆₀ an extensive area of study in the field of nanotechnology.⁵

There is a variety of organometallic complexes functionalized with C₆₀. [60] Fullerene can be coordinated to organometallic complexes because it has a high electron affinity¹² and can participate in π -back bonding with transition metals¹². [60] Fullerene coordinates transition metals in a dihapto (η^2) mode resembling an olefinic-metal mode of coordination.¹³ An example of these complexes are: *fac*-(η^2 -phen)(η^2 -C₆₀)W(CO)₃¹⁴ and *fac*-(η^2 -phen)(η^2 -C₆₀)Mo(CO)₃¹⁵. The functionalization of C₆₀ is also of interest in organometallic catalysis. [60] Fullerene has the potential to modify and enhance the catalytic capacity of existing organometallic catalysts because it can labilize, coordinate ligands and stabilize electron rich transition states or intermediate species involved in the complexes ligand exchange reactions.¹⁶⁻¹⁷

This work presents the kinetic and mechanistic studies on the dissociation of C₆₀ from *fac*-(η^2 -phen)(η^2 -C₆₀)Cr(CO)₃, and also establishes a relationship on the profile of the complexes *fac*-(η^2 -phen)(η^2 -C₆₀)M(CO)₃ (M = W, Mo and Cr).

1.1 Objectives

To establish a relationship between the electronic structure, molecular structure and the reactivity of fullerene-metal complexes of $fac-(^2-C_{60})(^2-phen)M(CO)_3$ ($M = Cr, W, Mo$), the electrochemical profile of [60] fullerene-metal carbonyl complexes needs to be studied. Similarly, the mechanistic pathway of $fac-(^2-C_{60})(^2-phen)M(CO)_3$ kinetics needs to be studied, as well. The kinetics and mechanistic pathway of $fac-(^2-C_{60})(^2-phen)M(CO)_3$ reactions ($M = W, Mo$) were previously reported in our research group.^{14,15} This will contribute to our efforts in obtain further comprehension on these systems.

Specific Project Objectives

1. To prepare and characterize the complex $fac-(^2-C_{60})(^2-phen)Cr(CO)_3$
2. To establish the mechanism of the C_{60}/L exchange reactions on $fac-(^2-C_{60})(^2-phen)Cr(CO)_3$
3. To measure the half-wave potential values ($E_{1/2}$) of $fac-(^2-C_{60})(^2-phen)M(CO)_3$ ($M = Cr, W, Mo$) complexes and compare these values with the corresponding values for the uncoordinated C_{60} .
4. To study the electronic profile and obtain electronic structure information of $fac-(^2-C_{60})(^2-phen)M(CO)_3$ ($M = Cr, W, Mo$) using electrochemical properties.

Chapter II

Previous Work

Since their discovery in the middle 1980s, fullerenes have been of great interest because of their unique structure and properties¹. It was then realized that C₆₀ was also unique among the experimentally available fullerenes because of its high symmetry and stability¹.

Previous investigations have demonstrated that a secondary amine undergoes multiple additions to C₆₀, under photochemical conditions in an aerobic environment to produce tetra (amino)- fullerene epoxide.³ The reaction of C₆₀ and piperidine (pip) was previously reported.^{18,27} The reaction product is a tetra (pip)- fullerene epoxide, presented in figure 2.1. The rate of the epoxide appearance was monitored by observing an increase in absorbance at 407 nm (Figure 2.2). The reactions were studied under flooding conditions and the rate constants values were dependent of the concentration of piperidine.^{18,27}

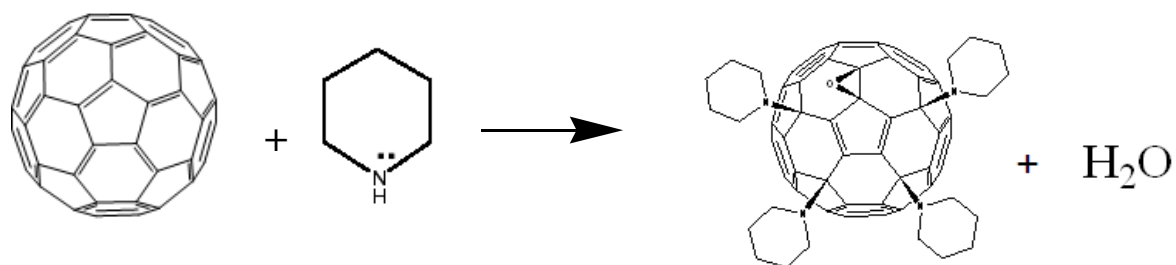


Figure 2.1 Schematic representation for reactions of C₆₀ with piperidine to produce tetra(pip)-fullerene epoxide¹⁸.

The coordination behavior of fullerenes was first reported by Fagan *et al.*, who crystallographically established the η^2 -bonding mode for [60] fullerene in $[\text{Pt}(\eta^2\text{-C}_{60})(\text{PPh}_3)_2]$ and $[\{\text{M}(\text{PEt}_3)_2\}_6(\eta^2\text{-C}_{60})]$ (M = Pd or Pt). Since then, several works reported this type of fullerene to metal coordination, for a range of transition metals.² Organometallic derivative complexes such as $(\eta^2\text{-chelate})(\eta^2\text{-C}_{60})\text{M}(\text{CO})_{5-2n}$ (M = Cr, Mo, W)^{14-15,19-20} are another example of η^2 -bonding mode for [60] fullerene. For instance, displacement reactions of C_{60} from $(\eta^2\text{-C}_{60})\text{Cr}(\text{CO})_5$ ($n = 0$) by piperidine (pip) producing $(\eta^1\text{-pip})\text{Cr}(\text{CO})_5$ (figure 2.2) has also been described²⁷. For these reactions, plots of absorbance versus time consist of three segments: the first decreasing segment of the plot was ascribed to the displacement of C_{60} from the parent complex, whereas the second and third increasing segments were assigned to stepwise additions of piperidine to uncoordinated C_{60} .^{18,20,27}

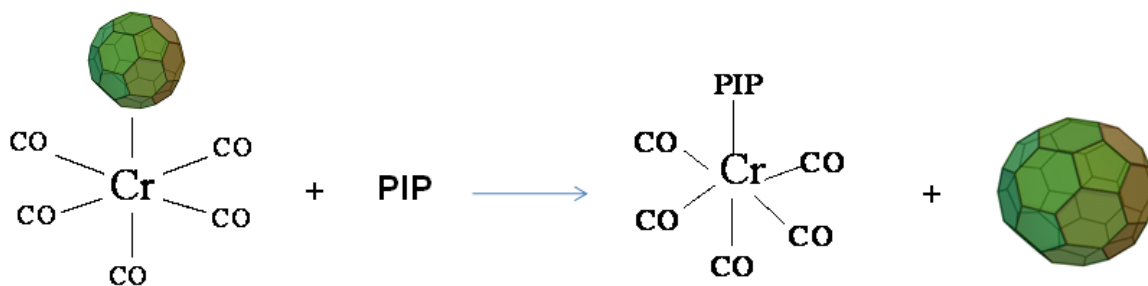


Figure 2.2 Schematic representation for displacement reactions of C_{60} from $\text{Cr}(\text{CO})_5(\text{C}_{60})$ through piperidine.

The displacement reaction of C_{60} from organometallic complexes such as $fac-(\eta^2-C_{60})(\eta^2\text{-phen})W(CO)_3$ ($n = 1$) with triphenyl phosphine (PPh_3) and tricyclohexyl phosphine ($P(Cy)_3$) can be obtained through a dissociative or an associative mechanistic pathway. Figure 2.3 presents both mechanisms: Path A involves an initial solvent assisted dissociation of C_{60} , while Path B describes a dissociative displacement.

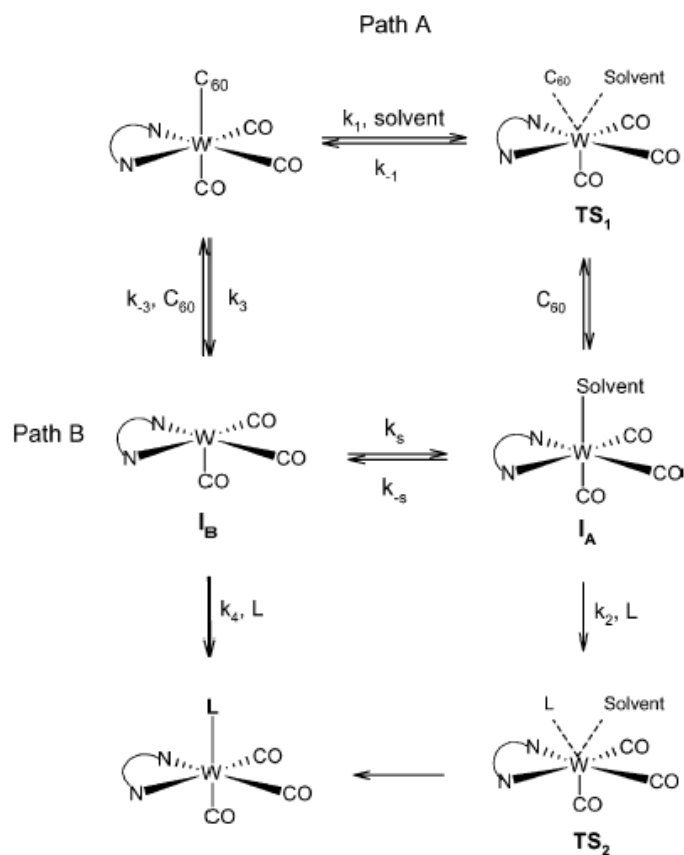


Figure 2.3 Proposed mechanisms for C_{60} displacement from $fac-(\eta^2-C_{60})(\eta^2\text{-phen})W(CO)_3$. Path A describes a solvent-assisted displacement of C_{60} , Path B describes a dissociative displacement. I_A and I_B are steady-state intermediates. TS_1 and TS_2 are plausible transition states¹⁴

The preferred dihapto (η^2) mode of coordination of C_{60} is due in part to its electronic structure, when the three-degenerated LUMOs are directed away from each other on the spherical surface of [60] fullerene. Comparison of the electrochemical profile of uncoordinated [60] fullerene with the corresponding profile of C_{60} -metal complexes permits assessment on the electron donor/acceptor capacity of [60] fullerene.² These [60] fullerene properties open a door in its use to design new inorganic catalysts and/or to modify precursors of existing ones.

Chapter III

Displacement of C_{60} from $fac-(\eta^2-C_{60})(\eta^2-phen)Cr(CO)_3$ by L (L = pip, PPh_3 and $P(Cy)_3$)

3.1 Materials and Methodology

3.1.1 General

Benzene, toluene and chlorobenzene were dried over phosphorous pentoxide and fractionally distilled under nitrogen. All reactions were performed on nitrogen atmosphere to avoid oxidation of reagents. Infrared spectra were performed with Bruker Vector 22TM Fourier transform, infrared spectrophotometer and a KBr cell of 0.10 mm light path was used for IR measurements. Concepts of group theory and symmetry were applied to predict the number of active IR bands in the CO stretching region (ν_{CO}).

UV/VIS spectra were obtained using a Perkin Elmer UV-Visible Lambda 25TM spectrophotometer. In order to determine radiation wavelength, (when L= PPh_3 and $P(Cy)_3$) where the reaction was monitored, a UV/VIS scan was performed to a solution with the complex $fac-(\eta^2-C_{60})(\eta^2-phen)Cr(CO)_3$ and the reacting ligands. The reactions progress was monitored until a significant change in absorbance was observed and this significant change occurred at 500 nm for L = PPh_3 and $P(Cy)_3$). Temperature was controlled using a Julabo F-12TM constant temperature bath, which consists of an EC model heating and refrigerating circulator and a K/J Fluke digital thermometer equipped with a bead thermocouple.

The rate constant values were determined from the plots of absorbance versus time using a non-linear regression computer program (OriginPro 7.5TM). The error limits of the rate constant values are given in parenthesis as the uncertainties of the last digit of the reported value and these are within one standard deviation.

3.1.2 Preparation of (*2*-phen)Cr(CO)₄

The complex (*2*-phen)Cr(CO)₄ was prepared thermally (figure 3.1) following a modified published procedure.⁴⁰ In a three-necked 100 mL round bottomed flask, equipped with a magnetic stirring bar, a condenser and a nitrogen inlet, 0.32773 g (0.149 mmol) of chromium hexacarbonyl (figure 3.2) and 0.25047 g (0.728 mmol) of 1,10-phenantroline were dissolved in 15 mL of toluene and heated under nitrogen for approximately four hours. The progress of the reaction was monitored by observing the decrease of the CO band intensity at 1982 cm⁻¹ of chromium hexacarbonyl and the growth of the (*2*-phen)Cr(CO)₄ CO bands intensities. The resulting reddish-brown product and solvent was purged with nitrogen and the product was characterized as (*2*-phen)Cr(CO)₄ from its CO absorbencies in toluene, (CO, cm⁻¹): 2007, 1898, 1890, and 1842 (figure 3.3).

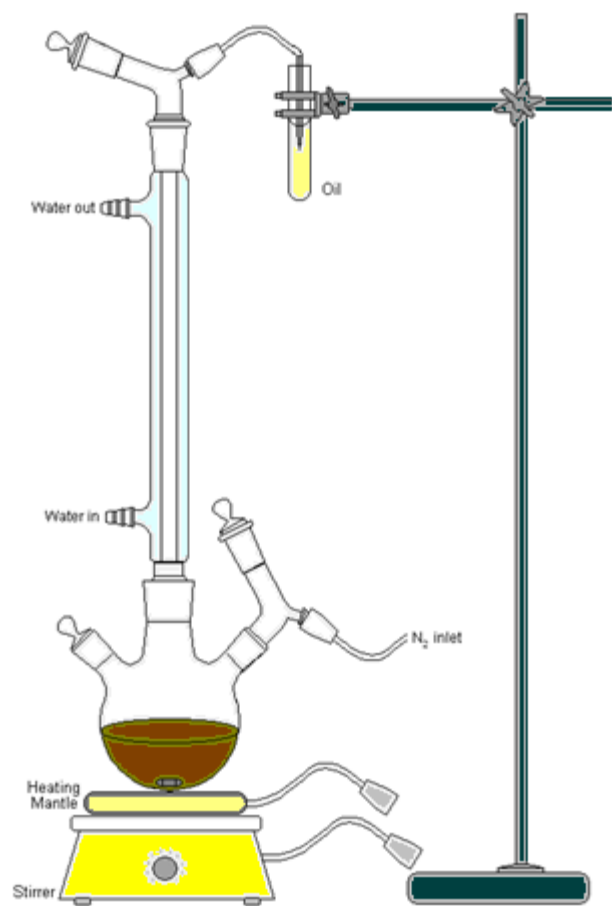


Figure 3.1 Schematic Representation of the equipment used for the thermal preparation of $(\text{}^2\text{-phen})\text{Cr}(\text{CO})_4$.¹⁸

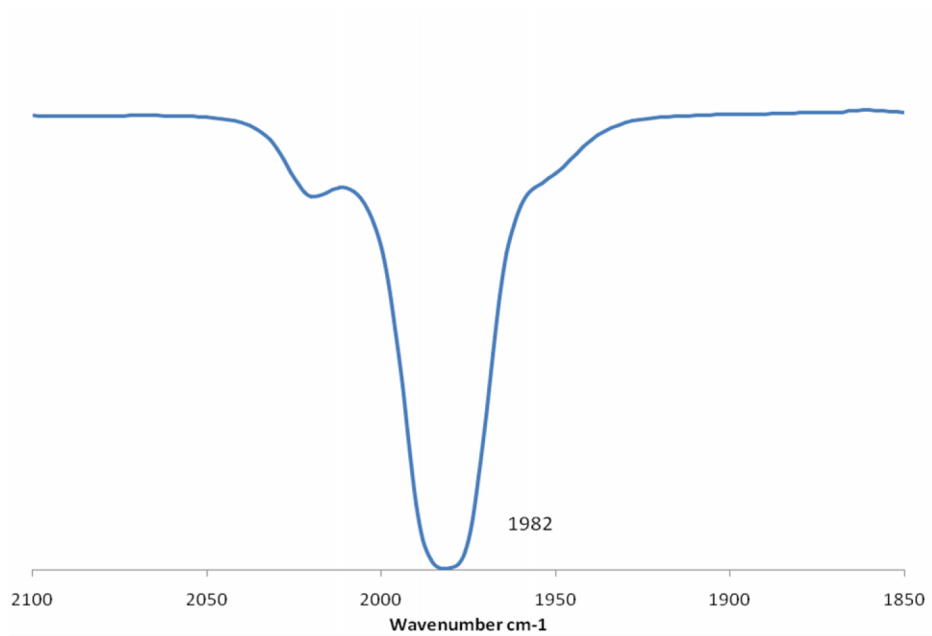


Figure 3.2 Infrared Spectrum in the carbonyl region of $\text{Cr}(\text{CO})_6$ in toluene.

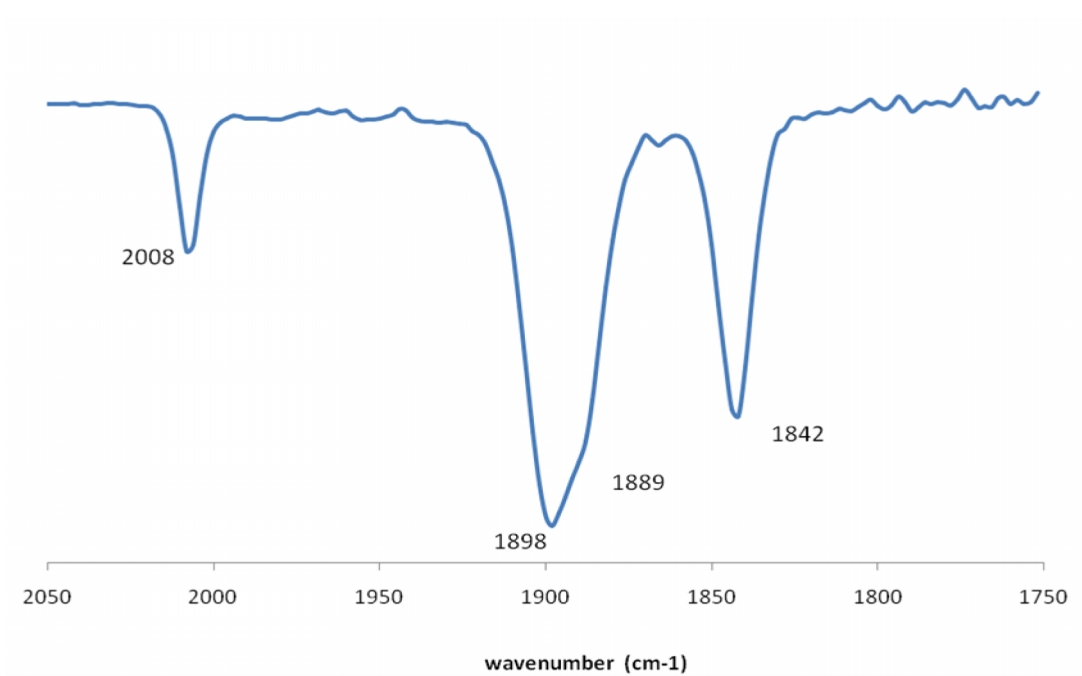


Figure 3.3 Infrared Spectrum in the carbonyl region of $(2\text{-phen})\text{Cr}(\text{CO})_4$, produced from the thermal reaction of $\text{Cr}(\text{CO})_6$ with 1,10-phenanthroline in toluene.

3.1.3 Preparation of *fac*-(²-C₆₀)(²-phen)Cr(CO)₃

The complex *fac*-(²-C₆₀)(²-phen)Cr(CO)₃ was prepared photochemically (figure 3.4) from (²-phen)Cr(CO)₄ and C₆₀ using a medium pressure mercury arc lamp. In a three-necked 100 mL round bottomed flask equipped with a magnetic stirring bar, a condenser and a nitrogen inlet, 0.03199 g (0.0930 mmol) of (²-phen)Cr(CO)₄ and 0.05070 g (0.0704 mmol) of [60] fullerene were dissolved in 15 mL dried toluene. After the reacting mixture was purged with nitrogen, it was irradiated with a medium pressure mercury arc lamp under a slow and continuous flow of nitrogen for approximately two hours. The reaction was considered complete after judging the infrared spectrum; consequently, toluene was purged with nitrogen from the reaction mixture. The resulting brown solid was then dissolved in approximately 10 mL of carbon disulfide (CS₂). Thin layer chromatography analysis showed two components. The two components were separated by column chromatography, using a 15 cm long and 1cm diameter glass column, packed with 62 grades, 60-2000 mesh, and 150 Å silica gel. The first component, identified as [60] fullerene from its distinctive purple color and its R_f value, was eluted using carbon disulfide. The second fraction was nitrogen-purged. After nitrogen-purged, the product was characterized as *fac*-(²-C₆₀)(²-phen)Cr(CO)₃ (figure 3.5) from its CO absorbencies in toluene, (CO, cm⁻¹): 1960, 1944, 1872, 1861, and 1804. The product was obtained in a low yield of 23%.

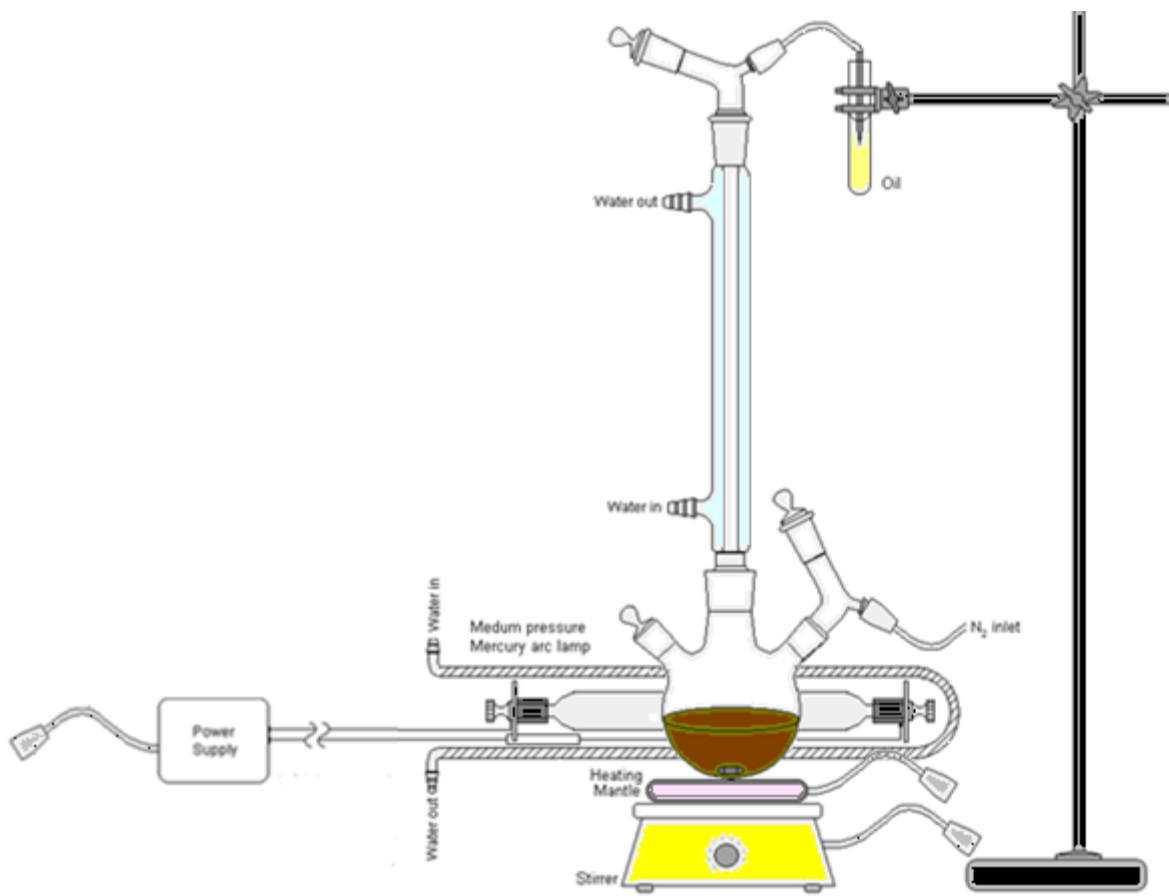


Figure 3.4 Schematic representation of the photochemical preparation of $fac-(^2-C_{60})(^2-phen)_3Cr(CO)_3$.

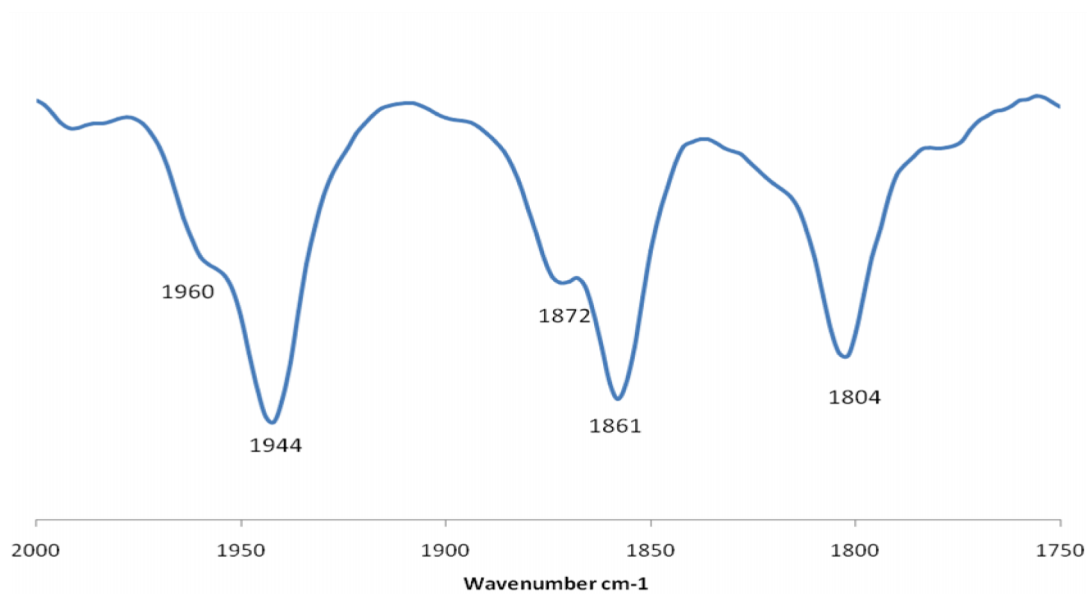


Figure 3.5 Infrared Spectrum in the Carbonyl region of *fac*-(²-C₆₀)(²-phen)Cr(CO)₃, produced from the photochemical reaction of (²-phen)Cr(CO)₄ with C₆₀ in toluene.

3.1.4 Preparation of (¹-pip)₃Cr(CO)₃

The complex (¹-pip)₃Cr(CO)₃ was prepared thermally from (²-phen)Cr(CO)₄ and piperidine. In a three-necked 100 mL round bottomed flask, equipped with a magnetic stirring bar, a condenser, and a nitrogen inlet, a solution of 0.03039 g (0.0883 mmol) of (²-phen)Cr(CO)₄ and a pinch of piperidine were poured into toluene (15 mL), followed by a two hours reflux. The intermediate species was characterized as *fac*-(¹-pip)(²-phen)Cr(CO)₃, from its CO absorbencies in toluene (CO, cm⁻¹): 1964, 1946, 1878, 1862, and 1808, followed by the characterization of the product (¹-pip)₃Cr(CO)₃ (figure 3.7) from its CO absorbencies in toluene, (CO, cm⁻¹):1958, 1942, 1870, 1858, and 1802.



Figure 3.6 Infrared Spectrum in the Carbonyl region for an actual sample of the intermediate species *fac*-(¹-pip)(²-phen)Cr(CO)₃ produced in the thermal reaction of (²-phen)Cr(CO)₄ with piperidine in toluene, t = 0:50minutes.

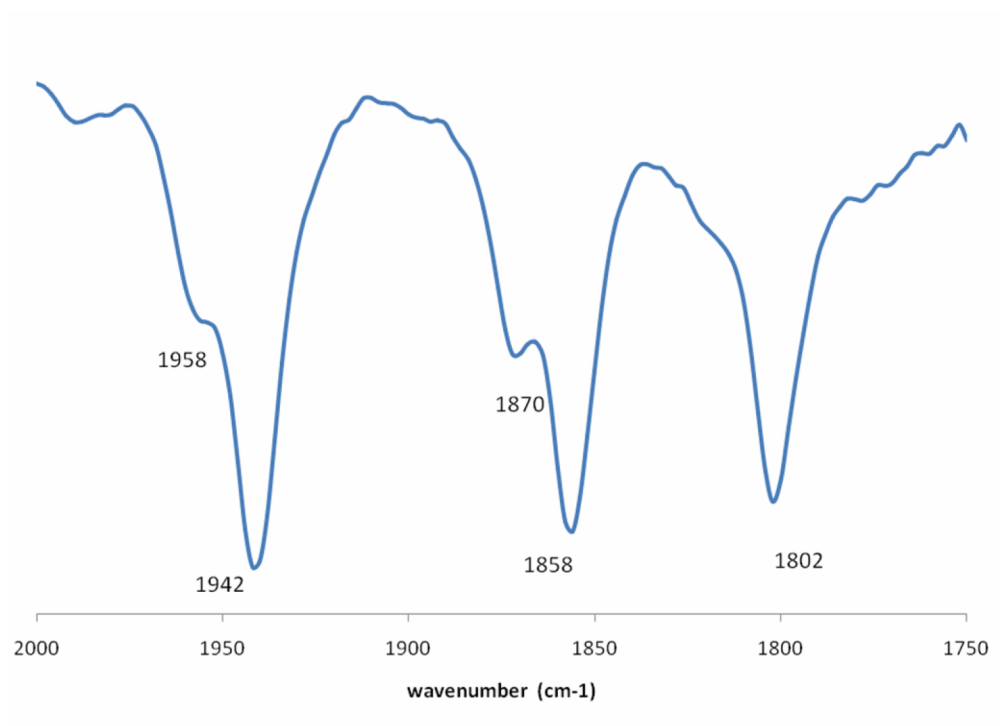


Figure 3.7 Infrared Spectrum in the carbonyl region for an actual sample of the product (¹-pip)₃Cr(CO)₃, produced in the thermal reaction of (²-phen)Cr(CO)₄ with piperidine in toluene, where t = 0:90minutes.

3.1.5 Preparation of (¹-pip)₃Cr(CO)₃

The complex (¹-pip)₃Cr(CO)₃ was prepared thermally, also from the complex *fac*-(²-C₆₀)(²-phen)Cr(CO)₃ and piperidine. In a three-necked 15mL round bottomed flask equipped with a magnetic stirring bar, a condenser, and a nitrogen inlet, a solution of 0.00339g (0.00327mmol) of *fac*-(²-phen)(²-C₆₀)Cr(CO)₃ and a pinch of piperidine were poured into 10 mL of toluene and thermally refluxed for 40 minutes. The solution was purged under nitrogen and characterized as (¹-pip)₃Cr(CO)₃, from its CO absorbencies in toluene, (ν_{CO}, cm⁻¹): 1958, 1942, 1868, 1858, and 1802.

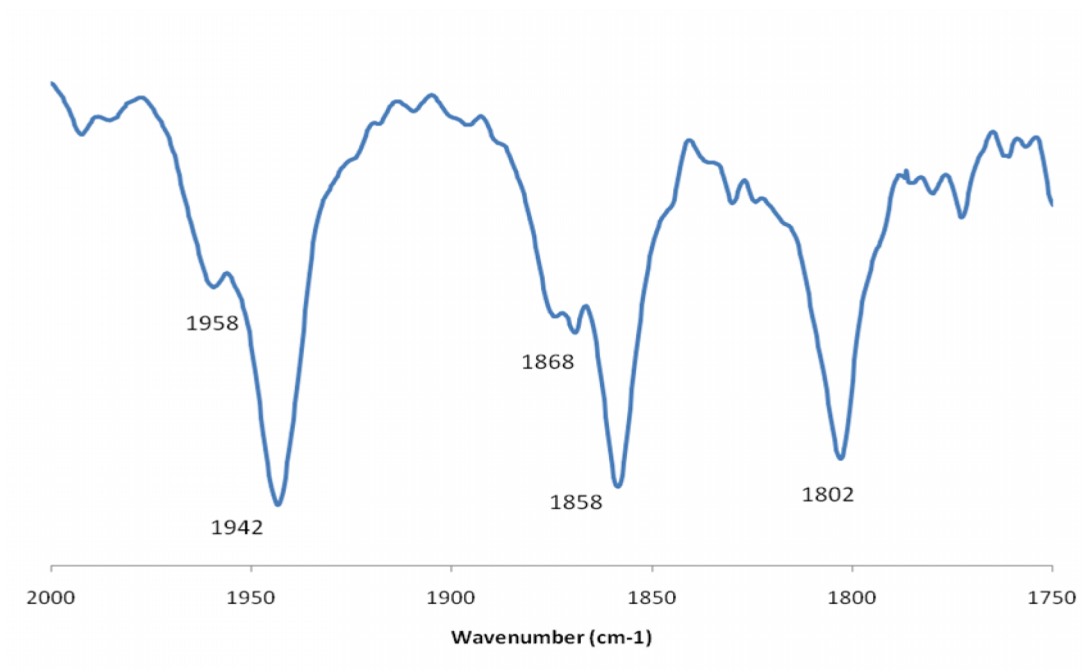


Figure 3.8 Infrared Spectrum in the Carbonyl region for an actual sample of the product (¹-pip)₃Cr(CO)₃ produced in the thermal reaction of *fac*-(²-C₆₀)(²-phen)Cr(CO)₃ with piperidine in toluene, where t = 0:40minutes.

3.2 Kinetic Experiments of $fac-(^2-C_{60})(^2-phen)Cr(CO)_3$

3.2.1 Kinetic Experiments for reactions of $fac-(^2-C_{60})(^2-phen)Cr(CO)_3$ with piperidine in chlorobenzene

The reactions of $fac-(^2-C_{60})(^2-phen)Cr(CO)_3$ with piperidine were studied, observing an increase in absorbance followed by a decrease in absorbance at 407 nm. The reactions were dissolved into chlorobenzene at 313.2, 323.2, and 333.2 K; under flooding conditions, where $[pip] \gg \gg [fac-(^2-C_{60})(^2-phen)Cr(CO)_3]$.

3.2.2 Kinetic Experiments for the reactions of $fac-(^2-C_{60})(^2-phen)Cr(CO)_3$ with PPh_3 in chlorobenzene

The reactions of $fac-(^2-C_{60})(^2-phen)Cr(CO)_3$ with PPh_3 , were studied observing a decrease in absorbance at 500 nm. The reactions were dissolved into chlorobenzene at 303.2, 313.2, 323.2, and 333.2 K under flooding conditions where $[PPh_3] \gg \gg [fac-(^2-C_{60})(^2-phen)Cr(CO)_3]$.

3.2.3 Kinetic Experiments for reactions of $fac-(^2-C_{60})(^2-phen)Cr(CO)_3$ with PPh_3 in toluene

The reactions of $fac-(^2-C_{60})(^2-phen)Cr(CO)_3$ with PPh_3 , were studied observing a decrease in absorbance at 500 nm. The reactions were dissolved into toluene at 303.2, 313.2, 323.2, and 333.2 K under flooding conditions where $[PPh_3] \gg \gg [fac-(^2-C_{60})(^2-phen)Cr(CO)_3]$.

3.2.4 Kinetic Experiments for the reactions of $fac-(^2-C_{60})(^2-phen)Cr(CO)_3$ with PPh_3 in benzene

The reactions of $fac-(^2-C_{60})(^2-phen)Cr(CO)_3$ with PPh_3 , were studied observing a decrease in absorbance at 500 nm. The reactions were studied into benzene at 303.2, 313.2, 323.2, and 333.2 K under flooding conditions, where $[PPh_3] \gg \gg [fac-(^2-C_{60})(^2-phen)Cr(CO)_3]$.

3.3 Data Analysis

3.3.1 Kinetics data for the displacement of C_{60} from $fac-(\eta^5-C_{60})(\eta^5-phen)Cr(CO)_3$ by PPh_3

Kinetics data was analyzed using OriginPro 7.5™, as the non-linear least-squares computer program. The graphs of absorbance vs. time for the reactions under flooding conditions when the ligands were PPh_3 and $P(Cy)_3$, consist of a mono-exponential decay. The fit that best describes the behavior of the experimental data points is of first order and the function that's provided by the computer program is given through:

$$Y = (A_1) e^{-x/t} + Y_0 \quad \text{Equation (3.1)}$$

Where Y is the dependant variable at time t; Y_0 is the value of Y at time 0 or initial value; A_1 is the amplitude; x is the independent variable and 1/t is the rate constant. The family of equations obtained by the computer program is mathematically equivalent to a first order rate equation that represents the monitored change of absorbance. The value of absorbance (A) is proportional to the concentration of the species involved in the reaction. The equation for a first order reaction is represented as:

$$A_t = (A_0 - A_{\infty}) e^{-k*t} + A_{\infty} \quad \text{Equation (3.2)}$$

Where the correspondence is: $A_t = Y$; $(A_0 - A_{\infty}) = A_1$; $k = 1/t$; $t = x$ and $A_{\infty} = Y_0$. A_t represents the value of absorbance at a given time, A_0 represents the absorbance at time zero, A_{∞} represents the absorbance at infinite time, k is the observed rate constant, and t represents time.

3.3.2 Kinetics data for the displacement of C₆₀ from *fac*-(²-C₆₀)(²-phen)Cr(CO)₃ by piperidine

Kinetic data was analyzed using OriginPro 7.5™. The graphs of absorbance vs. time for L = piperidine were biphasic consisting of two consecutive segments. The first segment, increased with time and the second segment, decreased with time. The rate constant values for the reaction were determined using a non-linear least squares computer program. The mathematical equation which best describes the behavior of the experimental data points for reactions that consists of two segments is:

$$Y = -A_1e^{-x/t_1} + A_2e^{-x/t_2} + Y_0 \quad \text{Equation (3.3)}$$

Where Y is the dependent variable, Y₀ is the Y offset, A₁ and t₁ are the amplitude and the decay constant for the second segment, respectively, A₂ and t₂ are the amplitude and the decay constant for the second segment, respectively, and x is the independent variable. The computer program performs the necessary parameters initialization. It also sets Y₀ to an appropriate fixed number, which is close to the asymptotic value of the Y variable for large x values. The creation of the mathematical fit is produced by an iterative procedure. The mainframe fitter computes the Variance-Covariance matrix in each of the iterations using the previous iteration value. This matrix depends on the fitting function, the number of parameters, and the data set assignments. The analysis made by the computer program is adaptable to chemical kinetics conditions since a physical property, such as absorbance, is monitored. Thus, the equation becomes:

$$A_t = -e^{-kAt} + e^{-kbt} + A \quad \text{Equation (3.4)}$$

Where the correspondence is: A_t = Y; = A₁; = A₂; k = 1/t ; t = x and A = Y₀. In which A_t is the value of the absorbance at a given time, A₀ represents the absorbance at time zero, A represents the absorbance at time infinite, and are pre-exponential constants, k is the observed rate constant, and t is the time.

3.3.3 Eyring Plots

Eyring plots were constructed to estimate the activation parameters. The Eyring equation (equation 3.5) expresses the temperature dependence of a rate constant, based on the transition state model. A plot of $\ln(k/T)$ versus $1/T$ is expected to be linear for small temperature ranges.

$$\ln \frac{k}{T} = -\frac{\Delta H^\ddagger}{R} \left(\frac{1}{T} \right) + \ln \frac{k_B}{h} + \frac{\Delta S^\ddagger}{R}$$

Equation (3.5)

Where k_B = Boltzmann's constant [$1.381 \times 10^{-23} \text{ J}\cdot\text{K}^{-1}$], T = absolute temperature in Kelvin (K), R = Gas constant [$8.3145 \text{ J/K}\cdot\text{mol}$], and h = Plank's constant [$6.626 \times 10^{-34} \text{ J}\cdot\text{s}$].

The values of enthalpy of activation can be estimated from the slope: $H = -R(\text{slope})$ and the values of the entropy of activation can be estimated from the intercept: $S = R (\text{intercept} - \ln(k_B/h))$.

3.4 Results

3.4.1 Displacement reactions of C₆₀ from *fac*-(²-C₆₀)(²-phen)Cr(CO)₃ by piperidine

The reaction of *fac*-(²-C₆₀)(²-phen)Cr(CO)₃ with piperidine producing *fac*-(¹-pip)₃Cr(CO)₃ in chlorobenzene were biphasic. The reactions were studied at temperatures of 313.2, 323.2, and 333.2 K. The plots of absorbance vs. time consisted of two consecutive segments. The first segment (increasing) of the plot was assigned to step-wise additions of piperidine to uncoordinated C₆₀. The second segment (decreasing) was ascribed to solvent-assisted displacement of C₆₀ from *fac*-(²-C₆₀)(²-phen)Cr(CO)₃. The rate of disappearance of *fac*-(²-C₆₀)(²-phen)Cr(CO)₃ was monitored observing an increase followed by a decrease of absorbance values at 407 nm.

The reactions' progress was also followed by monitoring the stretching carbonyl region (CO, cm⁻¹) 1700 to 2100. The results suggest the formation of *fac*-(¹-pip)(²-phen)Cr(CO)₃ as an intermediate species, followed by the formation of the corresponding kinetically inaccessible product (¹-pip)₃(²-phen)Cr(CO)₃ (figure 3.9).

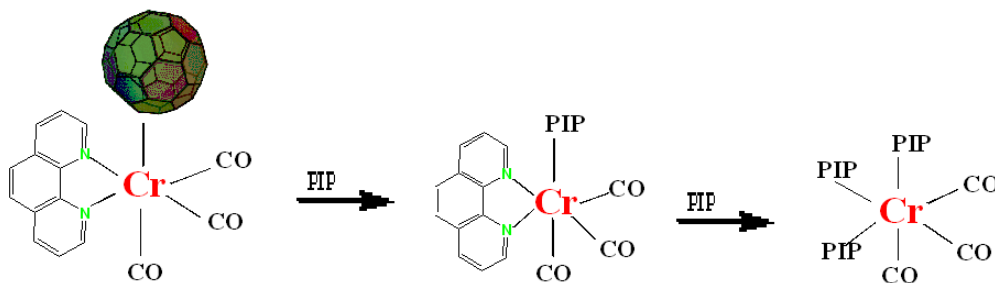


Figure 3.9 Schematic representation of the displacement of C₆₀ from *fac*-(²-C₆₀)(²-phen)Cr(CO)₃ by piperidine.

The nature of the reaction product was established by comparison of the CO spectrum of the reaction product with the spectra of the authentic samples. A plot of absorbance vs. time for the reaction of *fac*-(²-C₆₀)(²-phen)Cr(CO)₃ with piperidine ([pip] = 1.59 M in chlorobenzene at 313.2 K) is given in figure 3.10. The equation 3.3, describes the relation between Absorbance and time (where A₁ = 0.05301, A₂ = 0.09884; 1/t₁ = 1.92(5)*10⁻³ s⁻¹; 1/t₂ = 3.26(6)*10⁻⁴ s⁻¹ and Y₀ = 0.20062).

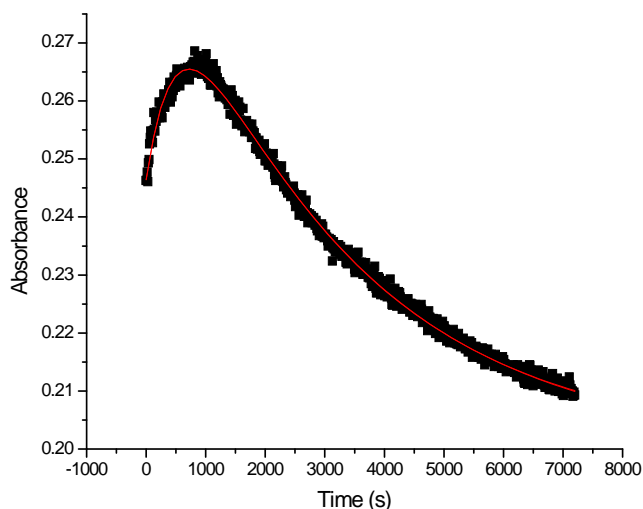


Figure 3.10 Plot of absorbance (407nm) vs. time (s) for C₆₀ displacement from *fac*-(²-C₆₀)(²-phen)Cr(CO)₃ through piperidine dissolved in chlorobenzene, producing *fac*-(¹-pip)₃Cr(CO)₃ at 313.2K under conditions, where [pip] >>> [*fac*-(²-C₆₀)(²-phen)Cr(CO)₃]. The dissociation of C₆₀ from *fac*-(²-C₆₀)(²-phen)Cr(CO)₃ to form *fac*-(¹-pip)Cr(²-phen)Cr(CO)₃ as an intermediated species was ascribed to the second segment of the plot, while the first segment was ascribed to the step-wise addition of piperidine to uncoordinated C₆₀. The function that best describes the relation between Absorbance vs. time is: $Y = -A_1e^{-x/t_1} + A_2e^{-x/t_2} + Y_0$; where A₁ = 0.05301, A₂ = 0.09884; 1/t₁ = 1.92(5)*10⁻³ s⁻¹, 1/t₂ = 3.26(6)*10⁻⁴ s⁻¹, and Y₀ = 0.20062.

The rate constant (k_{obsd1}) for the first segment is dependent on the concentration of piperidine.^{18, 20} The average rate constant value (k_{obsd1} and k_{obsd2}) determined for various piperidine concentrations and temperatures are presented in table 3.1.

Table 3.1 Average Rate constants values for the displacement reactions of C_{60} from $fac-(^2-C_{60})(^2-phen)Cr(CO)_3$ by piperidine (pip) in chlorobenzene at different temperature, under flooding conditions, where $[pip] \gg \gg [fac-(^2-C_{60})(^2-phen)Cr(CO)_3]$

Temp (K)	Average $k_{obsd1}(10^{-3} s^{-1})$	Average $k_{obsd2}(10^{-4} s^{-1})$
313.2	2.24 (± 0.94)	3.86 (± 0.60)
323.2	5.10 (± 3.8)	4.96 (± 0.85)
333.2	11.43 (± 2.9)	5.77 (± 1.77)

*The values in parenthesis are the standard deviation of the average rate constants.

**The single rate constant values (k_{obsd1} and k_{obsd2}) are presented on the Appendix D, tables D1, and D2 respectively.

The rate constants values (k_{obsd2}) for the second segment, were independent of piperidine concentration (figure 3.11) for the reactions of $fac-(^2-C_{60})(^2-phen)Cr(CO)_3$ with piperidine in chlorobenzene. The corresponding activation parameters, presented in table 3.2, were determined from the Eyring plot (3.12)

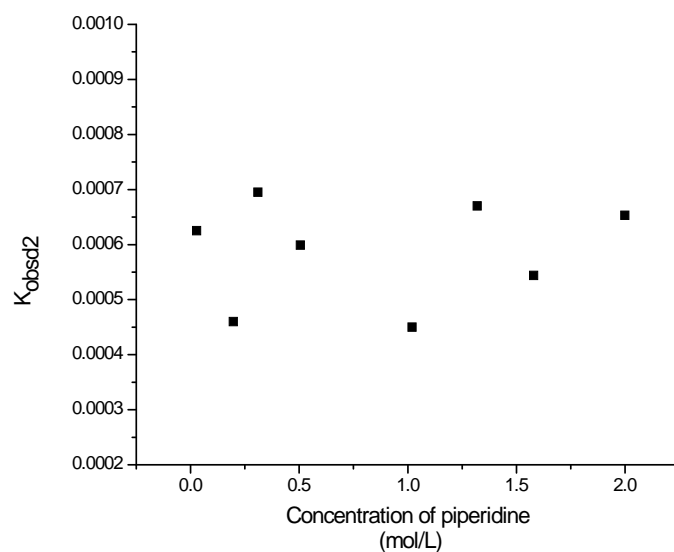


Figure 3.11 Plot of k_{obsd2} versus [pip] for C_{60} dissociation from $fac-(^2-C_{60})(^2-phen)Cr(CO)_3$ in chlorobenzene by piperidine at 333.2 K. The k_{obsd2} values were obtained under flooding conditions where $[pip] \gg [fac-(^2-C_{60})(^2-phen)Cr(CO)_3]$. The plot shows that the k_{obsd2} values are independent on the concentration of piperidine.

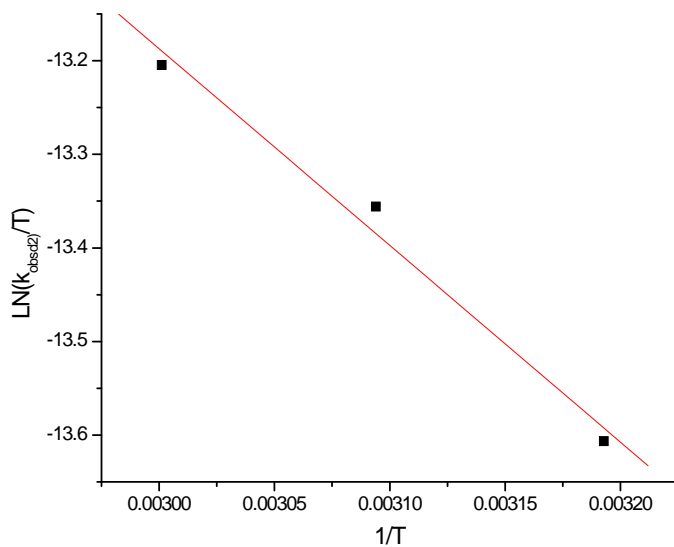


Figure 3.12 Eyring plot of $\ln(k_{obsd2}/T)$ vs. $1/T$ for C_{60} displacement from $(^2-C_{60})(^2-phen)Cr(CO)_3$ by piperidine in chlorobenzene. The k_{obsd} values were obtained under flooding conditions where the $[pip] \gg [fac-(^2-C_{60})(^2-phen)Cr(CO)_3]$, $H^\ddagger = 17(4)$ kJ/mol and $S^\ddagger = -177(64)$ J/K mol.

Table 3.2 Activation Parameters values for the dissociation of C_{60} from *fac*-(η^2-C_{60})(η^2 -phen)Cr(CO)₃ through piperidine in chlorobenzene. The values of enthalpy of activation can be estimated from the slope: $H^\ddagger = -R(\text{slope})$ and the values of the entropy of activation can be estimated from the intercept: $S^\ddagger = R(\text{intercept} - \ln(k_B/h))$ of the equation 3.5.

Ligand	H^\ddagger (kJ/mol)	S^\ddagger (J/K mol)
Piperidine (pip)	17 (4)	-177 (64)

**The values in parenthesis are the reported uncertainties.

3.4.2 Displacements of C₆₀ from *fac*-(²-C₆₀)(²-phen)Cr(CO)₃ by PPh₃ and P(Cy)₃

The complex *fac*-(²-C₆₀)(²-phen)Cr(CO)₃ was also studied with the ligands triphenylphosphine (PPh₃) and tricyclohexylphosphine (P(Cy)₃). The reactions of *fac*-(²-C₆₀)(²-phen)Cr(CO)₃ with PPh₃ and P(Cy)₃ in chlorobenzene, benzene and toluene were monophasic. The reactions were studied at temperatures of 303.2, 313.2, 323.2, and 333.2 K. The rate of *fac*-(²-C₆₀)(²-phen)Cr(CO)₃ disappearance was monitored by observing the decrease of the absorbance values at 500nm for both ligands. The reactions were studied under flooding conditions where (i) the concentrations of L and C₆₀ ($0 < [C_{60}]/[L] < 1$) were greater than the concentration of *fac*-(²-C₆₀)(²-phen)Cr(CO)₃ and (ii), where the concentrations where $[L] \gg [fac-(^{2}C_{60})(^{2}phen)Cr(CO)_3]$. For both conditions, the rate constant values were independent on the chemical nature of the L and of the concentration of L, but dependent of the nature of the solvent.

A plot of absorbance vs. time for the reaction of *fac*-(²-C₆₀)(²-phen)Cr(CO)₃ with PPh₃ ($[PPh_3] = 0.133$ M in chlorobenzene at 313.2 K) and with P(Cy)₃ ($[P(Cy)_3] = 0.103$ M in chlorobenzene) are given in figures 3.13 and 3.14, respectively.

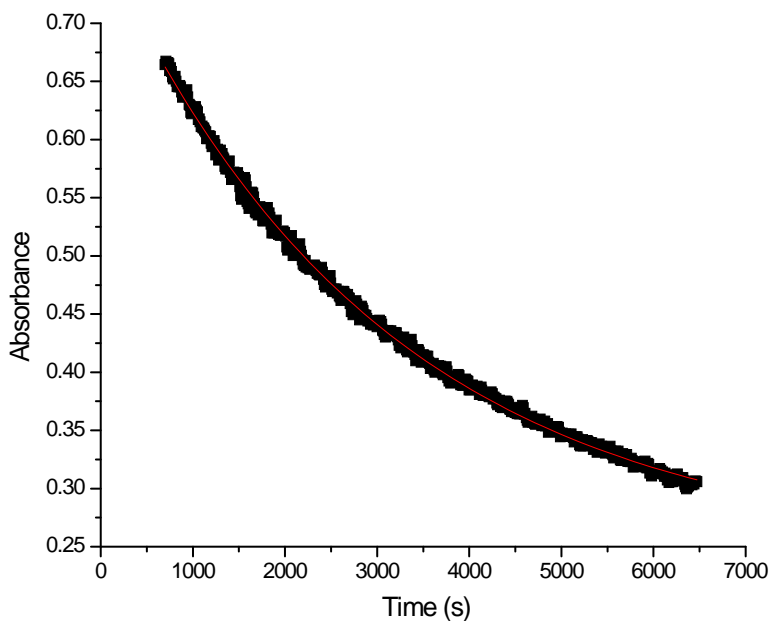


Figure 3.13 Plot of absorbance (500 nm) vs. time (s) for C_{60} displacement from $fac-(^2-C_{60})(^2-phen)Cr(CO)_3$ through PPh_3 ($[PPh_3] = 0.133$ M) in chlorobenzene to form $fac-(^1PPh_3)(^2-phen)Cr(CO)_3$ at 313.2 K, under flooding conditions, where $[PPh_3] \gg [fac-(^2-C_{60})(^2-phen)Cr(CO)_3]$. The equation that best describes the relation between absorbance and time is: $Y = (A_1) e^{-x/t} + Y_0$, where $A_1 = 0.52572$, $1/t_1 = 3.27(3) \cdot 10^{-4} s^{-1}$ and $Y_0 = 0.24434$.

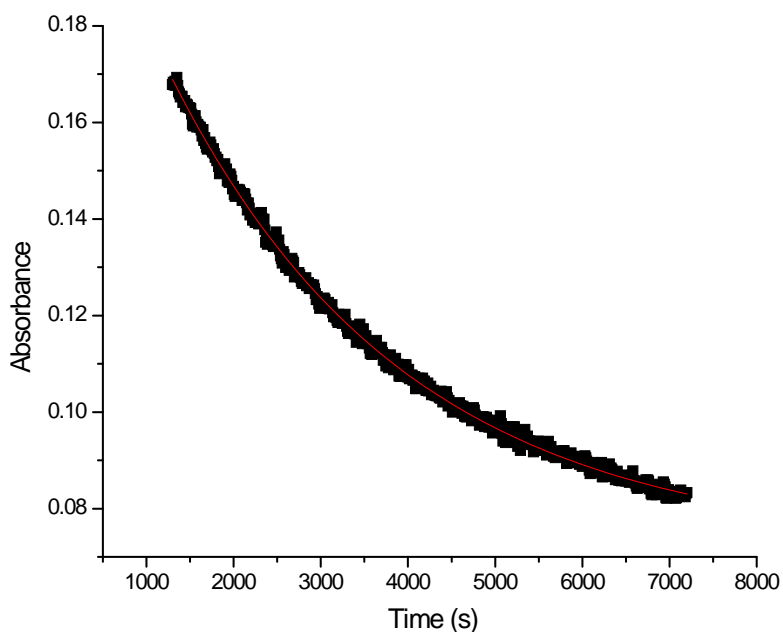


Figure 3.14 Plot of absorbance (500 nm) vs. time (s) for C_{60} displacement from $fac-(^2-C_{60})(^2-phen)Cr(CO)_3$ by $P(Cy)_3$ ($[P(Cy)_3] = 0.103$ M) in chlorobenzene to form $fac-(^1P(Cy)_3)(^2-phen)Cr(CO)_3$ at 313.2K, under flooding conditions where $[P(Cy)_3] \gg [fac-(^2-C_{60})(^2-phen)Cr(CO)_3]$. The equation that best describes the relation between absorbance and time is: $A_t = (A_0 - A) e^{-k \cdot t} + A$, where $A_0 - A = 0.52572$, $k_{obsd} = 3.70(2) \cdot 10^{-4}$ and $A = 0.07215$.

The average rate constant values (k_{obsd}) determined for various ligand concentrations and temperature in various solvents under conditions, where $[L] \gg [fac-(\eta^5-C_6O)(\eta^2\text{-phen})Cr(CO)_3]$, are presented in table 3.3. The k_{obsd} values, determined under conditions where $0 < [C_{60}]/[L] < 1$, are presented in table 3.4. The k_{obsd} values were independent of ligand's concentration under conditions where $0 < [C_{60}]/[L] < 1$ as shown in figures 3.15 and 3.16, respectively.

Table 3.3 Average rate constants values (k_{obsd}) for the displacement reactions of C_{60} from $fac-(\eta^5-C_6O)(\eta^2\text{-phen})Cr(CO)_3$ by triphenylphosphine (PPh_3) in chlorobenzene, benzene and toluene at various temperatures, under flooding conditions, such that $[PPh_3] \gg [fac-(\eta^5-C_6O)(\eta^2\text{-phen})Cr(CO)_3]$

Solvent	Temp (K)	Average $k_{\text{obsd}}(10^{-4} \text{ s}^{-1})$
Chlorobenzene	303.2	3.69 (± 0.56)
	313.2	4.39 (± 0.87)
	323.2	4.98 (± 0.66)
	333.2	5.52 (± 0.55)
Benzene	303.2	3.32
	313.2	4.06 (± 0.69)
	323.2	5.09 (± 0.67)
	333.2	6.04 (± 1.16)
Toluene	303.2	3.04
	313.2	4.09 (± 0.92)
	323.2	4.95 (± 0.24)
	333.2	5.72 (± 0.45)

*The values in parenthesis are the standard deviation of the average rate constants.

**The single rate constant values (k_{obsd1}) are presented in Appendix D, table D3.

Table 3.4 Rate constant values (K_{obsd}) for the displacement of C_{60} from $fac-(^2-C_{60})(^2\text{phen})Cr(CO)_3$ by triphenylphosphine and tricyclohexyl phosphine in chlorobenzene at various $[L]$ and $[C_{60}]/[L]$ at 313.2 K and 500 nm

Ligand	$[L] * 10^{-3} \text{ M}$	$[C_{60}] * 10^{-4} \text{ M}$	$[C_{60}]/[L] * 10^{-1} \text{ M}$	$k_{\text{obsd}} * 10^{-4} \text{ s}^{-1}$	
PPh ₃	2.61	7.56	2.89	4.97(3)	
	2.26	12.6	5.56	4.46(3)	
	1.09	7.14	6.55	4.68(3)	
	1.13	10.0	8.85	4.38(3)	
	0.496	4.50	9.07	3.06(1)	
	2.87	1.47	0.512	4.30(3)	
	100	0	0	3.54(7)	
	1.16	0	0	5.22(3)	
	14.5	0	0	4.79(2)	
	0.351	0	0	5.38(2)	
	13.3	0	0	3.27(3)	
	P(Cy) ₃	11.5	0	0	4.80(3)
		10.3	0	0	3.70(2)
46.3		0	0	3.38(3)	
3.09		3.78	1.22	4.68(2)	
2.75		7.19	2.61	3.93(4)	
2.24		9.69	4.33	3.82(2)	
1.10		5.92	5.38	3.75(3)	

*The values given in parenthesis are the uncertainties of the last digit reported for the rate constant.

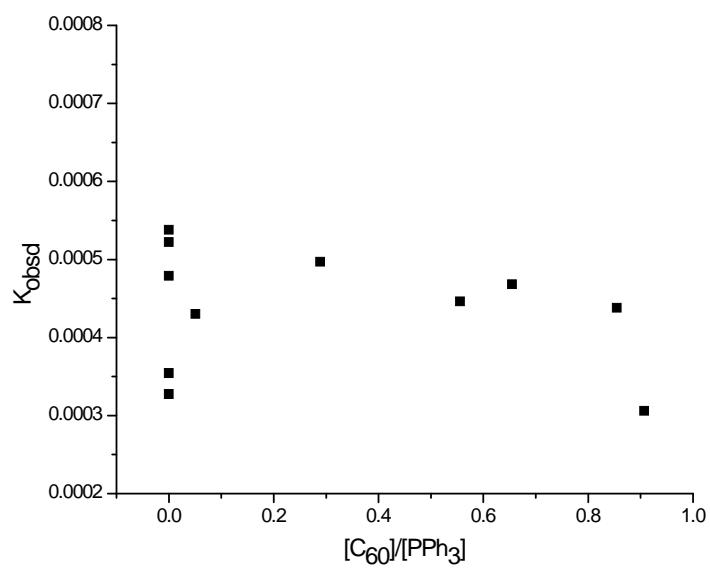


Figure 3.15 Plot of k_{obsd} versus $[C_{60}]/[PPh_3]$ for C_{60} dissociation from $fac-(^2-C_{60})(^2phen)Cr(CO)_3$ by triphenylphosphine at 313.2 K and 500 nm. The K_{obsd} values were obtained under flooding conditions, where $[C_{60}]/[PPh_3] \gg \gg [fac-(^2-C_{60})(^2phen)Cr(CO)_3]$. The plot shows that the k_{obsd} values are independent of the concentration of C_{60} and PPh_3 .

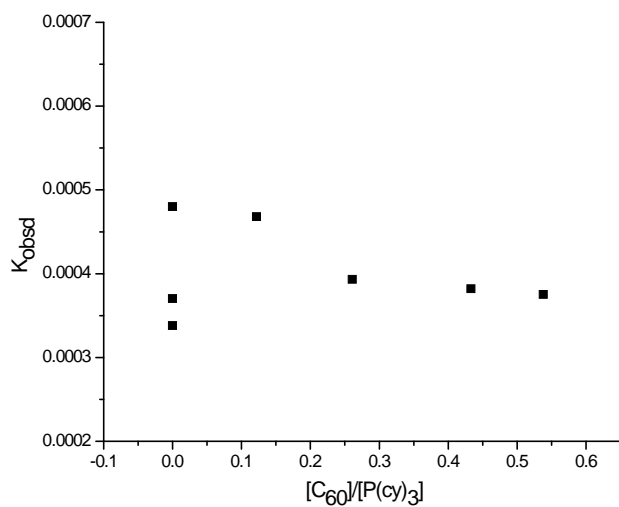


Figure 3.16 Plot of k_{obsd} versus $[C_{60}]/[P(Cy)_3]$ for C_{60} dissociation from $fac-(^2-C_{60})(^2phen)Cr(CO)_3$ by tricyclohexyl phosphine at 313.2 K and 500 nm. The K_{obsd} values were obtained under flooding conditions, where $[C_{60}]/[PPh_3] \gg \gg [fac-(^2-C_{60})(^2phen)Cr(CO)_3]$. The plot shows that the k_{obsd} values are independent on the concentration of C_{60} and PPh_3 .

The constructed Eyring plots for the displacement reactions of C_{60} from $fac-(^2-C_{60})(^2-phen)Cr(CO)_3$ by $L = PPh_3$ in chlorobenzene, benzene, and toluene are shown in figures 3.17, 3.18, and 3.19, respectively.

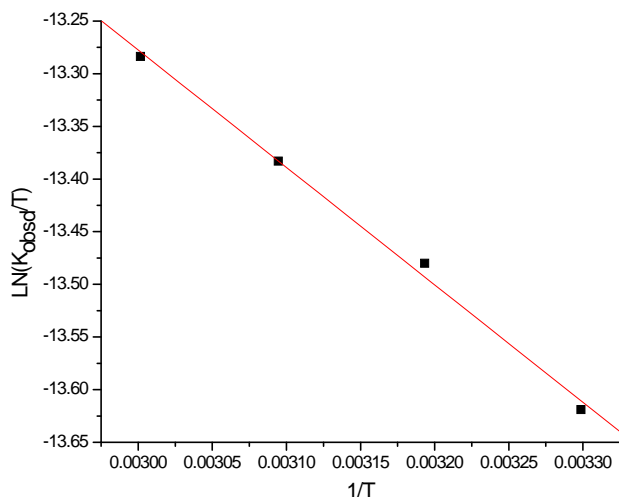


Figure 3.17 Plot of $\ln(k_{obsd}/T)$ vs. $1/T$ for C_{60} displacement from $fac-(^2-C_{60})(^2-phen)Cr(CO)_3$ in chlorobenzene by triphenylphosphine. The k_{obsd} values were obtained under flooding conditions where $[PPh_3] \gg [fac-(^2-C_{60})(^2-phen)Cr(CO)_3]$, where $H^\ddagger = 9(3)$ kJ/mol and $S^\ddagger = -280(38)$ J/K mol.

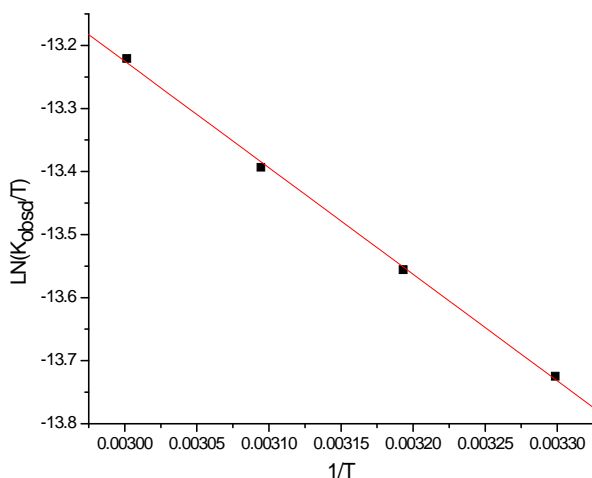


Figure 3.18 Plot of $\ln(k_{obsd}/T)$ vs. $1/T$ for C_{60} displacement from $fac-(^2-C_{60})(^2-phen)Cr(CO)_3$ in benzene by triphenylphosphine. The k_{obsd} values were obtained under flooding conditions where $[PPh_3] \gg [fac-(^2-C_{60})(^2-phen)Cr(CO)_3]$, where $H^\ddagger = 14(3)$ kJ/mol and $S^\ddagger = -265(33)$ J/K mol.

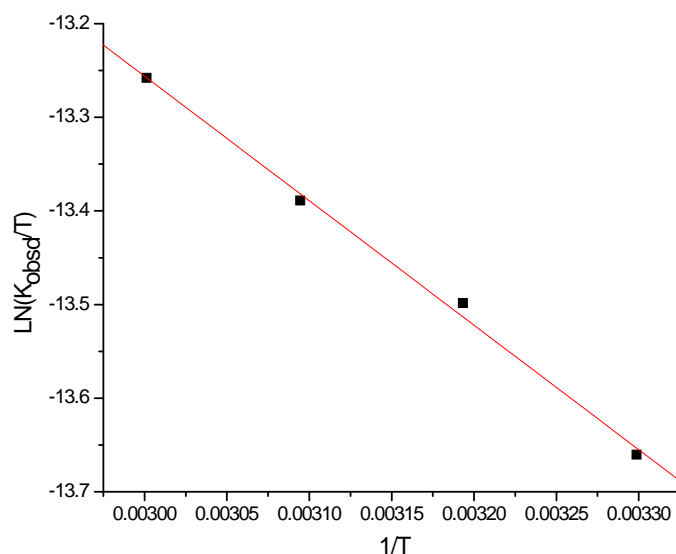


Figure 3.19 Plot of $\ln(k_{\text{obsd}}/T)$ vs. $1/T$ for the displacement of C_{60} from $fac-(^2-C_{60})(^2\text{-phen})Cr(CO)_3$ in toluene by triphenylphosphine. The k_{obsd} values were obtained under flooding conditions where $[PPh_3] \gg [fac-(^2-C_{60})(^2\text{-phen})Cr(CO)_3]$, where $H^\ddagger = 10(4)$ kJ/mol and the $S^\ddagger = -275(48)$ J/K mol.

Table 3.5 Activation Parameters values for the dissociation of C_{60} from $fac-(^2-C_{60})(^2\text{-phen})Cr(CO)_3$ by PPh_3 in chlorobenzene, benzene, and toluene. The values of enthalpy of activation can be estimated from the slope: $H^\ddagger = -R(\text{slope})$ and the values of the entropy of activation can be estimated from the intercept: $S^\ddagger = R(\text{intercept} - \ln(k_B/h))$ of the equation 3.5.

Solvent	H^\ddagger (kJ/mol)	S^\ddagger (J/K mol)
Chlorobenzene	9 (3)	-280 (38)
Benzene	14 (3)	-265 (33)
Toluene	10 (4)	-275 (48)

**The values in parenthesis are the reported uncertainties.

3.5 Discussion

The Lewis bases (L) piperidine (pip), triphenyl phosphine (PPh₃), and tricyclohexyl phosphine (P(Cy)₃) displace C₆₀ from *fac*-(²-C₆₀)(²-phen)Cr(CO)₃ to produce *fac*-(¹-L)(²-phen)Cr(CO)₃, as an intermediate species, and (¹-L)₃Cr(CO)₃ as a product of the reaction. Kinetic experiments were limited and to established the mechanistic pathway, it was assumed that *fac*-(¹-pip)(²-phen)Cr(CO)₃ was the product of reaction and not an intermediate species.

The k_{obsd} values are independent of chemical nature of L, [L] and of [C₆₀]/[L]. These observations suggest that L is not involved in the steps contributing to the k_{obsd} values. The proposed mechanism (figure 3.20) was reported for the molybdenum analogous and it is being adopted here for the reactions under study. This mechanisms involves a solvent-assisted C₆₀ displacement producing *fac*-(solvent)(²-phen)Cr(CO)₃ as an intermediate species (I_A). Assuming that the concentration of this intermediate species, I_A, is at steady-state concentration, this mechanism predicts the following rate-law (equations 3.6 and 3.7).

$$-\frac{d[S]}{dt} = k_{obsd}[S] \quad \text{Equation (3.6)}$$

Where S = substrate = *fac*-(²-C₆₀)(²-phen)Cr(CO)₃ and the value of K_{obsd} is given by:

$$k_{obsd} = \frac{k_1 k_2 [L]}{k_{-1} [C_{60}] + k_2 [L]} \quad \text{Equation (3.7)}$$

The observation that k_{obsd} values are [L] independent is in accord with the approximation that

$k_{-1}[C_{60}] \ll k_2[L]$ and equation 3.7 becomes:

$$k_{obsd} \approx k_1 \quad \text{Equation (3.8)}$$

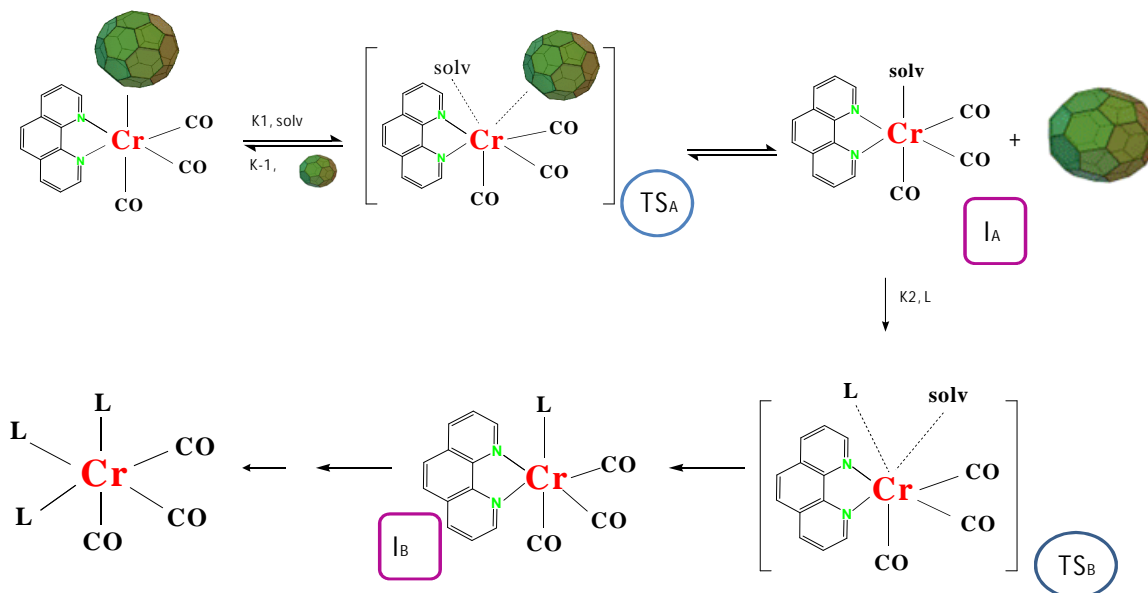


Figure 3.20 Proposed mechanisms for C_{60} displacement from $fac-(^2-C_{60})(^2-phen)Cr(CO)_3$. The mechanism describes a solvent assisted displacement of C_{60} . I_A and I_B are steady-state intermediates. TS_A and TS_B are plausible transition states.

Since the concentration of $[C_{60}]$ can be experimentally controlled when $L = PPh_3$ and $P(Cy)_3$, the rate constant values were determined under conditions where $0 < [C_{60}]/[L] < 1$. The observation that k_{obsd} values are independent of $[C_{60}]$ and of $[C_{60}]/[L]$, demonstrate, that $k_{-1} \ll k_2$. The high selectivity of the intermediate species ($k_{-1} \ll k_2$)^{15,22,29-30} and the activation parameters for the reactions of $fac-(^2-C_{60})(^2-phen)Cr(CO)_3$ with $L = PPh_3$ in chlorobenzene ($H^\ddagger = 9(3) \text{ kJ/mol}$, $S^\ddagger = -280(38) \text{ J/Kmol}$) indicate that the rupture $Cr-C_{60}$ bond in $fac-(^2-C_{60})(^2-phen)Cr(CO)_3$ is assisted by the solvent and that the TS_1 involves a concerted solvent- Cr bond making and $C_{60}-Cr$ bond breaking. The same results were observed for the reactions of $fac-(^2-C_{60})(^2-phen)Cr(CO)_3$ with $L = PPh_3$ in benzene and toluene. The role of the solvent in the ligand exchange reactions of metal carbonyl complexes have been previously reported.³¹⁻³⁷ Aromatic solvents may interact with the substrate and intermediate species through an

olefinic linkage³¹⁻³³, agnostic linkage,^{35,36} or a lone pair (in halogenated solvents).³⁴ The coordinated solvent may undergo a “chain walk” isomerization to attain the most stable mode of coordination³¹⁻³².

The k_{obsd} value depends on the nature of the solvent; activation parameters reflect a variation from solvent to solvent and the fact that k_{obsd} values for the reactions of *fac*-(η^2 -C₆₀)(η^2 -phen)Cr(CO)₃ with L = PPh₃ were almost the same at 323.2 K in chlorobenzene, benzene, and toluene (table 3.5) suggest that an isokinetic temperature should be observed. Figure 3.21 presents the plots of $\ln(k_{\text{obsd}}/T)$ vs. $1/T$ for the reactions in chlorobenzene (), benzene () and Toluene (). Activation parameters for these plots are presents in table 3.5. Notice that smaller H^\ddagger values are associated with more negative S^\ddagger values, indicative of an isokinetic point. In fact figure 3.21 shows a common region of intersection for all the plots.

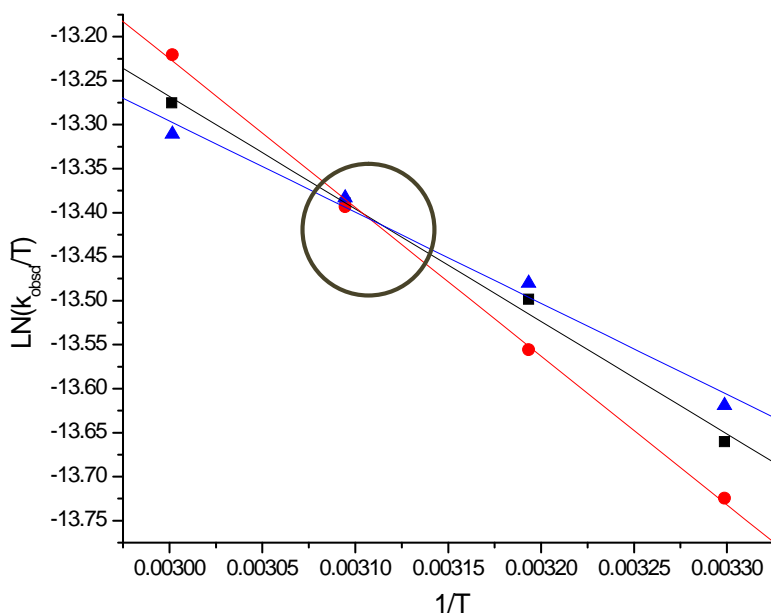


Figure 3.21 Plot of $\ln(k_{\text{obsd}}/T)$ vs. $1/T$ showing the isokinetic region in the vicinity of 323.2K for the solvent-assisted C_{60} displacement from *fac*-(η^5 - C_{60})(η^5 -phen)Cr(CO)₃ in chlorobenzene (), benzene () and Toluene () by tri-phenylphosphine. The k_{obsd} values were obtained under flooding conditions where $[PPh_3] \gg [(\eta^5-C_{60})(\eta^5\text{-phen})Cr(CO)_3]$.

This common point of intersection, in the vicinity of 323.2 K, corresponds to the isokinetic temperature or the temperature where the rate constant values are the same for all reactions in different solvents. The existence of an isokinetic temperature with chemical or physical meaning has been addressed elsewhere.^{15,30} Often, the common intersection occurs at temperatures experimentally-inaccessible and the uncertainty of the intersection is large. In the present study, the isokinetic temperature was experimentally accessible ($T_{\text{iso}} = 323.2$ K). This suggests that regardless of the variation of the activation parameters and rate constant values, the L/ C_{60} exchange takes place via a common mechanism.

Chapter IV

Profile of the ligand displacement reactions of *fac*-(η^2 -C₆₀)(η^2 -phen)M(CO)₃ (M = W, Mo and Cr)

4.1 Materials and Methodology

4.1.1 General

Electrochemical studies were performed at room temperature and at a low pressure atmosphere using a BAS CV-50W™ potentiostat. A high vacuum line (figure 4.1) was used to transfer and mix reagents. Dichloromethane was used as a solvent for all electrochemical experiments.

Tetrabutylammoniumhexafluorophosphate (TBPF₆) was used as a supporting electrolyte in all electrochemical measurements. The supporting electrolyte was recrystallized from an ethanol/H₂O (95:5) mixture and dried in vacuo prior to use. Decamethylferrocene (Fc)/ decamethylferrocenium (Fc⁺) couple was used as internal standard in all measurements.

A three-electrode configuration was used consisting of a glassy carbon working electrode (3 mm in diameter), a platinum wire (Pt-wire) counter electrode, and a non-aqueous silver wire in contact with a solution of approximately 0.01M TBPF₆ in CH₂Cl₂ separated from the bulk solution by a fine glass frit as pseudo reference electrode. The working electrode was polished before use with a 0.25 μm diamond polishing compound (Metadi II) and a microcloth (BAS). The Pt-wire was cleaned by exposing it to a flame for approximately 30 seconds, and the silver wire was rinsed with acetone and deionized water to remove impurities.

The electrochemical cell that was used in all electrochemical experiments was custom made. The cell contained two special arm adapters (figure 4.2), which allowed sequential mixing. The sample of the species that was to be studied was placed in one of the arm adapters (the enough amount to obtain a solution of approximately 0.5 mM to 1.0 mM in 3 mL) and ferrocene was placed in the other arm adapter.

In a typical electrochemical experiment, the supporting electrolyte is placed in the cell (ca. 0.12 g of TBPF6).

In order to remove moisture from the supporting electrolyte and the cell, the cell containing the electrolyte was heated with a heat gun for five seconds. This process was repeated until the supporting electrode was dry. The cell was then opened to the vacuum line (10^{-5} to 10^{-6} mmHg) for roughly 10 minutes. Approximately 3 mL of dichloromethane were transferred to the cell directly through the vacuum line. After direct solvent transfer was accomplished, the whole ensemble was disconnected from the vacuum line and allowed to warm at room temperature. Electrochemical measurements were obtained while the cell was kept at the equilibrium vapor pressure of the solvent. The solution was stirred between scans using a magnetic stir bar controlled by a stirring motor located beneath the electrochemical cell. The background voltammogram of the solvent and supporting electrolyte was recorded prior to the electrochemical measurement of the sample. All cyclic voltammograms, unless otherwise specified, were run at a scan rate of 100 mV/s.

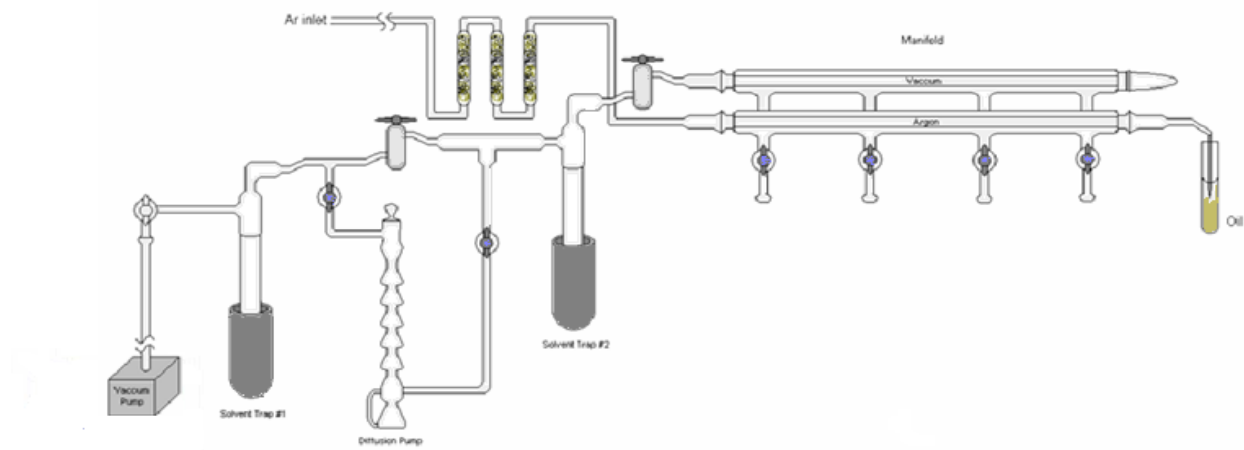


Figure 4.1 Schematic representation of the vacuum line used to transfer and mix reagents in electrochemical runs.²⁰

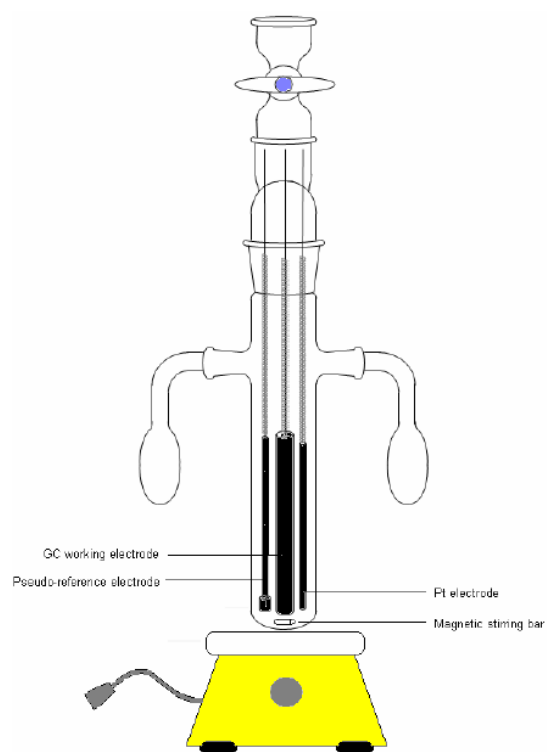


Figure 4.2 Electrochemical cell with a three-electrode configuration used for electrochemical runs.^{19,20}

4.1.2 Preparation of *fac*-(²-C₆₀)(²-phen)Mo(CO)₃

The complex *fac*-(²-C₆₀)(²-phen)Mo(CO)₃ was prepared photochemically following a published procedure,¹⁵ which uses (²-phen)Mo(CO)₄ and C₆₀. In a 100 mL round bottomed flask equipped with a magnetic stirring bar, a condenser, and a nitrogen inlet; 0.02508 g (0.123 mmol) of (²-phen)Mo(CO)₄ and 0.03784 g (0.053 mmol) of C₆₀ were dissolved in 15 mL of dried toluene followed by irradiation with the medium pressure mercury arc lamp under nitrogen during approximately 1.5 hours. After the reaction was completed, judging by the infrared spectrum, toluene was nitrogen-purged from the reaction mixture. The resulting brownish solid was then dissolved in approximately 10 mL of carbon disulfide (CS₂). Thin layer chromatography analysis showed two components. The two components were separated by column chromatography using a 15 cm long (1.0 cm diameter) column packed with 62 grades, 60-2000 mesh, 150 Å silica gel. The first component identified as unreacted C₆₀ was eluted using CS₂. The remaining component was isolated by dissolving the contents of the chromatography column in 10 mL of dichloromethane followed by suction filtration. Dichloromethane was then nitrogen purged, the yellowish-brown solid was characterized as *fac*-(²-C₆₀)(²-phen)Mo(CO)₃ from its CO absorbencies in chlorobenzene (ν_{CO}, cm⁻¹): 1971, 1896, and 1829.

4.1.3 Preparation of *fac*-(η^2 -C₆₀)(η^2 -phen)W(CO)₃

The complex *fac*-(η^2 -C₆₀)(η^2 -phen)W(CO)₃ was prepared thermally, following a published procedure.¹⁴ In a 100 mL round-bottomed flask equipped with a magnetic stirring bar, a condenser, and a nitrogen inlet; 0.02648 g (0.089 mmol) of (η^2 -phen)W(CO)₄ and 0.04011 g (0.056 mmol) of C₆₀ were dissolved in 15 mL of dried chlorobenzene. The resulting reddish solution was stirred under nitrogen and refluxed for 90 min. During reflux the solution turned brown. The progress of the reaction was monitored by observing and recording the decrease of the CO (cm⁻¹): 2003, 1889, 1872, and 1835 and the increase of the band intensities at 1966, 1889, and 1822, corresponding to (η^2 -phen)W(CO)₄ and *fac*-(η^2 -C₆₀)(η^2 -phen)W(CO)₃ complexes, respectively. After the reaction was complete, judged by the infrared spectrum, chlorobenzene was nitrogen purged directly into the mixture. The reddish-brown solid was then dissolved in approximately 10 mL of carbon disulfide. Thin layer chromatography analysis showed three components. The three fractions were separated by column chromatography using a 15 cm long (1 cm diameter) column packed with 62 grade, 60–2000 mesh, 150 silica gel. The first fraction was eluted using CS₂ and contained unreacted C₆₀. The other two fractions were eluted with chlorobenzene. The first of the two fractions eluted with chlorobenzene was identified as *fac*-(η^2 -C₆₀)(η^2 -phen)W(CO)₃. The second fraction was identified as (η^2 -phen)W(CO)₄. The CO of *fac*-(η^2 -C₆₀)(η^2 -phen)W(CO)₃ in dichloromethane showed three bands: (CO, cm⁻¹): 1966, 1890, and 1823.

4.2 Data Analysis

The cyclic voltammogram of the complexes $fac-(^2-C_{60})(^2-phen)M(CO)_3$ (where $M = Cr, Mo$ and W) in dichloromethane, are shown in Figure 4.4 to 4.6. The reversible waves half peak potentials ($E_{1/2}$) are calculated relative to the potential of ferrocene/ferrocenium (Fc/Fc^+) which was used as internal standard. Let's consider the case of $fac-(^2-C_{60})(^2-phen)Cr(CO)_3$ in Figure 4.3.

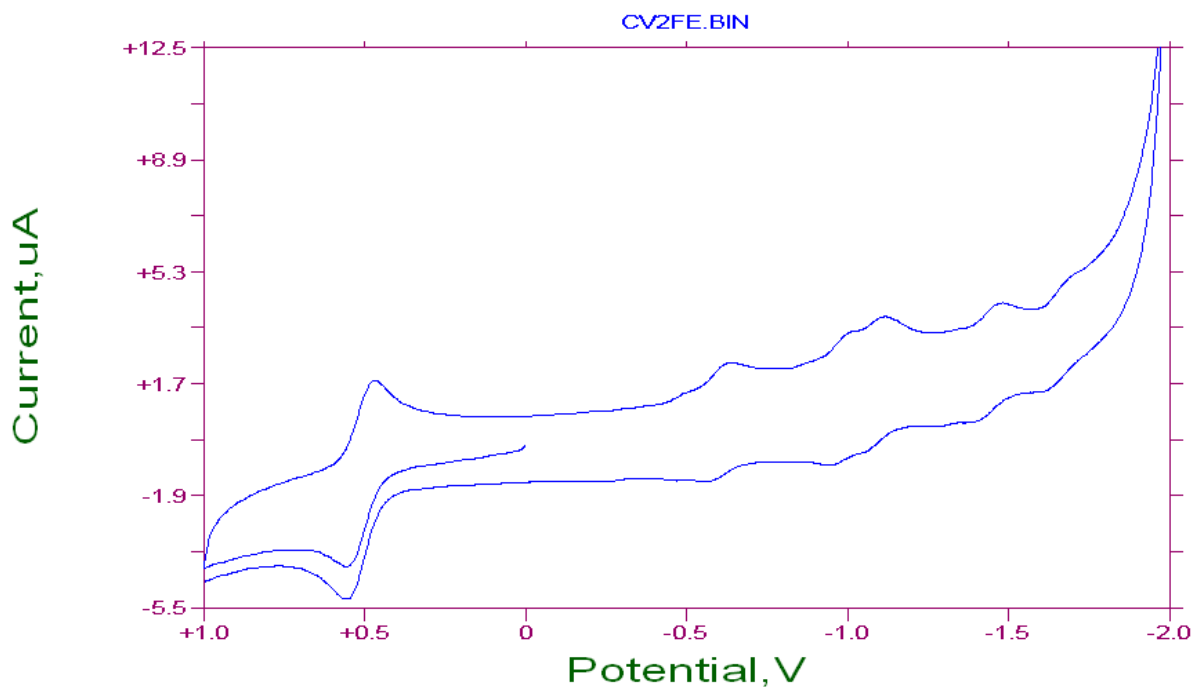


Figure 4.3 Cyclic voltammetric responses recorded at a glassy carbon working electrode on dichloromethane solution containing, 0.1M TBPF6, $fac-(^2-C_{60})(^2-phen)Cr(CO)_3$ (saturated solution), and traces of dexamethylferrocene (Fc) scan rate 100 mV/s. The $E_{1/2}$ for Fc/Fc^+ is 515mV. The $E_{1/2}$ for $fac-(^2-C_{60})(^2-phen)Cr(CO)_3$ are -1110, -1547 and -1933 mV and 2172 mV vs. Fc/Fc^+ . $T = 20\text{ }^\circ\text{C}$

In order to determine the internal standard potential ($STD E_{1/2}$) Fc/Fc^+ one must take the sum of the reduction potential (E_{red}) and the oxidation potential (E_{ox}) and divide the sum by two:

$$E_{1/2}^{std} = \frac{E_{red} + E_{ox}}{2}$$

Equation 4.1

In order to calculate each reversible one-electron reduction waves vs. Fe/Fe^+ the equation used is:

$$E_{1/2}^n = \frac{E_{red} + E_{ox}}{2} - E_{1/2}^{std}$$

Equation 4.2

Difference from equations 4.1 and 4.2 allow the calculation of the one-electron reduction waves, relatives to Fe/Fe^+ .

4.3 Results

The half peak potentials of $fac-(^2-C_{60})(^2-phen)M(CO)_3$ ($M = Cr, Mo, W$) and C_{60} are given in Table 4.1 and their corresponding cyclic voltammograms are shown in Figures 4.4 to 4.6. The cyclic voltammogram of the complex $fac-(^2-C_{60})(^2-phen)Cr(CO)_3$ in dichloromethane, shown in Figure 4.4, exhibits five reversible one-electron reduction waves corresponding to the formation of $fac-(^2-C_{60})(^2-phen)Cr(CO)_3^-$, $fac-(^2-C_{60})(^2-phen)Cr(CO)_3^{2-}$, $fac-(^2-C_{60})(^2-phen)Cr(CO)_3^{3-}$ and $fac-(^2-C_{60})(^2-phen)Cr(CO)_3^{4-}$ and $fac-(^2-C_{60})(^2-phen)Cr(CO)_3^{5-}$ respectively. The reversible waves have peak potentials ($E_{1/2}$) at -1110, -1547, -1603, -1933, and -2172 mV, relative to the potential of ferrocene/ferrocenium (Fc/Fc+), which was used as internal standard.

The cyclic voltammogram of the complex $fac-(^2-C_{60})(^2-phen)Mo(CO)_3$ in dichloromethane, shown in Figure 4.5, exhibits four reversible one-electron reduction waves corresponding to the formation of $fac-(^2-C_{60})(^2-phen)Mo(CO)_3^-$, $fac-(^2-C_{60})(^2-phen)Mo(CO)_3^{2-}$, $fac-(^2-C_{60})(^2-phen)Mo(CO)_3^{3-}$ and $fac-(^2-C_{60})(^2-phen)Mo(CO)_3^{4-}$, respectively. The reversible waves have peak potentials ($E_{1/2}$) at -1323, -1909, -2456 mV, and -271 mV relative to the potential of ferrocene/ferrocenium (Fc/Fc+), which was used as an internal standard.

The complex $fac-(^2-C_{60})(^2-phen)W(CO)_3$ exhibits three reversible one-electron reductions waves. The peak potentials ($E_{1/2}$) are located at -1189, -1485, and -2183 mV relative to the potential of ferrocene/ferrocenium (Fc/Fc⁺) (Figure 4.6).

The previously reported cyclic voltammogram of C_{60} under same conditions shows three reversible reductions.¹⁹ The potential values of the complexes $fac-(^2-C_{60})(^2-phen)M(CO)_3$ (were $M = Cr, W,$ and Mo) were shifted to more negative potentials relative to the corresponding potentials of the uncoordinated C_{60} .

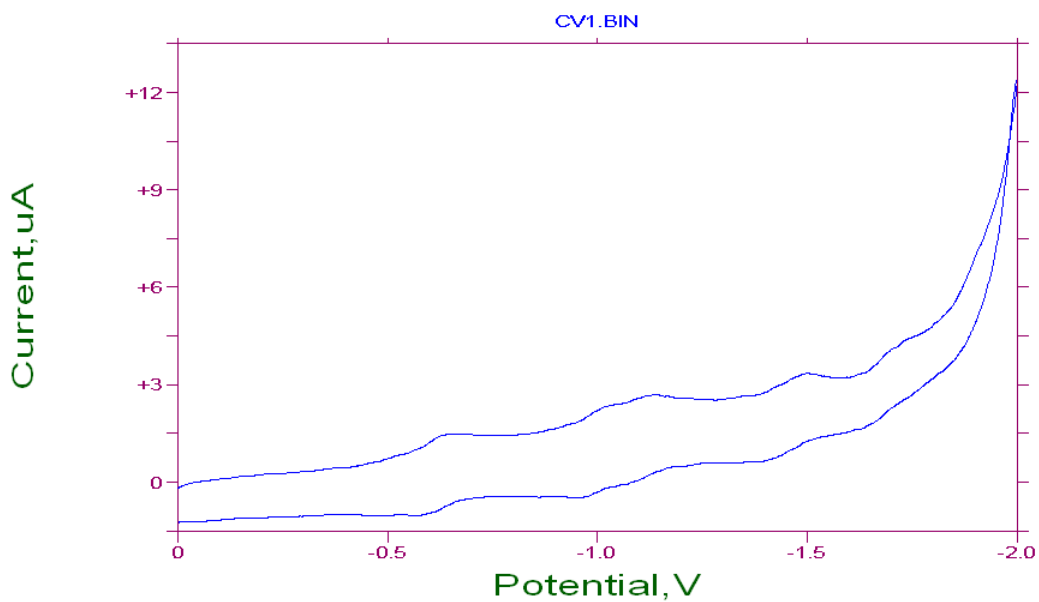


Figure 4.4 Cyclic voltammetric responses recorded at a glassy carbon working electrode on dichloromethane solution containing, 0.1 M TBPF6, *fac*-(η^5 -C₆₀)(η^2 -phen)Cr(CO)₃ (saturated solution), and traces of decamethylferrocene (Fc) scan rate 100 mV/s.

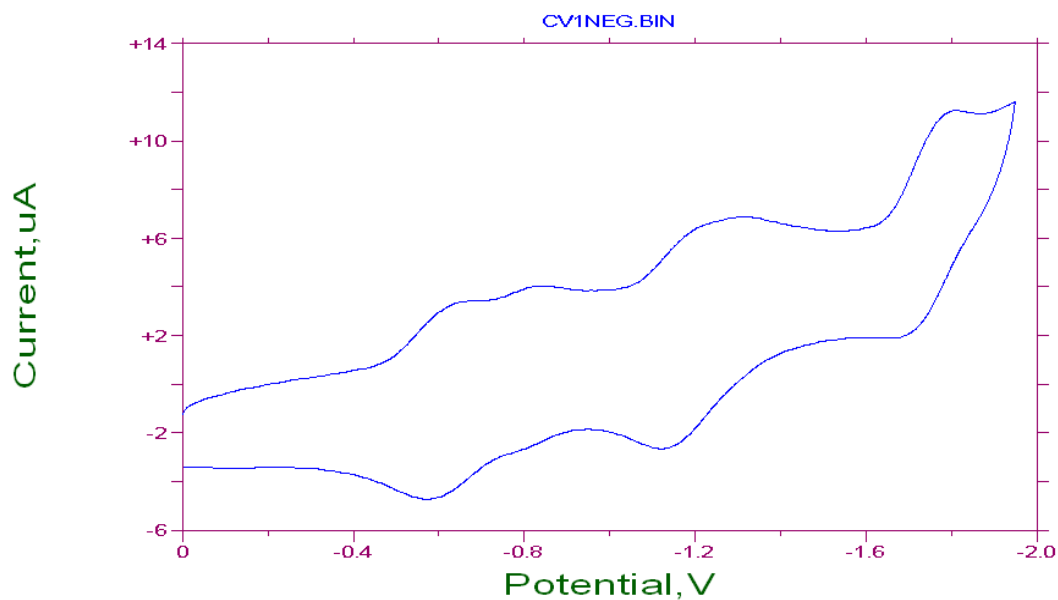


Figure 4.5 Cyclic voltammetric responses recorded at a glassy carbon working electrode on dichloromethane solution containing, 0.1 M TBPF6, *fac*-(η^5 -C₆₀)(η^2 -phen)Mo(CO)₃ (saturated solution), and traces of decamethylferrocene (Fc) scan rate 100 mV/s.

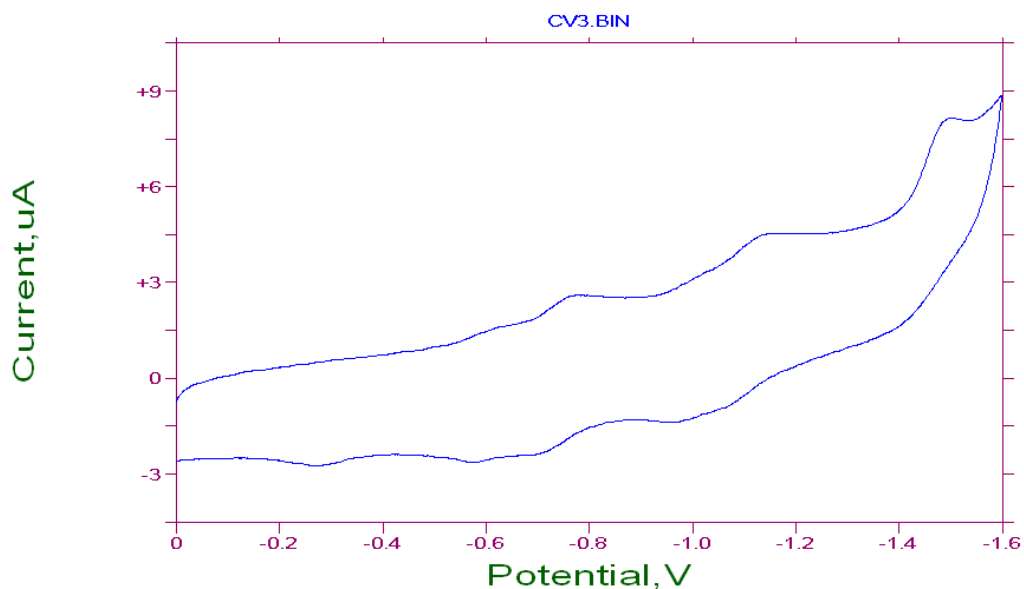


Figure 4.6 Cyclic voltammetric responses recorded at a glassy carbon working electrode on dichloromethane solution containing, 0.1 M TBPF6, *fac*-(²⁻C₆₀)(²⁻phen)W(CO)₃ (saturated solution), and traces of decamethylferrocene (Fc) scan rate 100 mV/s.

Table 4.1: Half-wave potentials ($E_{1/2}$) of the *fac*-(²⁻C₆₀)M(CO)₃ complexes (M = Cr, Mo and W) and C₆₀ in dichloromethane at room temperature.

Complexes	$E^1_{1/2, \text{red}}$ (mV)	$E^2_{1/2, \text{red}}$ (mV)	$E^3_{1/2, \text{red}}$ (mV)	$E^4_{1/2, \text{red}}$ (mV)	$E^5_{1/2, \text{red}}$ (mV)
**C ₆₀	-998	-1391	-1860		
<i>fac</i> -(²⁻ C ₆₀)(²⁻ phen)Cr(CO) ₃	-1110	-1547	-1603	-1933	-2172
<i>fac</i> -(²⁻ C ₆₀)(²⁻ phen)Mo(CO) ₃	-1323	-1909	-2456	-2711	
<i>fac</i> -(²⁻ C ₆₀)(²⁻ phen)W(CO) ₃	-1189	-1485	-2183		

All half wave potential are in mV vs. Fc/Fc+ at 100 mV/s scan rate.

** Previously reported values found in reference 19

4.4 Discussion

The Lewis bases (L) piperidine (pip), triphenyl phosphine (PPh₃), and tricyclohexyl phosphine (P(Cy)₃) displace C₆₀ from *fac*-(²-C₆₀)(n²-phen)M(CO)₃ to produce *fac*-(²-phen)(n¹-L)M(CO)₃ and *fac*-(¹-L)₃M(CO)₃, which depends on M. The progress of the reactions was followed by observing the change of absorbance values at various wavelengths, depending on M and entering ligand (L). The reactions were also monitored by observing the carbonyl stretching region from 1700 to 2100 cm⁻¹ to establish the nature of non-steady-state intermediate species and products. For example, the reactions of *fac*-(²-phen)(²-C₆₀)W(CO)₃ produced *fac*-(²-phen)(¹-L)W(CO)₃ as the only product. The plots of absorbance vs. time are monophasic, where k_{obsd} is independent of L and [L] when [C₆₀] <<< [L]; but dependent of the solvent nature and [C₆₀], when 0 < [C₆₀]/[L] < 1. Activation parameters suggest that the displacement of C₆₀ takes place via an initial solvent-assisted dissociation of C₆₀ when the solvent is benzene, but also the activation parameters and competition ratios values support a dissociative displacement of C₆₀ for the reactions in chlorobenzene and toluene¹⁴.

In the case of M = Mo, the formation of *fac*-(²-phen)(¹-L)Mo(CO)₃ was followed by thermal decomposition and the plots of absorbance vs. time are biphasic. The k_{obsd} is independent from L, [L] and of [C₆₀]/[L] but dependent on the solvents nature. Activation parameters suggest that the displacement of C₆₀ take place via an initial solvent-assisted dissociation of C₆₀. Eyring plots also show an isokinetic temperature in the vicinity of 323.2 K (figure 4.7).

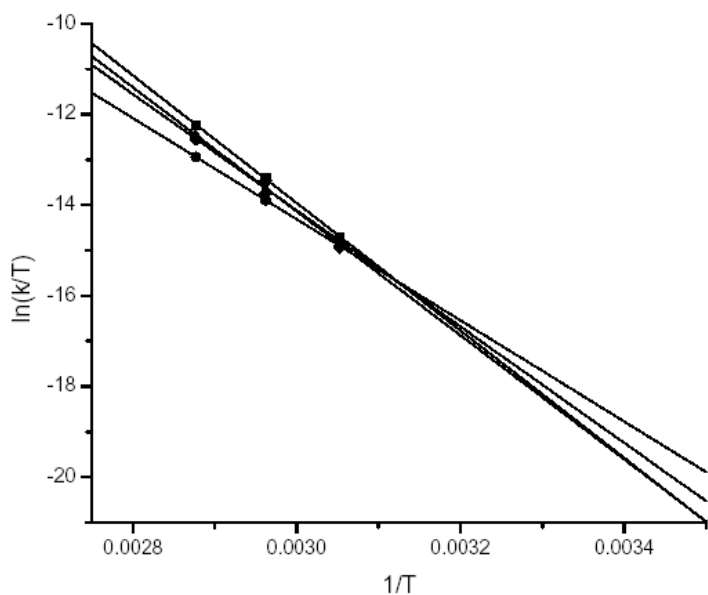


Figure 4.7 Plots of $\ln(k/T)$ vs. $1/T$ showing the isokinetic region for the solvent-assisted C_{60} displacement from $fac-(2-C_{60})(2-phen)Mo(CO)_3$ in chlorobenzene (), toluene (), bromobenzene (), and benzene ().^{15,19}

Interestingly, the complex $fac-(2-C_{60})(2-phen)Cr(CO)_3$ also exhibits an isokinetic temperature in the vicinity of 323.2 K, but the fact that the complex $fac-(2-C_{60})(2-phen)W(CO)_3$, does not exhibit an isokinetic temperature opens an interrogative regarding the behavior of the Eyring plots for the three complexes. The figure 4.8 presents the plots of $\ln(k_{obsd}/T)$ vs. $1/T$ for the complexes $fac-(2-C_{60})(2-phen)M(CO)_3$ (where $M = W, Mo$ and Cr).

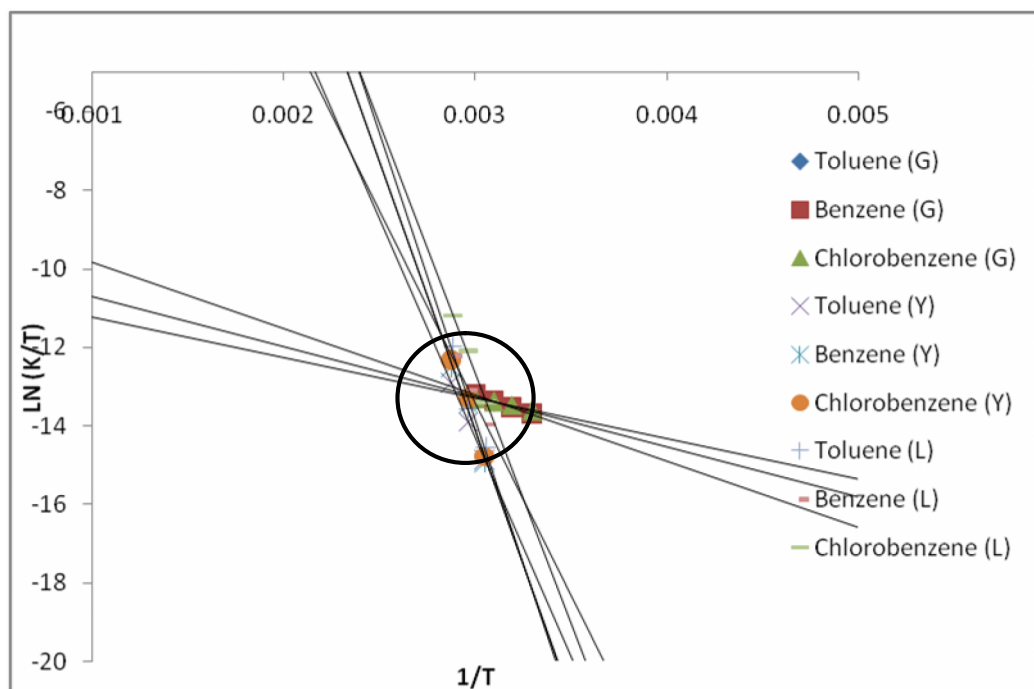


Figure 4.8 Plots of $\text{LN}(k_{\text{obsd}}/T)$ versus $1/T$ showing the isokinetic region for the solvent-assisted C_{60} displacement from the complexes $\text{fac}-(2\text{-C}_{60})(2\text{-phen})\text{M}(\text{CO})_3$ (where $\text{M}=\text{Cr}, \text{W}$ and Mo) in toluene, benzene and chlorobenzene

The fact that the plots of the complexes $\text{fac}-(2\text{-C}_{60})(2\text{-phen})\text{M}(\text{CO})_3$ ($\text{M} = \text{Mo}$ and Cr) present a common region of interception in the vicinity of 323 K; confirms the existence of an isokinetic temperature, but because the complex $\text{fac}-(2\text{-C}_{60})(2\text{-phen})\text{W}(\text{CO})_3$ passes through this common region it confirms that not only we were working on an isokinetic temperature, in fact we were working on an isokinetic region. For that reason, regardless of the variation on the activation parameters, constant values and also of the complex involved ($\text{M} = \text{Mo}, \text{W}$ or Cr) the L/C_{60} exchange reactions would take place via a common mechanism.

Chapter V

Conclusion

The Lewis bases (L): piperidine (pip), triphenyl phosphine (PPh₃) and tricyclohexyl phosphine (P(Cy)₃) displace [60] fullerene (C₆₀) from *fac*-(²-C₆₀)(²-phen)M(CO)₃ to produce *fac*-(²-phen)(¹-L)M(CO)₃ and *fac*-(¹-L)₃M(CO)₃, depending on M. The progresses of the reactions were followed by observing the change of absorbance values at various wavelengths, depending on M and entering ligand (L). The reactions were also monitored by observing the stretching carbonyl region from 1700 to 2100 cm⁻¹ to establish the nature of non-steady-state intermediate species and products.

The reactions of *fac*-(²-phen)(²-C₆₀)W(CO)₃ produced *fac*-(²-phen)(¹-L)W(CO)₃ as the only product. For M = Mo, the formation of *fac*-(²-phen)(¹-L)Mo(CO)₃ was followed by thermal decomposition. For, M = Cr, the formation of *fac*-(²-phen)(¹-L)Cr(CO)₃ was followed displacement of phenantroline producing *fac*-(¹-L)₃Cr(CO)₃. For example, plots of absorbance vs. time were biexponential for reactions under flooding conditions, where [pip] >>> [*fac*-(²-C₆₀)(²-phen)Cr(CO)₃]. The plots of absorbance vs. time consisted of two consecutive segments. The first segment (increasing) of the plot was assigned to step-wise additions of piperidine to uncoordinated C₆₀. The second segment (decreasing) was ascribed to the displacement of C₆₀ from *fac*-(²-C₆₀)(²-phen)Cr(CO)₃.

The dissociation of C₆₀ is solvent-assisted. The activation parameter values, the high selectivity of the intermediate species, the non-dependence of k_{obsd} values on the nature of L and [L], the dependence of k_{obsd} values on the nature of the solvent support, to some degree, the conclusion that was reached. This was that the solvent–Cr bond formation in the TS₁ leads to the formation of *fac*-(solvent)(²-phen)Cr(CO)₃.

The observation of an experimentally-accessible isokinetic temperature suggests that the seemingly different mechanistic path for the systems investigated, is actually limiting case of the general mechanism.

The reduction and oxidation potentials of the metal-fullerene complexes studied in this work seem to depend on (i) the extent of π -back donation between C_{60} and (ii) the degree of distortion of the spherical surface of C_{60} upon coordination. The extent of π -back donation favors negative potential shifts relative to uncoordinated C_{60} .

5.2 Future works

Following the investigations described in this thesis, a number of projects could be taken up, involving the modified infrared and kinetics studied:

1. It would be interesting to obtain information on:
 - a. The bond distance of M-C₆₀ and M-benzene on the complexes *fac*-(²-C₆₀)(²-phen)M(CO)₃ (M = C, W, Mo).
 - b. The energy of M-C₆₀ and M-benzene on the complexes *fac*-(²-C₆₀)(²-phen)M(CO)₃ (M = C, W, Mo).

These studies will contribute to our efforts in obtain further comprehension on these systems and establish a better explanation of the solvent-assisted mechanism for the displacement of C₆₀ from the complexes *fac*-(²-C₆₀)(²-phen)M(CO)₃ (M = C, W, Mo).

References

1. Krätschmer, W.; Lamb, L. D.; Fostiropoulos, K; Huffman, D. R. *Nature* **1990**,347, 354. Bürgi, H. B.; Blanc, E.; Schwarzenbach, D.; Liu, S.; Lu, Y.; Kappes, M. M.; Ibers, J. *Angew. Chem., Int. Ed. Engl.* **1992**, 31, 640. Satpathy, S. *Chem.Phys. Lett.* **1986**, 130, 545. Hawkins, J. M; Meyer, A.; Lewis, T. A.; Loren, S.; Hollander, F. J., *Science* **1991**, 252, 313.
2. Zanello P.; Laschi F.; Fontani M.; Mealli C.; Ienco A.; Tang K.; Jin X.; Li L., *J. Chem. Soc., Dalton Trans.*, 1999, 965–970.
3. Isobe, H.; Tomita, N.; Nakamura, E. *Org. Lett.*, **2000**, 2, 3663-3665.
4. Modin, J.; Johansson, H. Grennberg, H. *Org. Lett.*, **2005**, 7, 3977 -3979.
5. Kroto, H. W., Heath, J. R.; O'Brien, S. C.; Curl, R. F.; Smalley, R. E. *Nature*, **1985**, 318, 162-3.
6. Ruoff, R.S.; Tse, D. S.; Malhotra, R.; Lorents, D.C. *J. Phys. Chem.*, **1993**, 91, 3379-3383.
7. Fukami T., Mugishima A., Suzuki T., Hidaka S., Endo T., Ueda H., Tomono K., *Chem. Pharm. Bull.* **2004**. 52(8) 961—964.
8. Miki S., Kitao M. and Fukunishi K, *Tet. Lett.*, **1996**, 37: 2049-2052.
9. Tamisier-Karolak S., Pagliarusco S., Herrenknecht C., Brettreich M., Hirsch A., Céolin R., Bensasson R.V., Szwarc H., Moussa F., *Electrophoresis* **2001**, 22, 4341–4346.
10. Tegos, G.; Demidova, T.; Arcila-Lopez, D.; Lee, H.; Wharton, T.; Gali, H.; Hamblin, M. *Chem. & Biol.*, **2005**, 12, 1127-1135.
11. Tumanskii B.L., Bashilov V.V., Kalina O.G, Sokolov V.I., *J. Organomet. Chem.* **2000**, 599: 28–31.
12. Lerke, S.A., Parkinson, B.A., Evans, D.H., Fagan, P.J., *J. Am. Chem. Soc.*, **1992**, 114, 7807.
13. Chernega A.N., Green H., Haggitt J., Stephens H.H., *J. Chem. Soc. Dalton Trans.* **1998**, 755.
14. Rivera-Rivera, L. A.; Crespo-Román, G.; Acevedo-Acevedo, D.; Ocasio-Delgado, Y.; Cortés-Figueroa, J. E. *Inorg. Chim. Acta*, **2004**, 357, 881-887.

15. Ocasio-Delgado, Y., De Jesus-Segarra, J.; Cortés-Figueroa, J. E., *J. Organomet. Chem.* **2005**, 690, 3366–3372.
16. Hsu, H.F., Du, Y., Albrecht-Schmitt, T.E., Wilson, S.R., Shapley, J.R., *Organometallics* **1998**, 17, 1756.
17. Song, L.-C., Zhu, Y.-H., Hu, Q.-M. *Polyhedron*, **1997**, 16, 72, 2141.
18. Capella-Capella, C., Thesis M.S. University of Puerto Rico, Mayagüez, P.R. May 2008.
19. Ocasio-Delgado, Y. Thesis M.S. University of Puerto Rico, Mayagüez, Jul 2005.
20. Igartua-Nieves, E. Thesis MS. University of Puerto Rico at Mayagüez, Jul 2006.
21. Perrin, L. Maron, O. Eisentein, L.F. Lapert. *New J. Chem*, **2003**, 27, 121–127.
22. Ocasio-Delgado, Y., Rivera-Rivera, L.A., Crespo-Roman, G., Cortés-Figueroa, J.E., *Inorg. React. Mech.* **2003**, 5, 13-19.
23. Igartúa-Nieves, E.; Ocasio-Delgado, Y.; Cortés-Figueroa, J. E. *J. Coord. Chem.*, **2007**, 60, 449-456.
24. Balch A.L., Hao L., Olmstead M.M, *Angew. Chem., Int. Ed. Engl.* **1996**, 35, 188.
25. Fagan P.J., Calabrese J.C, Malone B., *Science* **1991**, 252, 1160.
26. Balch A. L., Costa D.A., Olmstead M.M., *Chem. Commun.*, **1996**, 2449; H.-F. Hsu, S. R. Wilson and J. R. Shapley, *Chem. Commun.*, **1997**, 1125.
27. Igartúa-Nieves, E.; Ocasio-Delgado, Y.; Torres-Castillo, María D. L. A.; Rivera- Betancourt, O.; Rivera-Pagán, J. A.; Rodriguez, D.; López, G. E.; Cortés- Figueroa, J. E. *Dalton Trans.* **2007**, 1293-1299.
28. Langford, C.H., Moralejo, C., Sharma, D.K., *Inorg. Chim. Acta* 126, **1987**, L11.
29. Yang, G.K., Vaida, V., Peters, K.S., *Polyhedron* 7, **1989**, 1619.
30. McBane, G.C., *J. Chem. Educ.* 75, **1998**, 919.
31. Simon, J.D., Xie, X., *J. Phys. Chem.* 93, **1989**, 291.

32. Xie X., Simon J.D., *J. Am. Chem. Soc.* 112, **1990**, 1130.
33. Zhang S., Dobson G.R., *Inorg. Chem.* 29, **1990**, 3477.
34. Zhang S., Dobson G.R., *Polyhedron* 9, **1990**, 2511.
35. Brookhart M., Green M.L.H., *J. Organomet. Chem.* 250, **1983**, 395.
36. Saillard J.-Y., Hoffmann R., *J. Am. Chem. Soc.* 106, **1984**, 206.
37. Dobson G. R., Asali K.J., Cate C.D., Cate C. W., *Inorg. Chem.* 30, **1991**, 4471.
38. Lewis K.E., Golden D.M., Smith G.P., *J. Am. Chem. Soc.* 106, **1984**, 3905.
39. Graham G.R., Angelici R.J., *Inorg. Chem.* 6, **1967**, 2082.
40. Morse J., Parker G., Burkey T.J., *Organometallics* 7, **1989**, 2471.
41. Grim, S. O., Briggs, W.L., Barth, R. C., Tolman, C. A., *Inorg. Chem.* 13, **1974**, 1095.
42. Shapley, J.R., Koefod, R. S., Xu, C., Lu, W, *J. Phys. Chem.*, **1992**, 96, 2928.
43. Alexander N. Chernega, Malcolm L. H. Green, Jane Haggitt and Adam H. H. Stephens, *J. Chem. Soc., Dalton Trans.*, **1998**, 755–767.
44. Li-Cheng S., Ying-Huai Z., Qing-Mei H., *J. Chem. Research*, **1999**, 56.
45. Chatt J., Leigh G.H. , Thankarajan N.. *J. Organomet. Chem.*, **1971**, 29, 105.

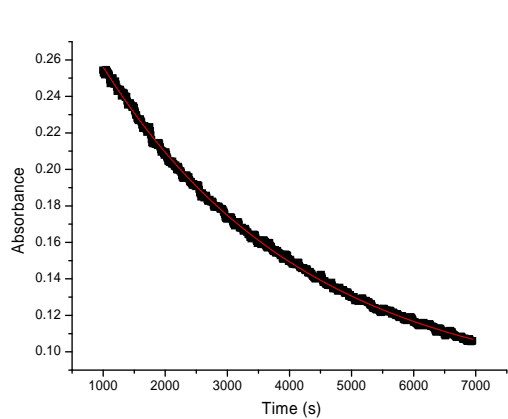
APPENDICES

APPENDICES A

APPENDIX A-1

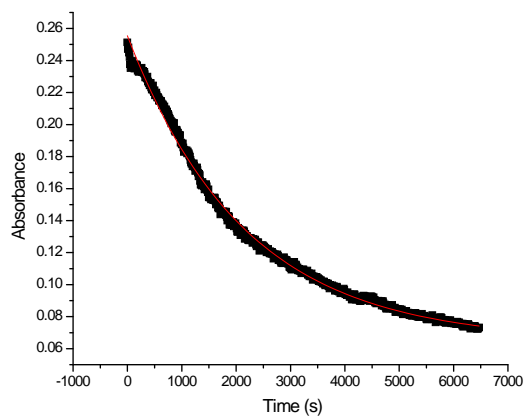
Plot of Absorbance versus time for the reaction of *fac*-(²-C₆₀)(²-phen)Cr(CO)₃
with the Lewis base Tri-phenylphosphine in Toluene

Plot of Absorbance versus time for the reaction of PPh3 (0.0569M) with (²-C₆₀)(²-phen)Cr(CO)₃ in Toluene at 303.2 K



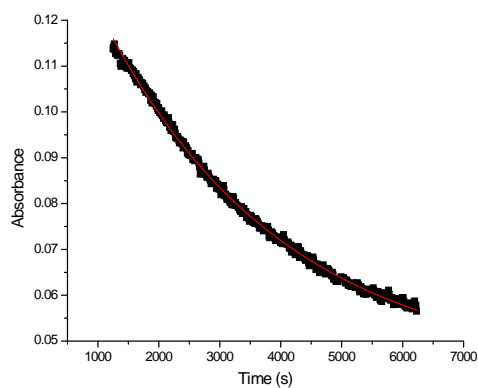
Data: Data1_B
 Model: ExpDec1
 Equation: $y = A1 * \exp(-x/t1) + y0$
 Weighting: y No weighting
 Chi²/DoF = 1.5328E-6
 R² = 0.99914
 y0 0.0776 0.00045
 A1 0.24177 0.00029
 t1 3291.35032 18.29037
 K1 3.04E-04

Plot of Absorbance versus time for the reaction of PPh3 (0.0519M) with (²-C₆₀)(²-phen)Cr(CO)₃ in Toluene at 313.2 K



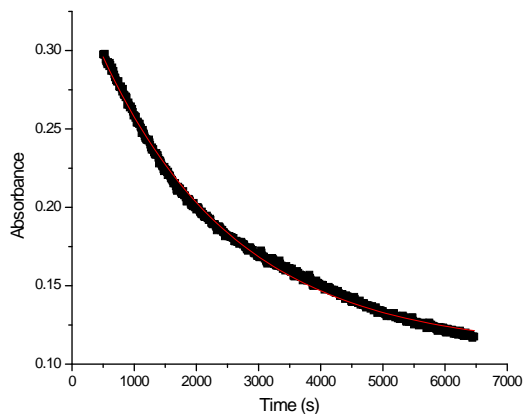
Data: Data1_B
 Model: ExpDec1
 Equation: $y = A1 * \exp(-x/t1) + y0$
 Weighting: y No weighting
 Chi²/DoF = 9.3834E-6
 R² = 0.99614
 y0 0.06484 0.00045
 A1 0.19068 0.00047
 t1 2146.23777 16.31428
 K1 4.65E-04

Plot of Absorbance versus time for the reaction of PPh₃ (0.552M) with (²-C₆₀)(²-phen)Cr(CO)₃ in Toluene at 313.2 K



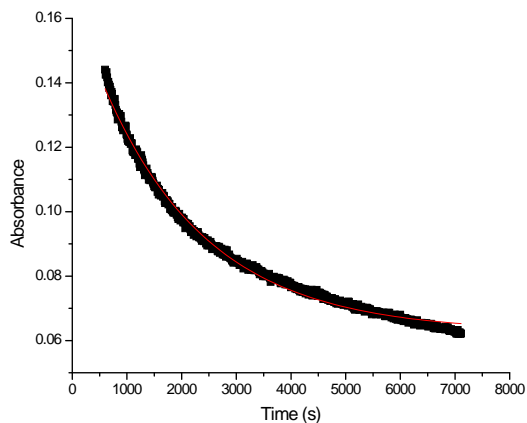
Data: Data1_B
 Model: ExpDec1
 Equation: $y = A1 \cdot \exp(-x/t1) + y0$
 Weighting:
 y No weighting
 Chi²/DoF = 1.03E-6
 R² = 0.99693
 y0 0.03985 0.0005
 A1 0.10875 0.00028
 t1 3302.64255 41.29319
 K1 3.028E-04

Plot of Absorbance versus time for the reaction of PPh₃ (0.0966M) with (²-C₆₀)(²-phen)Cr(CO)₃ in Toluene at 313.2 K



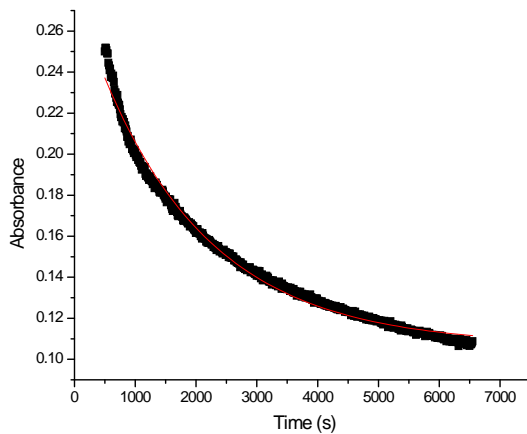
Data: Data1_B
 Model: ExpDec1
 Equation: $y = A1 \cdot \exp(-x/t1) + y0$
 Weighting:
 y No weighting
 Chi²/DoF = 7.7791E-6
 R² = 0.99662
 y0 0.10931 0.00049
 A1 0.23493 0.00062
 t1 2177.33746 17.20391
 K1 4.592E-04

Plot of Absorbance versus time for the reaction of PPh3 (0.0589M) with (²⁻C₆₀)(²⁻-phen)Cr(CO)₃ in Toluene at 323.2 K



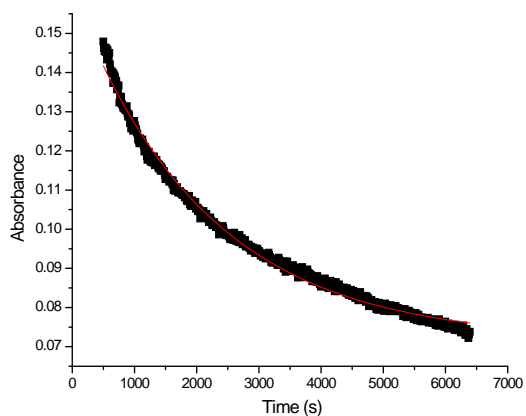
Data: Data1_B
 Model: ExpDec1
 Equation: $y = A1 * \exp(-x/t1) + y0$
 Weighting:
 y No weighting
 Chi²/DoF = 2.3399E-6
 R² = 0.99389
 y0 0.06267 0.00019
 A1 0.10318 0.00044
 t1 1925.03993 17.06468
 K1 5.19E-04

Plot of Absorbance versus time for the reaction of PPh3 (0.152M) with (²⁻C₆₀)(²⁻-phen)Cr(CO)₃ in Toluene at 323.2 K



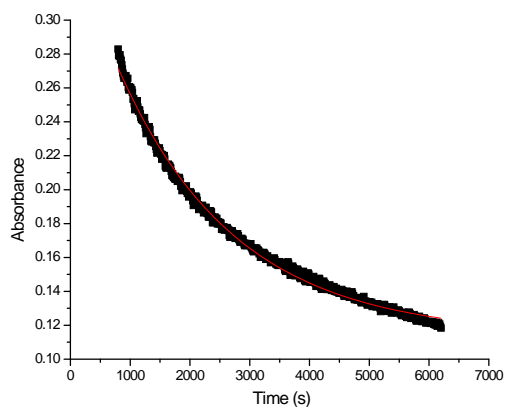
Data: Data1_B
 Model: ExpDec1
 Equation: $y = A1 * \exp(-x/t1) + y0$
 Weighting:
 y No weighting
 Chi²/DoF = 4.6757E-6
 R² = 0.99481
 y0 0.10343 0.00036
 A1 0.15999 0.00061
 t1 2073.33253 19.95242
 K1 4.82E-04

Plot of Absorbance versus time for the reaction of PPh₃ (0.632M) with (²-C₆₀)(²-phen)Cr(CO)₃ in Toluene at 323.2 K



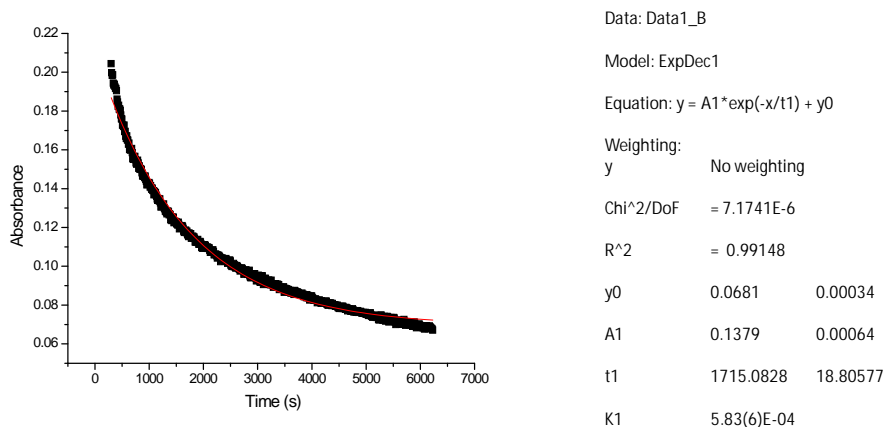
Data: Data1_B
 Model: ExpDec1
 Equation: $y = A1 * \exp(-x/t1) + y0$
 Weighting:
 y No weighting
 Chi²/DoF = 2.6444E-6
 R² = 0.9919
 y0 0.07159 0.00029
 A1 0.08857 0.00037
 t1 2137.76549 26.30685
 K1 4.67E-04

Plot of Absorbance versus time for the reaction of PPh₃ (0.0461M) with (²-C₆₀)(²-phen)Cr(CO)₃ in Toluene at 323.2 K

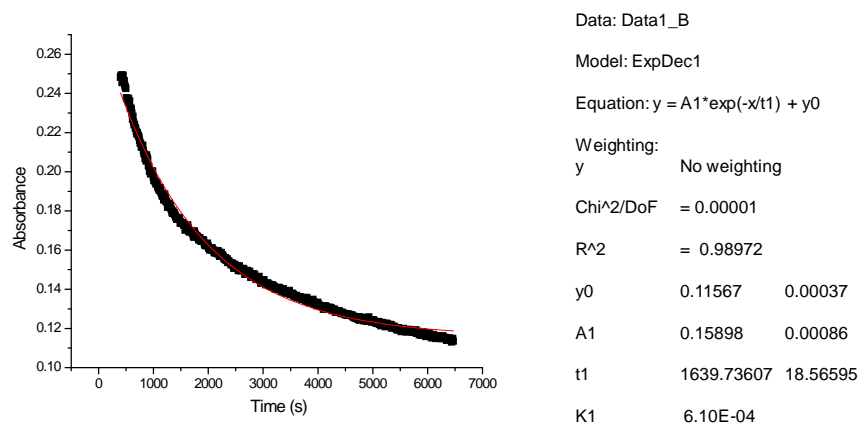


Data: Data1_B
 Model: ExpDec1
 Equation: $y = A1 * \exp(-x/t1) + y0$
 Weighting:
 y No weighting
 Chi²/DoF = 7.5102E-6
 R² = 0.99543
 y0 0.11417 0.0005
 A1 0.23697 0.00101
 t1 1959.9158 18.87918
 K1 5.10E-04

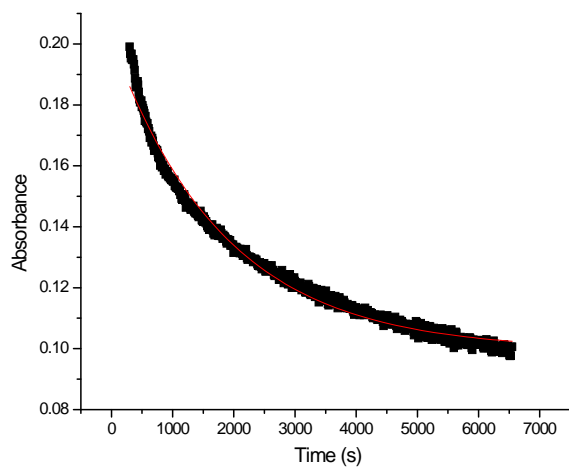
Plot of Absorbance versus time for the reaction of PPh3 (0.402M) with (η^5 -C₆₀)(η^2 -phen)Cr(CO)₃ in Toluene at 333.2 K and 500nm



Plot of Absorbance versus time for the reaction of PPh3 (0.611M) with (η^5 -C₆₀)(η^2 -phen)Cr(CO)₃ in Toluene at 333.2 K



Plot of Absorbance versus time for the reaction of PPh3
(0.0461M) with (²-C₆₀)(²-phen)Cr(CO)₃ in Toluene at 333.2 K



Data: Data1_B

Model: ExpDec1

Equation: $y = A1 \cdot \exp(-x/t1) + y0$

Weighting:
y No weighting

Chi²/DoF = 5.7859E-6

R² = 0.98782

y0 0.09888 0.00032

A1 0.10011 0.0005

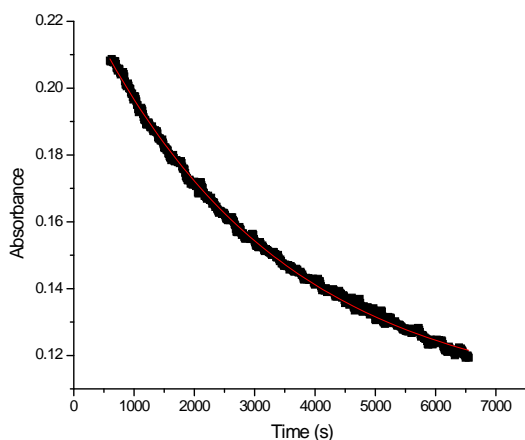
t1 1912.76365 25.22639

K1 5.23E-04

APPENDIX A-2

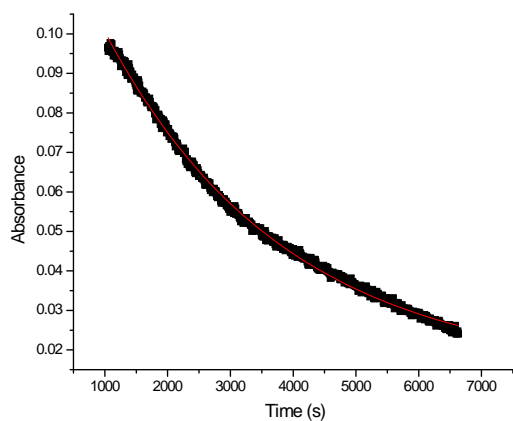
Plot of Absorbance versus time for the reaction of *fac*-(²-C₆₀)(²-phen)Cr(CO)₃
with the Lewis base Tri-phenylphosphine in Benzene

Plot of Absorbance vs time for the reaction of
 $(\eta^2\text{-phen})(\eta^2\text{-C}_{60})\text{Cr}(\text{CO})_3$ with $\text{PPh}_3(0.187\text{M})$ in
 benzene at 303.2 K



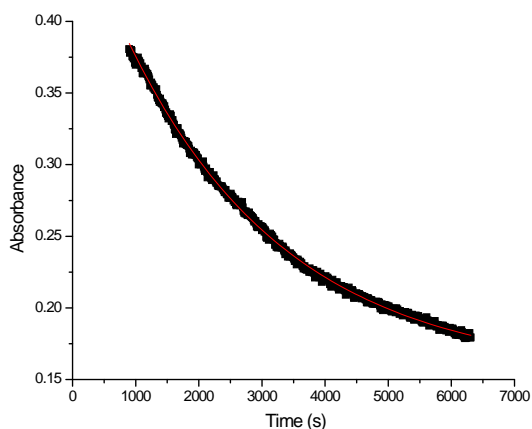
Data: Data1_B
 Model: ExpDec1
 Equation: $y = A1 \cdot \exp(-x/t1) + y0$
 Weighting:
 y No weighting
 $\chi^2/\text{DoF} = 1.0857\text{E-}6$
 $R^2 = 0.99821$
 y0 0.10526 0.00036
 A1 0.12471 0.00024
 T1 2993.22237 25.22024
 K1 3.32E-04

Plot of Absorbance vs time for the reaction of
 $(\eta^2\text{-C}_{60})(\eta^2\text{-phen})\text{Cr}(\text{CO})_3$ with $\text{PPh}_3(0.541\text{M})$ in benzene
 at 500nm and 313.2 K



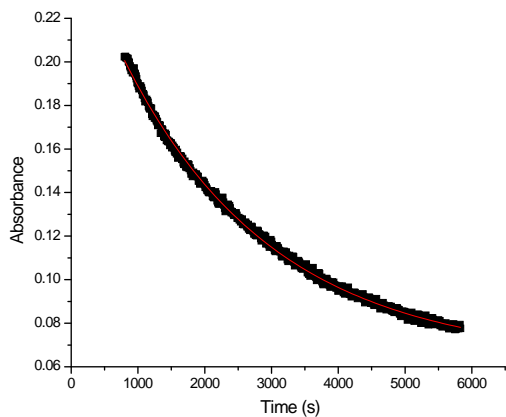
Data: Data1_B
 Model: ExpDec1
 Equation: $y = A1 \cdot \exp(-x/t1) + y0$
 Weighting:
 y No weighting
 $\chi^2/\text{DoF} = 1.0138\text{E-}6$
 $R^2 = 0.99773$
 y0 0.01354 0.00033
 A1 0.1221 0.00025
 t1 2909.6968 25.29412
 K1 3.44(3)E-04

Plot of Absorbance vs time for the reaction of
 $(n2-C60)(n2-phen)Cr(CO)3$ with PPh_3 (0.0516M) in benzene
 at 500nm and 313.2 K



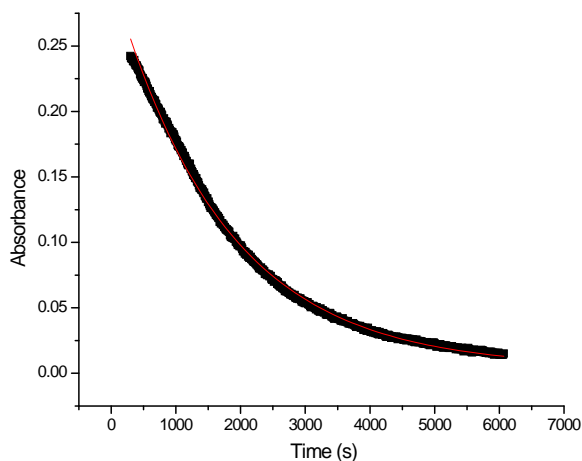
Data: Data1_B
 Model: ExpDec1
 Equation: $y = A1 * \exp(-x/t1) + y0$
 Weighting:
 y No weighting
 $\chi^2/DoF = 3.391E-6$
 $R^2 = 0.99896$
 y0 0.15351 0.00052
 A1 0.32956 0.00052
 t1 2533.58234 14.11724
 K1 3.9E-04

Plot of Absorbance vs time for the reaction of
 $(n2-C60)(n2-phen)Cr(CO)3$ with PPh_3 (0.531M) in benzene
 at 500nm and 323.2 K



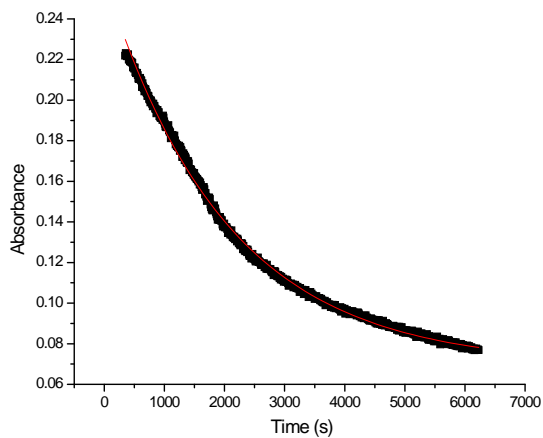
Data: Data1_B
 Model: ExpDec1
 Equation: $y = A1 * \exp(-x/t1) + y0$
 Weighting:
 y No weighting
 $\chi^2/DoF = 1.9791E-6$
 $R^2 = 0.99847$
 y0 0.06398 0.00036
 A1 0.19639 0.00038
 t1 2220.9149 14.46871
 K1 4.50E-04

Plot of Absorbance vs time for the reaction of (n2-C60)(n2-phen)Cr(CO)3 with PPh3 (0.0517M) in benzene at 500nm and 323.2 K



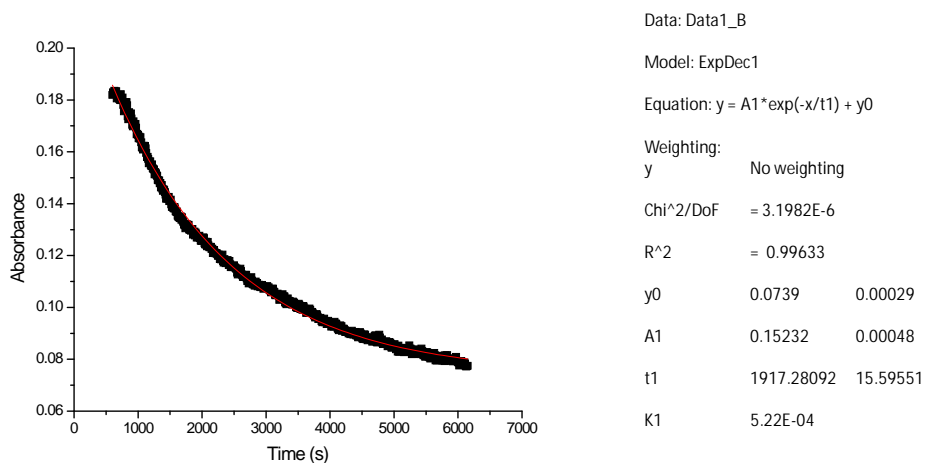
Data: Data1_B
 Model: ExpDec1
 Equation: $y = A1 * \exp(-x/t1) + y0$
 Weighting:
 y No weighting
 Chi^2/DoF = 8.6954E-6
 R^2 = 0.99794
 y0 0.00421 0.00039
 A1 0.29889 0.00065
 t1 1721.59713 9.44775
 K1 5.81E-04

Plot of Absorbance vs time for the reaction of (n2-C60)(n2-phen)Cr(CO)3 with PPh3 (0.147M) in benzene at 500nm and 323.2 K

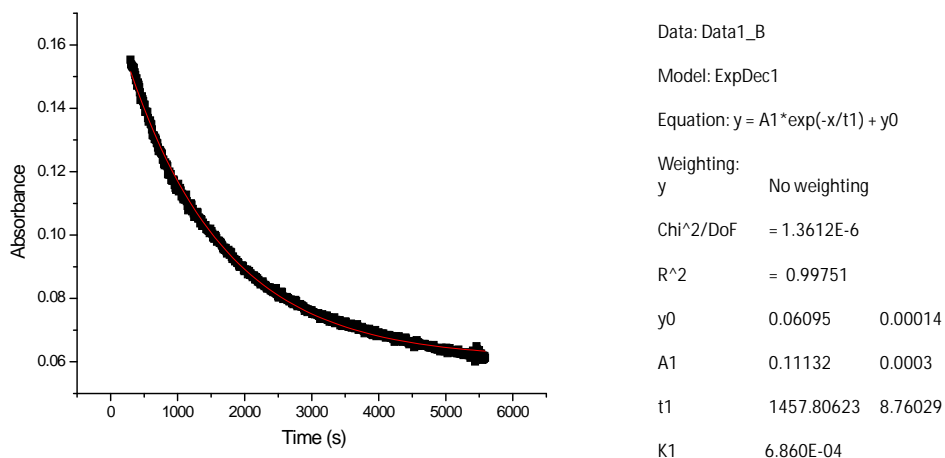


Data: Data1_B
 Model: ExpDec1
 Equation: $y = A1 * \exp(-x/t1) + y0$
 Weighting:
 y No weighting
 Chi^2/DoF = 4.2098E-6
 R^2 = 0.99754
 y0 0.06942 0.00033
 A1 0.19079 0.00042
 t1 2019.84727 13.14474
 K1 4.95E-04

Plot of Absorbance vs time for the reaction of
 (n2-C60)(n2-phen)Cr(CO)3 with PPh3 (0.207M) in benzene
 at 500nm and 333.2 K



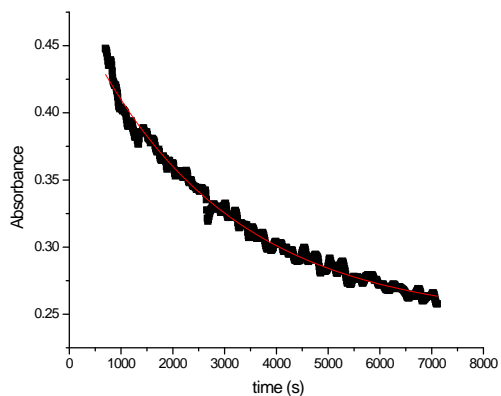
Plot of Absorbance vs time for the reaction of
 (n2-C60)(n2-phen)Cr(CO)3 with PPh3 (0.478M) in benzene
 at 500nm and 333.2 K



APPENDIX A-3

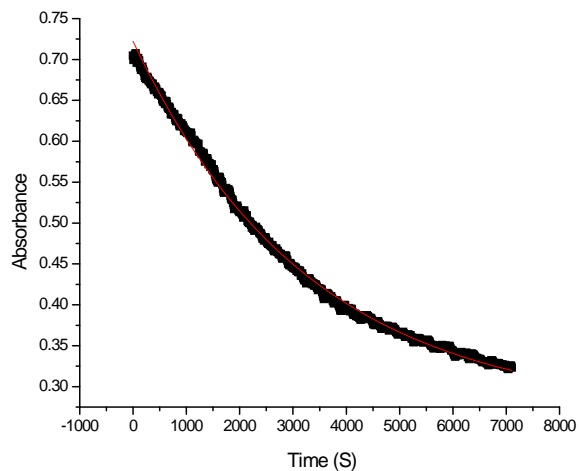
Plot of Absorbance versus time for the reaction of *fac*-(²-C₆₀)(²-phen)Cr(CO)₃ with the Lewis base Tri-phenylphosphine in chlorobenzene

Plot of Absorbance vs time for the reaction of
 (n2-phen)(n2-C60)Cr(CO)3 with PPh3(0.301M) in chlorobenzene
 at 303.2 K and 500nm



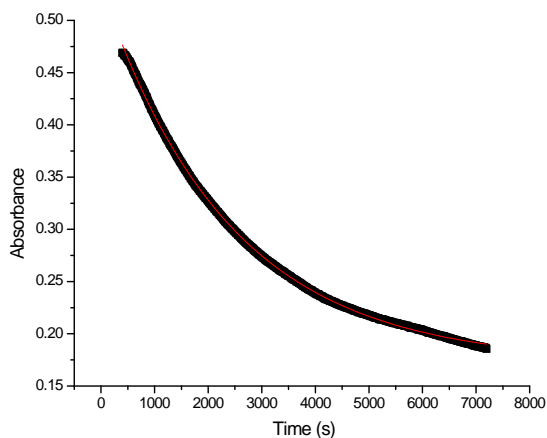
Data: Data1_B
 Model: ExpDec1
 Equation: $y = A1 \cdot \exp(-x/t1) + y0$
 Weighting:
 y No weighting
 Chi²/DoF = 0.00003
 R² = 0.99285
 y0 0.24924 0.00084
 A1 0.242 0.0008
 t1 2571.66675 26.97823
 K1 3.89(4)E-04

Plot of Absorbance vs time for the reaction of
 (n2-phen)(n2-C60)Cr(CO)3 with PPh3(0.100M) in chlorobenzene
 at 303.2 K



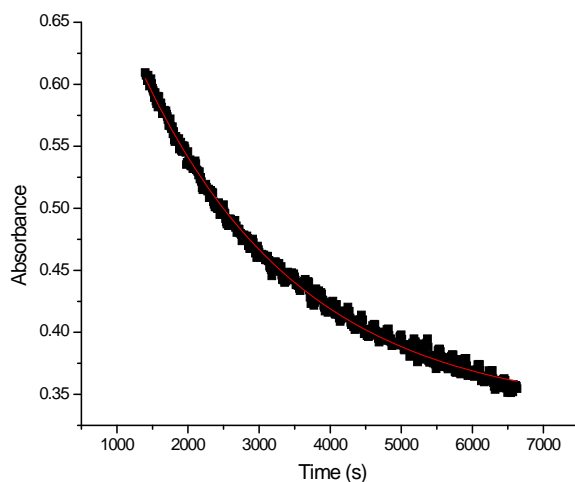
Data: Data1_B
 Model: ExpDec1
 Equation: $y = A1 \cdot \exp(-x/t1) + y0$
 Weighting:
 y No weighting
 Chi²/DoF = 0.00004
 R² = 0.99723
 y0 0.26778 0.00142
 A1 0.45457 0.00117
 t1 3275.1575 25.62482
 K1 3.053E-04

Plot of Absorbance vs time for the reaction of
 (n2-phen)(n2-C60)Cr(CO)3 with PPh3(0.879M) in chlorobenzene
 at 303.2 K and 500nm



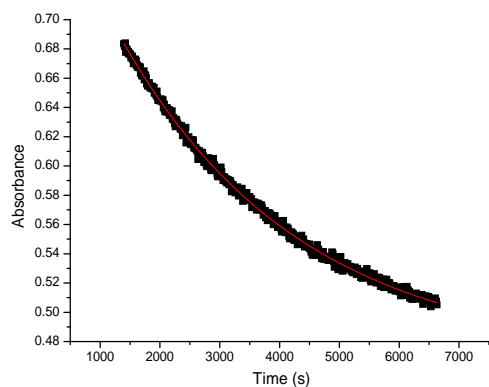
Data: Data1_B
 Model: ExpDec1
 Equation: $y = A1 * \exp(-x/t1) + y0$
 Weighting:
 y No weighting
 Chi^2/DoF = 3.4885E-6
 R^2 = 0.99947
 y0 0.17122 0.00029
 A1 0.35711 0.00032
 t1 2427.79435 6.87746
 K1 4.12(1)E-04

Plot of Absorbance vs time for the reaction of
 (n2-phen)(n2-C60)Cr(CO)3 with PPh3 (0.272) in clorobenzene
 at 313.2 K and 355nm



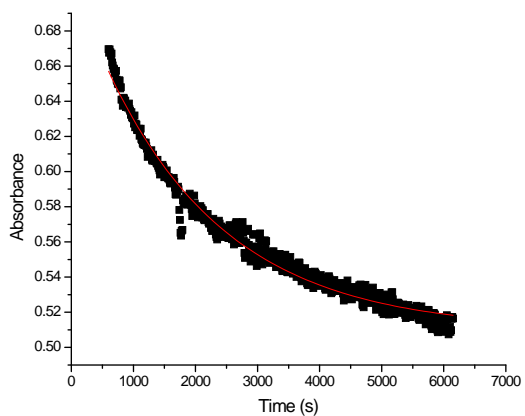
Data: Data1_B
 Model: ExpDec1
 Equation: $y = A1 * \exp(-x/t1) + y0$
 Weighting:
 y No weighting
 Chi^2/DoF = 0.00002
 R^2 = 0.99559
 y0 0.33428 0.00111
 A1 0.50562 0.00289
 t1 2238.59146 24.36114
 K1 4.47E-04

Plot of Absorbance vs time for the reaction of
 (n2-phen)(n2-C60)Cr(CO)3 with PPh3 (0.151) in clorobenzene
 at 313.2 K and 355nm



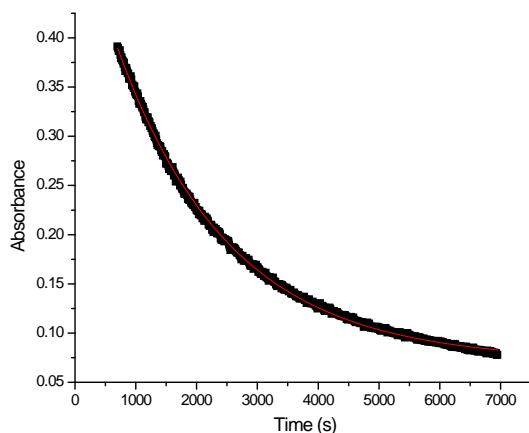
Data: Data1_B
 Model: ExpDec1
 Equation: $y = A1 \cdot \exp(-x/t1) + y0$
 Weighting:
 y No weighting
 Chi^2/DoF = 4.1498E-6
 R^2 = 0.99835
 y0 0.46916 0.00084
 A1 0.34237 0.00074
 t1 2993.87237 25.27412
 K1 3.34E-04

Plot of Absorbance vs time for the reaction of
 (n2-phen)(n2-C60)Cr(CO)3 with PPh3 (0.149) in clorobenzene
 at 313.2 K and 355nm



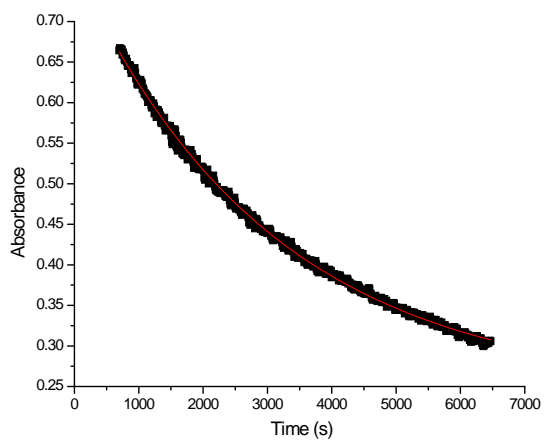
Data: Data1_B
 Model: ExpDec1
 Equation: $y = A1 \cdot \exp(-x/t1) + y0$
 Weighting:
 y No weighting
 Chi^2/DoF = 0.00003
 R^2 = 0.98161
 y0 0.5097 0.00089
 A1 0.2004 0.00147
 t1 1951.34545 36.63571
 K1 5.12E-04

Plot of Absorbance vs time for the reaction of
 $(\eta^5\text{-C}_5\text{H}_5)_2(\eta^5\text{-C}_6\text{H}_6)\text{Cr}(\text{CO})_3$ with $\text{PPh}_3(0.000351\text{M})$ in
 chlorobenzene at 313.2 K



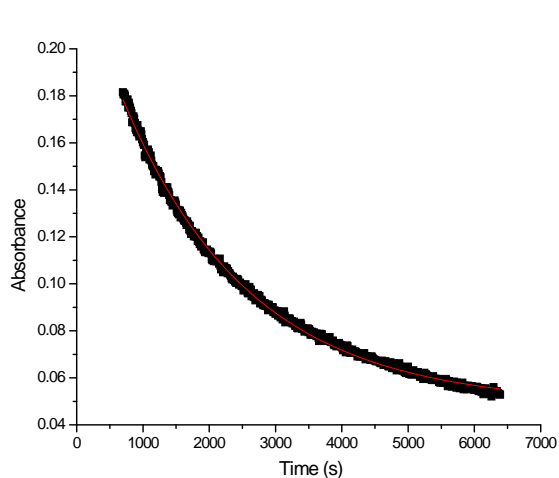
Data: Data1_B
 Model: ExpDec1
 Equation: $y = A1 \cdot \exp(-x/t1) + y0$
 Weighting:
 y No weighting
 Chi²/DoF = 5.4704E-6
 R² = 0.99919
 y0 0.07207 0.00029
 A1 0.46289 0.0008
 t1 1857.46751 6.13047
 K1 5.38E-04

Plot of Absorbance vs time for the reaction of
 $(\eta^5\text{-C}_5\text{H}_5)_2(\eta^5\text{-C}_6\text{H}_6)\text{Cr}(\text{CO})_3$ with $\text{PPh}_3(0.133\text{M})$ in chlorobenzene
 at 313.2 K



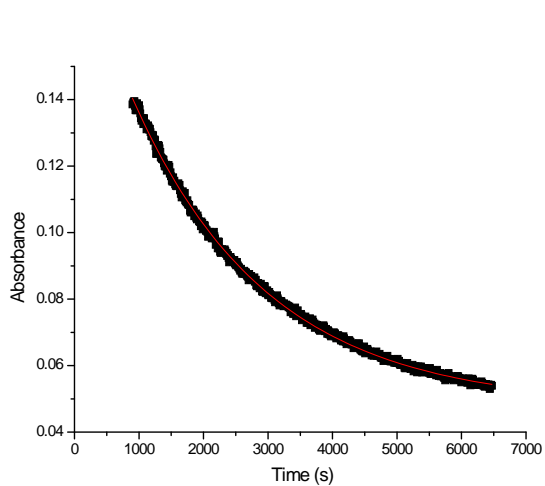
Data: Data1_B
 Model: ExpDec1
 Equation: $y = A1 \cdot \exp(-x/t1) + y0$
 Weighting:
 y No weighting
 Chi²/DoF = 0.00002
 R² = 0.9983
 y0 0.24434 0.0014
 A1 0.52572 0.00093
 t1 3052.04713 23.25659
 K1 3.27E-04

Plot of Absorbance vs time for the reaction of
 $(\eta^5\text{-phen})(\eta^5\text{-C}_6\text{O})\text{Cr}(\text{CO})_3$ with $\text{PPh}_3(0.1.16\text{E-}03\text{M})$ in
 chlorobenzene at 313.2 K



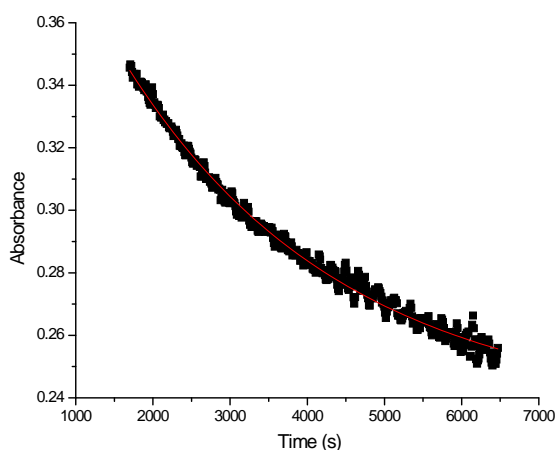
Data: Data1_B
 Model: ExpDec1
 Equation: $y = A1 \cdot \exp(-x/t1) + y0$
 Weighting:
 y No weighting
 Chi²/DoF = 2.2914E-6
 R² = 0.99796
 y0 0.04862 0.00024
 A1 0.187 0.0005
 t1 1915.25166 11.38591
 K1 5.22E-04

Plot of Absorbance vs time for the reaction of
 $(\eta^5\text{-phen})(\eta^5\text{-C}_6\text{O})\text{Cr}(\text{CO})_3$ with $\text{PPh}_3(1.45\text{E-}03\text{M})$ in
 chlorobenzene at 313.2 K



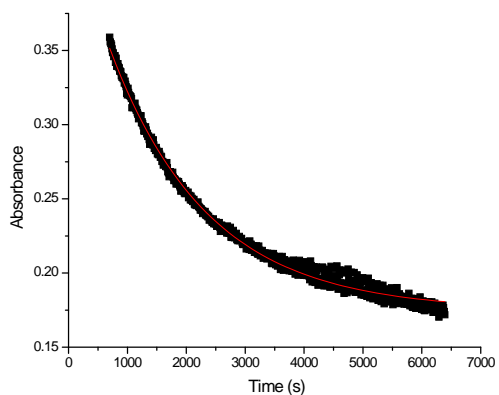
Data: Data1_B
 Model: ExpDec1
 Equation: $y = A1 \cdot \exp(-x/t1) + y0$
 Weighting:
 y No weighting
 Chi²/DoF = 5.9504E-7
 R² = 0.99894
 y0 0.04795 0.00015
 A1 0.14243 0.00029
 t1 2085.61169 9.72767
 K1 4.79E-04

Plot of Absorbance vs time for the reaction of
 (n2-phen)(n2-C60)Cr(CO)3 with PPh3(1.00M) in chlorobenzene
 at 313.2 K



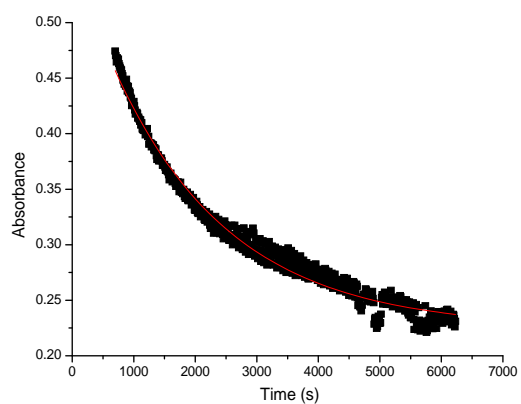
Data: Data1_B
 Model: ExpDec1
 Equation: $y = A1 \cdot \exp(-x/t1) + y0$
 Weighting:
 y No weighting
 Chi²/DoF = 4.9503E-6
 R² = 0.99232
 y0 0.23552 0.00102
 A1 0.19958 0.00131
 t1 2820.91232 55.5827
 K1 3.54E-04

Plot of Absorbance vs time for the reaction of
 (n2-phen)(n2-C60)Cr(CO)3 with PPh3 (0.0146M) in chlorobenzene
 at 323.2 K



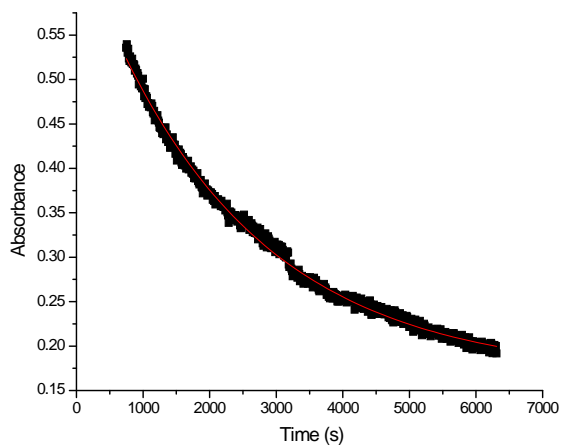
Data: Data1_B
 Model: ExpDec1
 Equation: $y = A1 \cdot \exp(-x/t1) + y0$
 Weighting:
 y No weighting
 Chi²/DoF = 0.00001
 R² = 0.99357
 y0 0.17488 0.00047
 A1 0.26887 0.00147
 t1 1665.43317 16.11422
 K1 6.004E-04

Plot of Absorbance vs time for the reaction of
 (n2-phen)(n2-C60)Cr(CO)3 with PPh3 (0.0510M) in chlorobenzene
 at 323.2 K



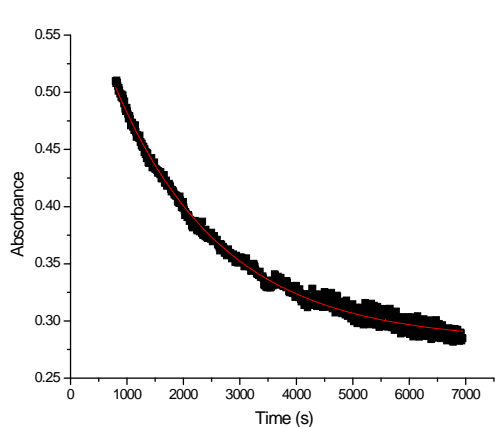
Data: Data1_B
 Model: ExpDec1
 Equation: $y = A1 \cdot \exp(-x/t1) + y0$
 Weighting:
 y No weighting
 Chi²/DoF = 0.00007
 R² = 0.98105
 y0 0.22481 0.00137
 A1 0.33582 0.00281
 t1 1890.71297 35.41882
 K1 5.289E-04

Plot of Absorbance vs time for the reaction of
 (n2-phen)(n2-C60)Cr(CO)3 with PPh3 (0.720M) in chlorobenzene
 at 323.2 K



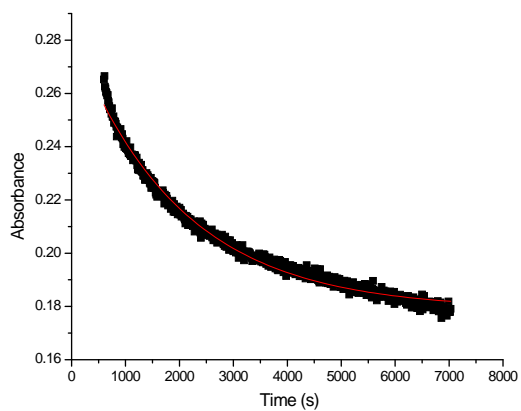
Data: Data1_B
 Model: ExpDec1
 Equation: $y = A1 \cdot \exp(-x/t1) + y0$
 Weighting:
 y No weighting
 Chi²/DoF = 0.00003
 R² = 0.99606
 y0 0.16662 0.00131
 A1 0.49191 0.00152
 t1 2336.01008 22.96639
 K1 4.281E-04

Plot of Absorbance vs time for the reaction of
 (n2-phen)(n2-C60)Cr(CO)3 with PPh3 (0.309M) in chlorobenzene
 at 323.2 K



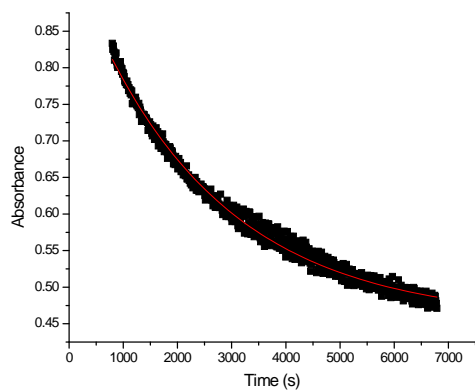
Data: Data1_B
 Model: ExpDec1
 Equation: $y = A1 \cdot \exp(-x/t1) + y0$
 Weighting:
 y No weighting
 Chi²/DoF = 0.00002
 R² = 0.99374
 y0 0.28211 0.00062
 A1 0.3376 0.00171
 t1 1910.95663 18.20678
 K1 5.23E-04

Plot of Absorbance vs time for the reaction of
 (n2-phen)(n2-C60)Cr(CO)3 with PPh3 (0.155M) in chlorobenzene
 at 323.2 K



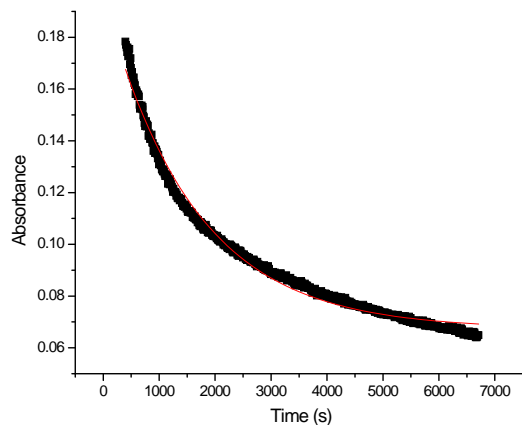
Data: Data1_B
 Model: ExpDec1
 Equation: $y = A1 \cdot \exp(-x/t1) + y0$
 Weighting:
 y No weighting
 Chi²/DoF = 4.1802E-6
 R² = 0.9895
 y0 0.1789 0.00027
 A1 0.10396 0.00057
 t1 1982.79619 23.85185
 K1 5.04E-04

Plot of Absorbance vs time for the reaction of
 (n2-phen)(n2-C60)Cr(CO)3 with PPh3 (0.519M) in chlorobenzene
 at 323.2 K



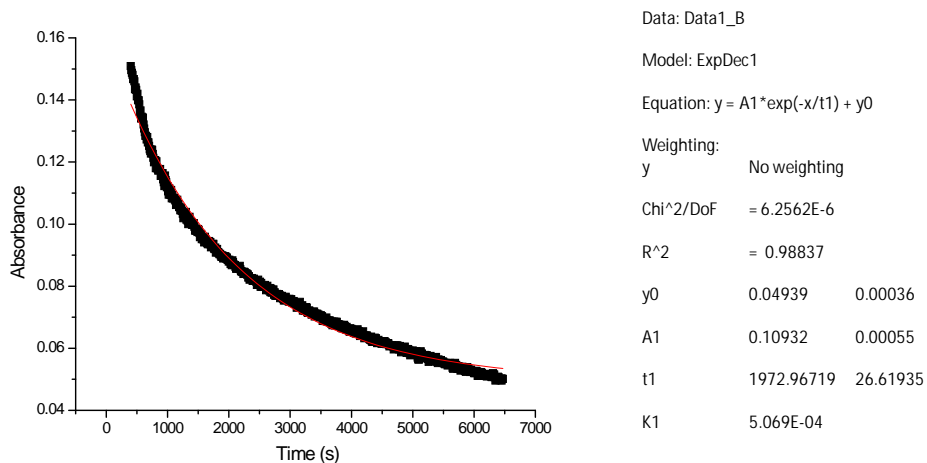
Data: Data1_B
 Model: ExpDec1
 Equation: $y = A1 \cdot \exp(-x/t1) + y0$
 Weighting:
 y No weighting
 Chi²/DoF = 0.00008
 R² = 0.99081
 y0 0.4546 0.00188
 A1 0.49289 0.00228
 t1 2476.62696 35.46571
 K1 4.04E-04

Plot of Absorbance vs time for the Reaction of
 (n2-C60)(n2-phen)Cr(CO)3 with PPh3 (0.241M) in chlorobenzene
 at 333.2 K

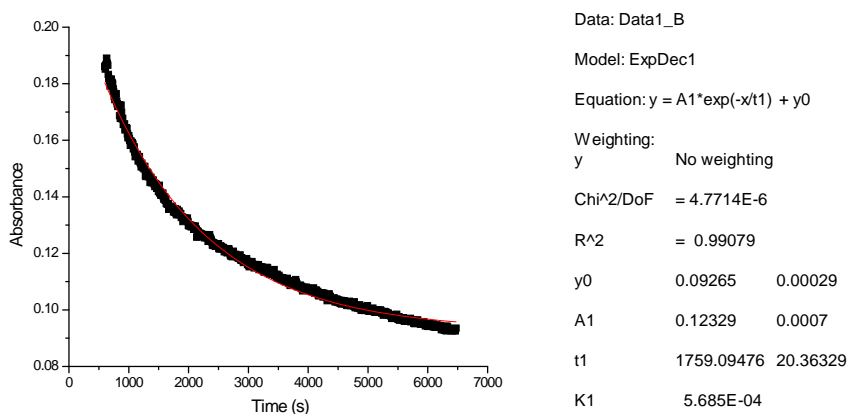


Data: Data1_B
 Model: ExpDec1
 Equation: $y = A1 \cdot \exp(-x/t1) + y0$
 Weighting:
 y No weighting
 Chi²/DoF = 6.2973E-6
 R² = 0.98892
 y0 0.06608 0.00029
 A1 0.12296 0.00072
 t1 1720.58103 20.29828
 K1 5.81E-04

Plot of Absorbance vs time for the Reaction of (n2-C60)(n2-phen)Cr(CO)3 with PPh3 (0.0679M) in chlorobenzene at 333.2 K



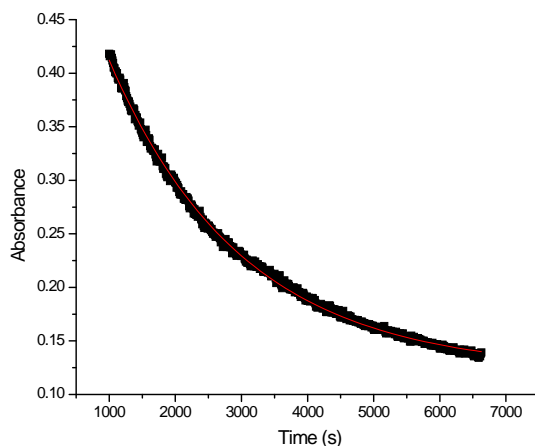
Plot of Absorbance vs time for the Reaction of (n2-C60)(n2-phen)Cr(CO)3 with PPh3 (0.484M) in chlorobenzene at 333.2 K



APPENDIX A-4

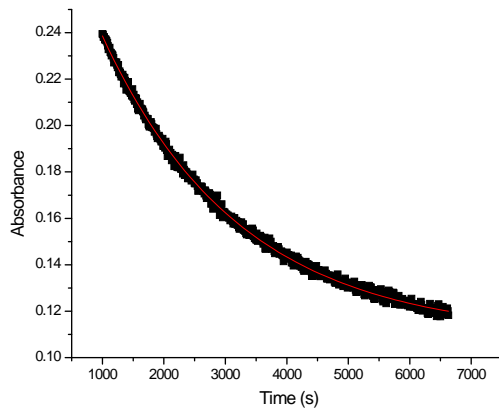
Plot of Absorbance versus time for the reaction of the ratio between PPh_3 and C_{60} with *fac*-($\eta^2\text{-C}_{60}$)($\eta^2\text{-phen}$) $\text{Cr}(\text{CO})_3$ in Chlorobenzene

Plot of Absorbance vs time for a Ratio of 0.289 between C60(7.56E-04M) and PPh3(2.61E-03M) reacting with (n2-phen)(n2-C60)Cr(CO)3 in chlorobenzene at 313.2 K



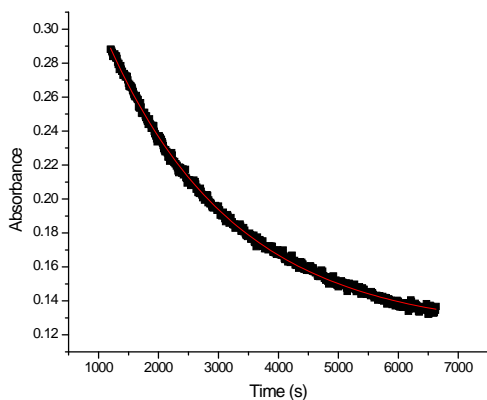
Data: Data1_B
 Model: ExpDec1
 Equation: $y = A1 \cdot \exp(-x/t1) + y0$
 Weighting:
 y No weighting
 Chi²/DoF = 9.0652E-6
 R² = 0.99837
 y0 0.12238 0.00053
 A1 0.47642 0.00138
 t1 2010.31877 11.18864
 K1 4.97E-04

Plot of Absorbance vs time for a Ratio of 0.556 between C60(1.26E-03M) and PPh3(2.26E-03M) reacting with (n2-phen)(n2-C60)Cr(CO)3 in chlorobenzene at 313.2 K



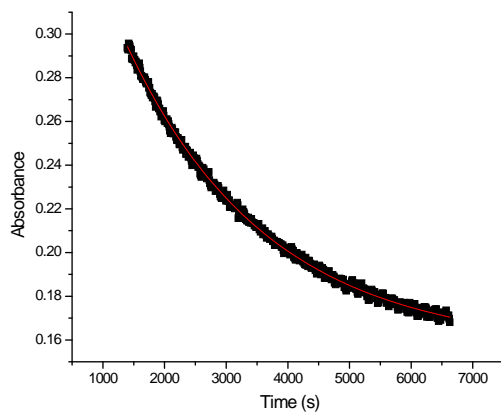
Data: Data1_B
 Model: ExpDec1
 Equation: $y = A1 \cdot \exp(-x/t1) + y0$
 Weighting:
 y No weighting
 Chi²/DoF = 1.6907E-6
 R² = 0.99843
 y0 0.10948 0.00027
 A1 0.20169 0.0005
 t1 2242.37057 13.24726
 K1 4.46E-04

Plot of Absorbance vs time for a Ratio of 0.655 between C60(7.14E-04M) and PPh3(1.09E-03M) reacting with (n2-phen)(n2-C60)Cr(CO)3 in chlorobenzene at 313.2 K



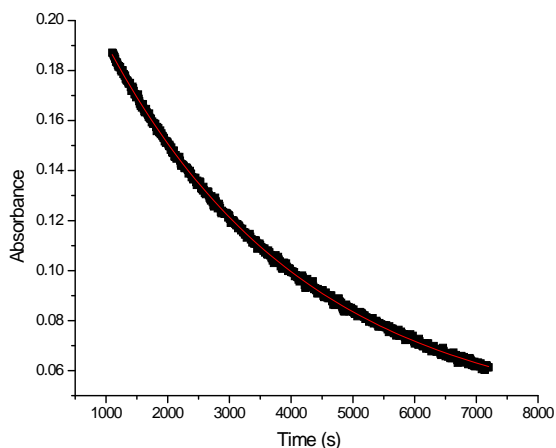
Data: Data1_B
 Model: ExpDec1
 Equation: $y = A1 \cdot \exp(-x/t1) + y0$
 Weighting:
 y No weighting
 Chi²/DoF = 2.6582E-6
 R² = 0.99853
 y0 0.12193 0.00034
 A1 0.29251 0.00088
 t1 2137.27541 12.34515
 K1 4.68E-04

Plot of Absorbance vs time for a Ratio of 0.885 between C60(1.0E-03M) and PPh3(1.13E-03M) reacting with (n2-phen)(n2-C60)Cr(CO)3 in chlorobenzene at 313.2 K



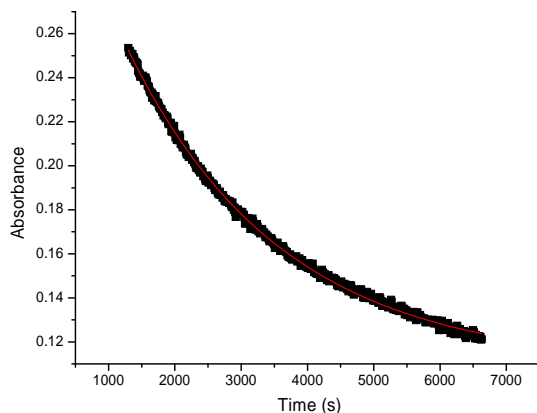
Data: Data1_B
 Model: ExpDec1
 Equation: $y = A1 \cdot \exp(-x/t1) + y0$
 Weighting:
 y No weighting
 Chi²/DoF = 1.8175E-6
 R² = 0.99848
 y0 0.15646 0.00034
 A1 0.25437 0.00083
 t1 2285.00945 14.81972
 K1 4.38E-04

Plot of Absorbance vs time for a Ratio of 0.907 between C60(4.5E-04M) and PPh3(4.96E-04M) reacting with (n2-phen)(n2-C60)Cr(CO)3 in chlorobenzene at 313.2 K



Data: Data1_B
 Model: ExpDec1
 Equation: $y = A1 \cdot \exp(-x/t1) + y0$
 Weighting:
 y No weighting
 Chi²/DoF = 6.7748E-7
 R² = 0.99945
 y0 0.03888 0.00028
 A1 0.20659 0.0002
 t1 3264.79124 13.87436
 K1 3.06E-04

Plot of Absorbance vs time for a Ratio of 0.051 between C60(1.47E-04M) and PPh3(2.87E-03M) reacting with (n2-phen)(n2-C60)Cr(CO)3 in chlorobenzene at 313.2 K

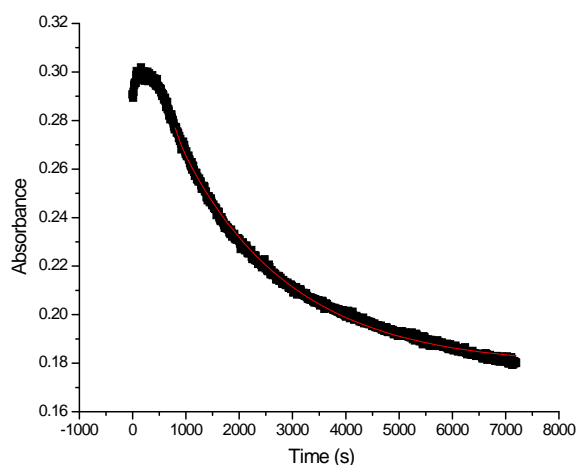


Data: Data1_B
 Model: ExpDec1
 Equation: $y = A1 \cdot \exp(-x/t1) + y0$
 Weighting:
 y No weighting
 Chi²/DoF = 1.7339E-6
 R² = 0.99865
 y0 0.10941 0.00033
 A1 0.25037 0.0007
 t1 2321.01212 13.99518
 K1 4.30E-04

APPENDIX B

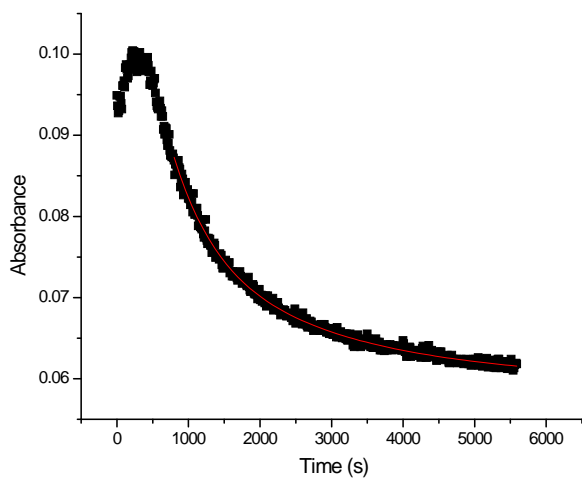
Plot of Absorbance versus time for the reaction of *fac*-(²-C₆₀)(²-phen)Cr(CO)₃
with the Lewis base Piperidine in chlorobenzene

Plot of Absorbance vs time for the Reaction of
 $(\eta^2\text{-C}_6\text{O})(\eta^2\text{-phen})\text{Cr}(\text{CO})_3$ with PIP (0.254M)
 at 323.2 K



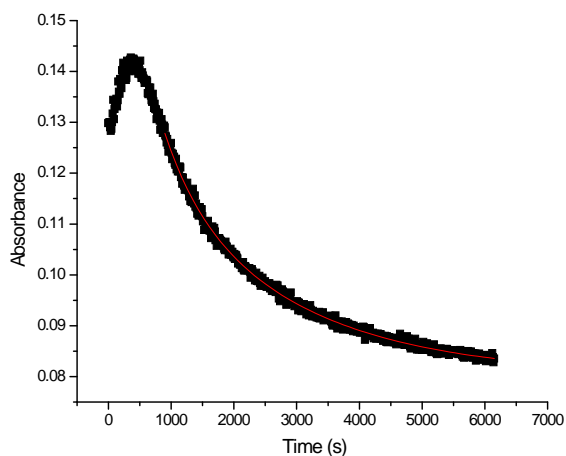
Data: Data1_B
 Model: BifCreciente2
 Weighting:
 y No weighting
 $\chi^2/\text{DoF} = 2.1301\text{E-}6$
 $R^2 = 0.99649$
 y0 0.17878 0.00024
 A1 -4.28765 15.96051
 t1 110.71053 54.92345
 A2 0.1402 0.00085
 t2 2056.64456 19.9343
 K1 9.03E-03
 K2 4.86E-04

Plot of Absorbance vs time for the Reaction of
 $(\eta^2\text{-C}_6\text{O})(\eta^2\text{-phen})\text{Cr}(\text{CO})_3$ with PIP (0.591M)
 at 323.2 K



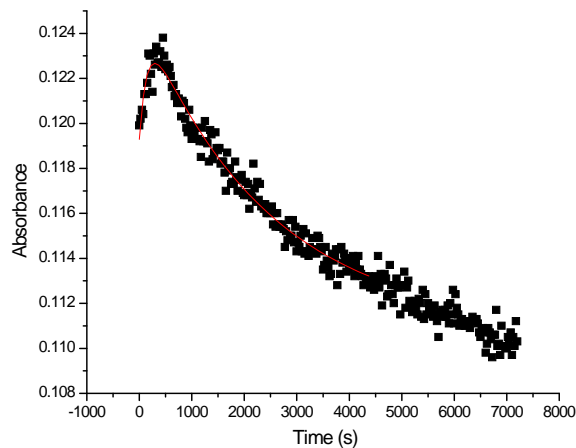
Data: Data1_B
 Model: BifCreciente2
 Weighting:
 y No weighting
 $\chi^2/\text{DoF} = 1.9289\text{E-}7$
 $R^2 = 0.99501$
 y0 0.05961 0.00052
 A1 -0.05155 0.00194
 t1 568.08042 55.01907
 A2 0.02121 0.00286
 t2 2340.38371 364.49388
 K1 1.76E-04
 K2 4.27E-04

Plot of Absorbance vs time for the Reaction of
 $(\eta^2\text{-C}_6\text{O})(\eta^2\text{-phen})\text{Cr}(\text{CO})_3$ with PIP (0.516M)
 at 323.2 K



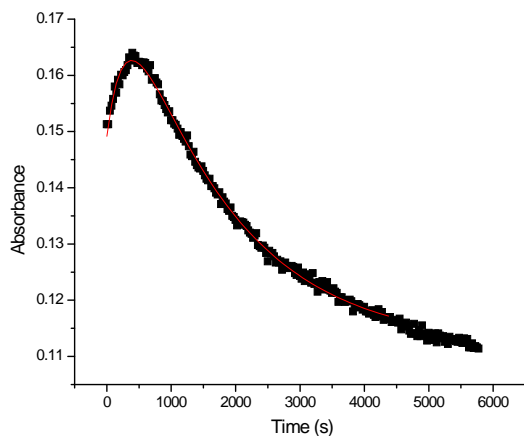
Data: Data1_B
 Model: BifCreciente2
 Weighting:
 y No weighting
 $\chi^2/\text{DoF} = 3.3504\text{E-}7$
 $R^2 = 0.99734$
 y0 0.0802 0.00044
 A1 -0.06022 0.00376
 t1 560.49742 65.83319
 A2 0.05324 0.00366
 t2 2227.09323 143.99614
 K1 1.784E-03
 K2 4.49E-04

Plot of Absorbance vs time for the Reaction of
 $(\eta^2\text{-C}_6\text{O})(\eta^2\text{-phen})\text{Cr}(\text{CO})_3$ with PIP (1.32M)
 at 323.2 K



Data: Data14_B
 Model: BifCreciente
 Weighting:
 y No weighting
 $\chi^2/\text{DoF} = 2.3425\text{E-}7$
 $R^2 = 0.97529$
 y0 0.11091 0.00045
 A1 0.00573 0.00041
 t1 142.70537 20.90303
 A2 0.01411 0.00027
 t2 2413.30349 195.08419
 K1 7.01E-03
 K2 4.14E-04

Plot of Absorbance vs time for the Reaction of
 $(\eta^2\text{-C}_6\text{O})(\eta^2\text{-phen})\text{Cr}(\text{CO})_3$ with PIP (0.287M)
 at 323.2 K



Data: Data7_B

Model: BifCreciente

Weighting:
 y No weighting

Chi²/DoF = 5.5678E-7

R² = 0.99767

y0 0.11174 0.0005

A1 0.04145 0.00159

t1 298.69123 13.99046

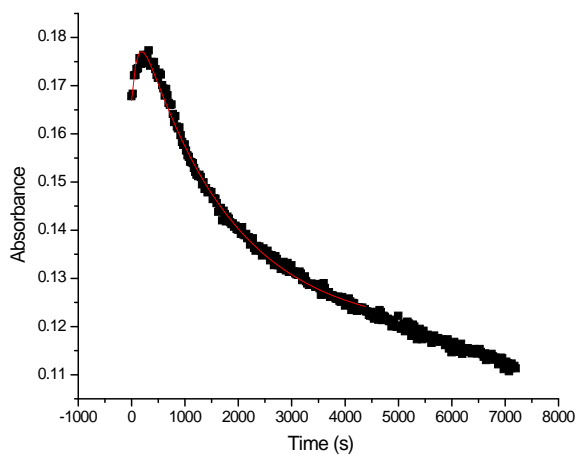
A2 0.07889 0.0013

t2 1633.99257 49.97346

K1 3.35E-03

K2 6.12E-04

Plot of Absorbance vs time for the Reaction of
 $(\eta^2\text{-C}_6\text{O})(\eta^2\text{-phen})\text{Cr}(\text{CO})_3$ with PIP (0.0584M)
 at 323.2 K



Data: Data3_B

Model: BifCreciente

Weighting:
 y No weighting

Chi²/DoF = 1.2476E-6

R² = 0.99559

y0 0.11885 0.00051

A1 0.02127 0.001

t1 108.29038 10.36633

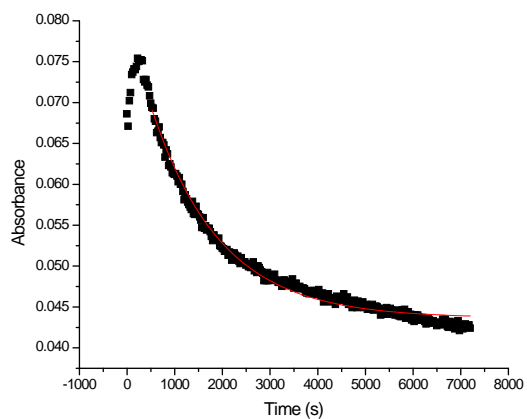
A2 0.06933 0.00047

t2 1704.01265 42.11857

K1 9.23 E-03

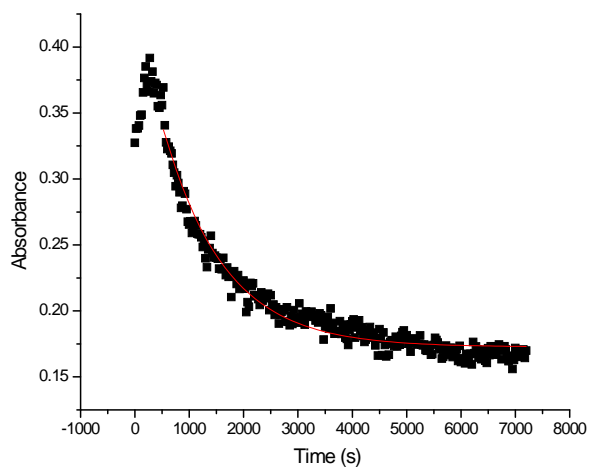
K2 5.87 E-04

Plot of Absorbance vs time for the Reaction of
 $(\eta^2\text{-C}_6\text{O})(\eta^2\text{-phen})\text{Cr}(\text{CO})_3$ with PIP (0.311M)
 at 333.2 K



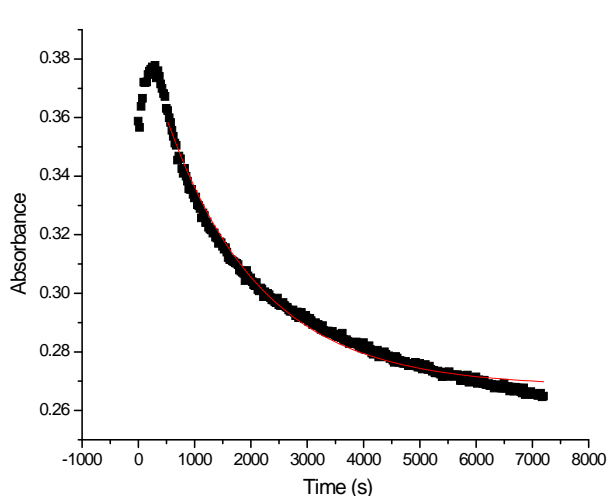
Data: Data1_B
 Model: BifCreciente
 Weighting:
 y No weighting
 Chi²/DoF = 5.2781E-7
 R² = 0.9931
 y0 0.04365 0
 A1 0.01411 0.00063
 t1 86.54915 7.64945
 A2 0.03671 0.0003
 t2 1438.60818 13.48768
 K1 1.16E-02
 K2 6.95E-04

Plot of Absorbance vs time for the Reaction of
 $(\eta^2\text{-C}_6\text{O})(\eta^2\text{-phen})\text{Cr}(\text{CO})_3$ with PIP (0.0434M)
 at 333.2 K



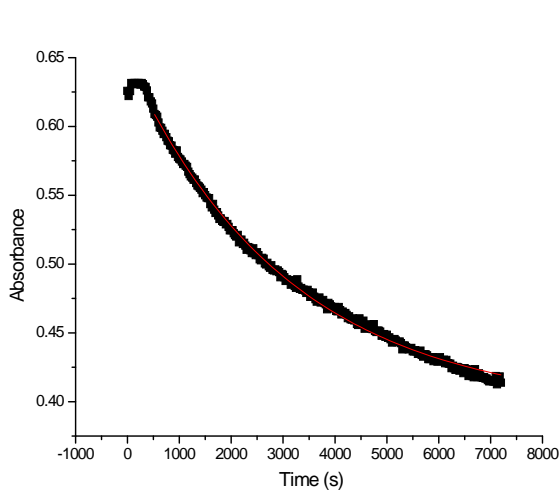
Data: Data8_B
 Model: BifCreciente
 Weighting:
 y No weighting
 Chi²/DoF = 0.00007
 R² = 0.98058
 y0 0.17265 0.00091
 A1 0.12491 0.00765
 t1 115.51539 14.22907
 A2 0.26585 0.00569
 t2 1115.76411 30.71684
 K1 8.64 E-03
 K2 8.96E-04

Plot of Absorbance vs time for the Reaction of
 $(\eta^2\text{-C}_6\text{O})(\eta^2\text{-phen})\text{Cr}(\text{CO})_3$ with PIP (0.506M)
 at 333.2 K



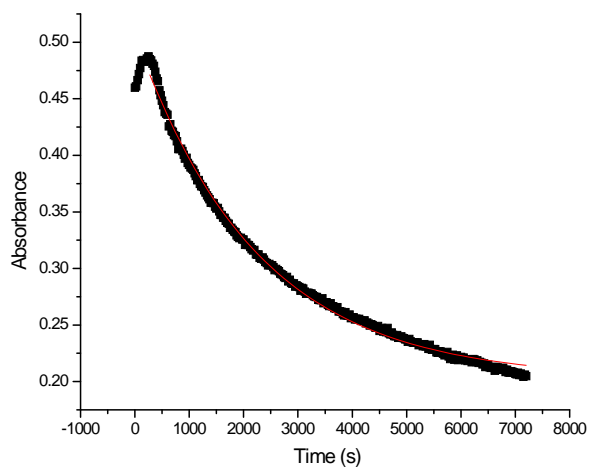
Data: Data10_B
 Model: BifCreciente
 Weighting:
 y No weighting
 Chi²/DoF = 6.574E-6
 R² = 0.993
 y0 0.26818 0.00042
 A1 0.04291 0.00237
 t1 64.88898 7.08751
 A2 0.12356 0.00086
 t2 1670.57196 26.39439
 K1 1.54 E-02
 K2 5.99 E-04

Plot of Absorbance vs time for the Reaction of
 $(\eta^2\text{-C}_6\text{O})(\eta^2\text{-phen})\text{Cr}(\text{CO})_3$ with PIP (0.614M)
 at 333.2 K



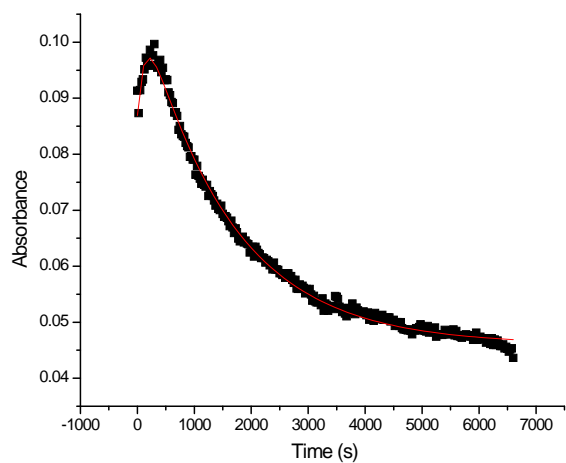
Data: Data13_B
 Model: BifCreciente
 Weighting:
 y No weighting
 Chi²/DoF = 7.6514E-6
 R² = 0.99804
 y0 0.39451 0.00122
 A1 0.02983 0.00243
 t1 74.87647 11.6294
 A2 0.25358 0.00091
 t2 3107.44186 39.70729
 K1 1.34 E-02
 K2 3.22 E-04

Plot of Absorbance vs time for the Reaction of
 (n2-C60)(n2-phen)Cr(CO)3 with PIP (1.02M)
 at 333.2 K



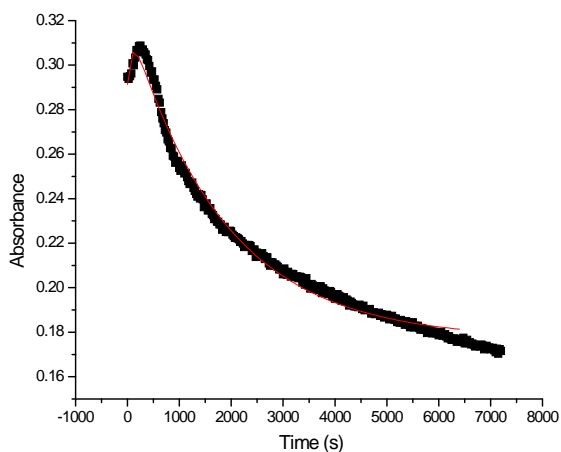
Data: Data1_B
 Model: BifCreciente
 Weighting:
 y No weighting
 Chi²/DoF = 0.00002
 R² = 0.99643
 y0 0.20242 0.00108
 A1 0.05273 0.00424
 t1 67.21701 10.44308
 A2 0.30506 0.00129
 t2 2223.44441 28.59655
 K1 1.49 E-02
 K2 4.50 E-04

Plot of Absorbance vs time for the Reaction of
 (n2-C60)(n2-phen)Cr(CO)3 with PIP (2.00M)
 at 333.2 K



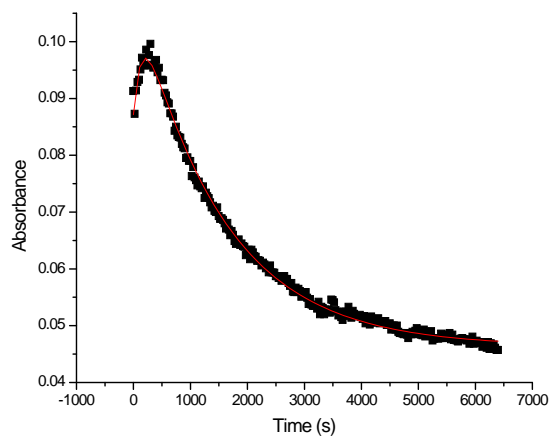
Data: Data1_B
 Model: BifCreciente
 Weighting:
 y No weighting
 Chi²/DoF = 9.2644E-7
 R² = 0.99597
 y0 0.04605 0.00015
 A1 0.02281 0.00082
 t1 126.58715 9.22602
 A2 0.06367 0.0005
 t2 1530.69737 21.17491
 K1 7.90 E-03
 K2 6.53 E-04

Plot of Absorbance vs time for the Reaction of
 $(n2-C60)(n2-phen)Cr(CO)_3$ with PIP (1.58M)
 at 333.2 K



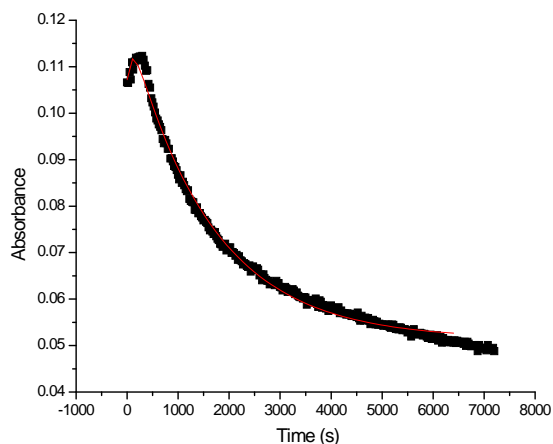
Data: Data3_B
 Model: BifCreciente
 Weighting:
 y No weighting
 Chi²/DoF = 0.00001
 R² = 0.99036
 y0 0.1769 0.00074
 A1 0.03016 0.00322
 t1 77.77265 16.31769
 A2 0.14453 0.00119
 t2 1837.52682 39.3045
 K1 1.29 E-02
 K2 5.44 E-04

Plot of Absorbance vs time for the Reaction of
 $(n2-C60)(n2-phen)Cr(CO)_3$ with PIP (1.32M)
 at 333.2 K



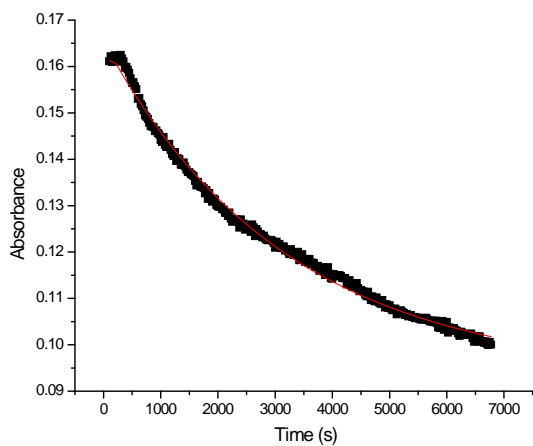
Data: Data1_B
 Model: BifCreciente
 Weighting:
 y No weighting
 Chi²/DoF = 8.1755E-7
 R² = 0.99644
 y0 0.04638 0.00015
 A1 0.02335 0.00078
 t1 136.07335 9.21721
 A2 0.06413 0.00052
 t2 1493.02822 20.45014
 K1 7.35 E-03
 K2 6.70 E-04

Plot of Absorbance vs time for the Reaction of
 $(\eta^2\text{-C}_6\text{O})(\eta^2\text{-phen})\text{Cr}(\text{CO})_3$ with PIP (0.0287M)
 at 333.2 K



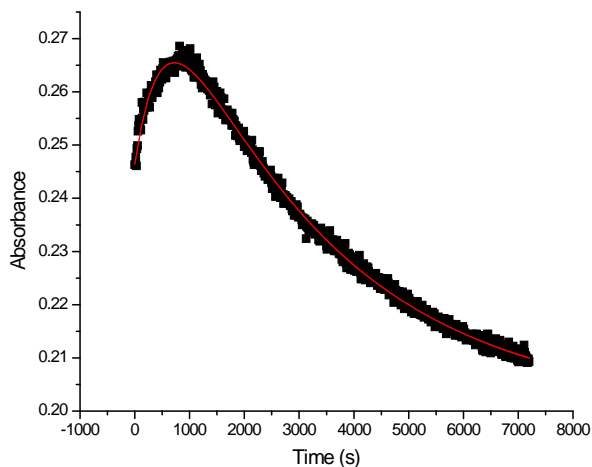
Data: Data8_B
 Model: BifCreciente
 Weighting:
 y No weighting
 Chi²/DoF = 1.5096E-6
 R² = 0.99493
 y0 0.0514 0.00021
 A1 0.01288 0
 t1 90.60553 14.89002
 A2 0.06869 0.00047
 t2 1598.75185 22.93328
 K1 1.10 E-02
 K2 6.25 E-04

Plot of Absorbance vs time for the Reaction of
 $(\eta^2\text{-C}_6\text{O})(\eta^2\text{-phen})\text{Cr}(\text{CO})_3$ with PIP (0.799M)
 at 333.2 K



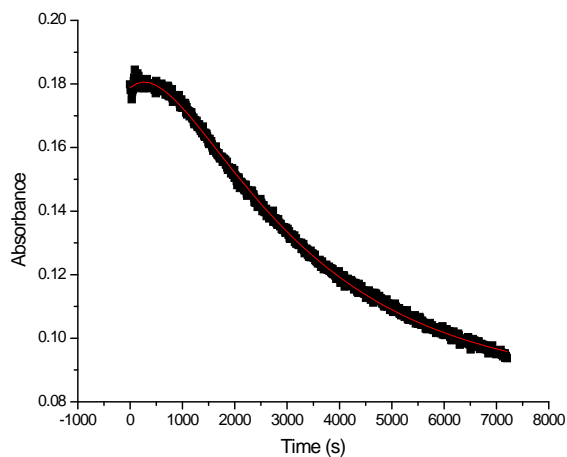
Data: Data10_B
 Model: BifCreciente
 Weighting:
 y No weighting
 Chi²/DoF = 1.5724E-6
 R² = 0.9948
 y0 0.09336 0.00054
 A1 0.04063 0.1748
 t1 32.87984 43.78596
 A2 0.07207 0.00041
 t2 3150.66644 61.27574
 K1 3.04 E-02
 K2 3.17 E-04

Plot of Absorbance vs time for the Reaction of
 $(\eta^2\text{-C}_6\text{O})(\eta^2\text{-phen})\text{Cr}(\text{CO})_3$ with PIP (1.59M) in chlorobenzene
 at 313.2 K and 407nm



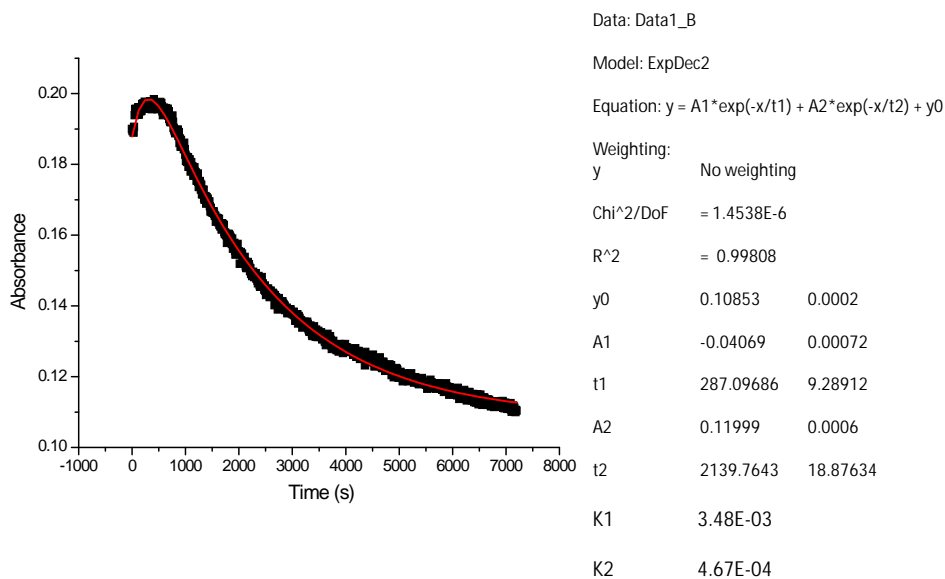
Data: Data17_B
 Model: BifCreciente
 Weighting:
 y No weighting
 Chi²/DoF = 1.1176E-6
 R² = 0.99678
 y0 0.20062 0.00047
 A1 0.05301 0.00109
 t1 520.11056 13.51063
 A2 0.09884 0.0008
 t2 3065.8267 60.29881
 K1 1.92 E-03
 K2 3.26 E-04

Plot of Absorbance vs time for the Reaction of
 $(\eta^2\text{-C}_6\text{O})(\eta^2\text{-phen})\text{Cr}(\text{CO})_3$ with PIP (0.0552M) in chlorobenzene
 at 313.2 K and 407nm

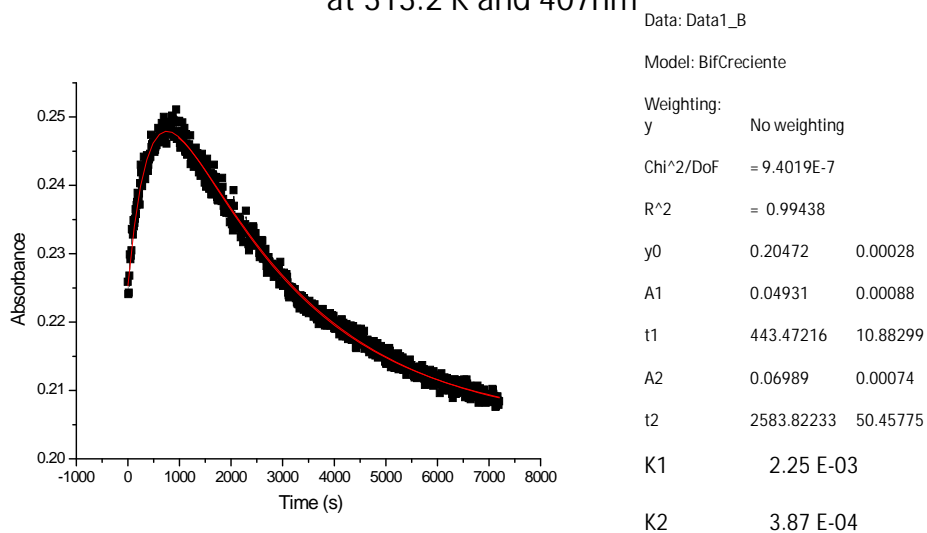


Data: Data11_B
 Model: BifCreciente
 Weighting:
 y No weighting
 Chi²/DoF = 1.0291E-6
 R² = 0.99871
 y0 0.085 0
 A1 0.05306 0.00124
 t1 784.85776 18.73876
 A2 0.14686 0.00134
 t2 2765.25892 14.87993
 K1 1.27 E-03
 K2 3.62 E-04

Plot of Absorbance vs time for the reaction of PIP (0.107M) with (n2-phen)(n2-C60)Cr(CO)3 in chlorobenzene at 313.2 K and 407nm

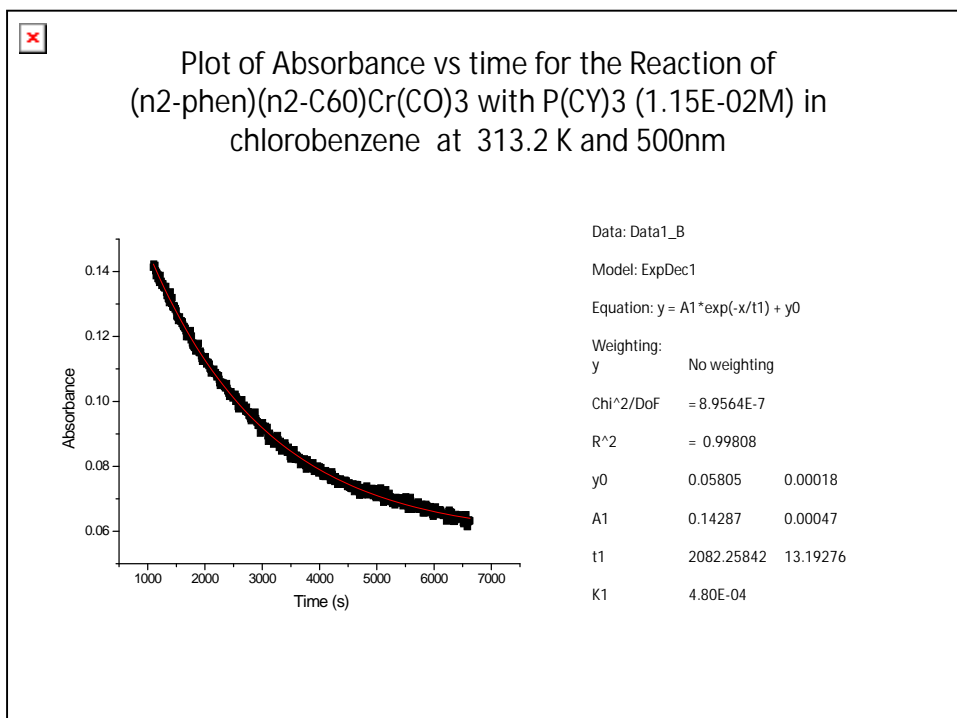


Plot of Absorbance vs time for the Reaction of (n2-C60)(n2-phen)Cr(CO)3 with PIP (1.99M) in chlorobenzene at 313.2 K and 407nm

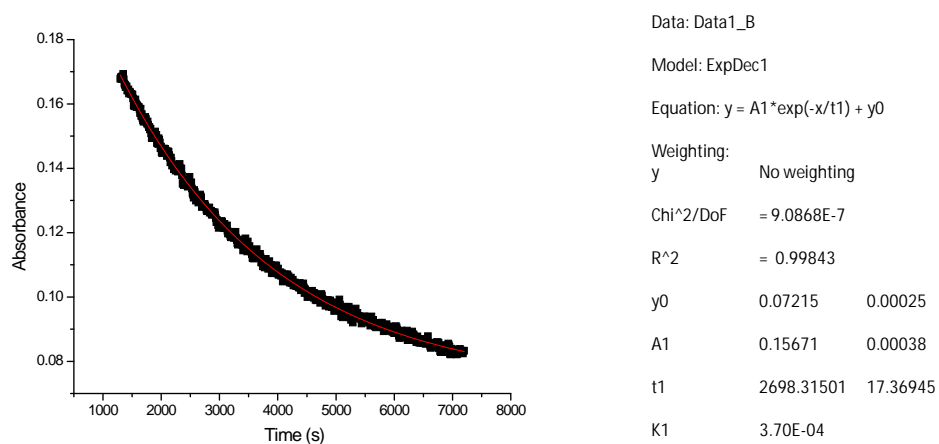


APPENDIX C

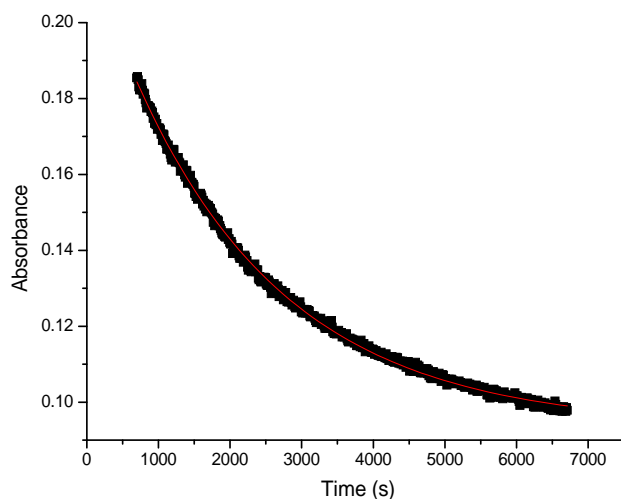
Plot of Absorbance versus time for the reaction of the ratio between $P(Cy)_3$ and C_{60} with $fac-(\eta^2-C_{60})(\eta^2-phen)Cr(CO)_3$ in Chlorobenzene



Plot of Absorbance vs time for the Reaction of (n2-phen)(n2-C60)Cr(CO)3 with P(CY)3 (0.103M) in chlorobenzene at 313.2 K and 500nm



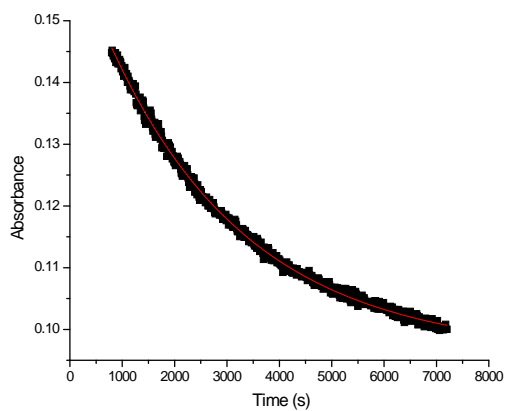
Plot of Absorbance vs time for a ratio of 0.122 between C60(3.78E-04M) and P(CY)3 (3.09E-03M) Reacting with (n2-phen)(n2-C60)Cr(CO)3 in chlorobenzene at 313.2 K and 500nm



Data: Data1_B
 Model: ExpDec1
 Equation: $y = A1 \cdot \exp(-x/t1) + y0$
 Weighting:
 y No weighting
 Chi²/DoF = 7.7113E-7
 R² = 0.99859
 y0 0.09357 0.00015
 A1 0.12606 0.00025
 t1 2134.81468 10.65845
 K1 4.68E-04

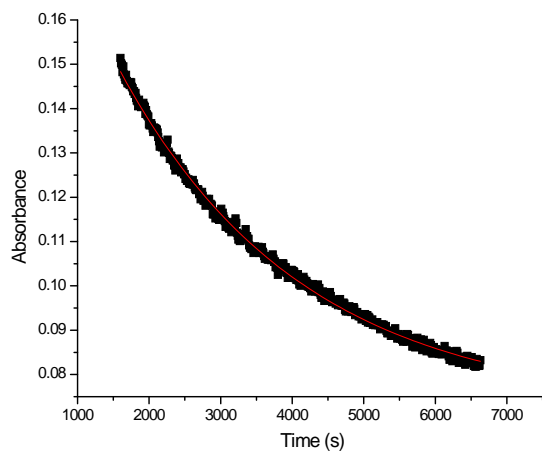
bv

Plot of Absorbance vs time for a ratio of 0.538 between C60(5.92E-04M) and P(CY)3 (1.10E-03M) Reacting with (n2-phen)(n2-C60)Cr(CO)3 in chlorobenzene at 313.2 K and 500nm



Data: Data1_B
 Model: ExpDec1
 Equation: $y = A1 \cdot \exp(-x/t1) + y0$
 Weighting:
 y No weighting
 Chi²/DoF = 3.2983E-7
 R² = 0.99788
 y0 0.09618 0.00012
 A1 0.06669 0.00014
 t1 2667.86297 17.7923
 K1 3.75E-04

Plot of Absorbance vs time for a ratio of 0.261 between C60(5.92E-04M) and P(CY)3 (1.10E-03M) Reacting with (n2-phen)(n2-C60)Cr(CO)3 in chlorobenzene at 313.2 K and 500nm



Data: Data1_B
Model: ExpDec1
Equation: $y = A1 \cdot \exp(-x/t1) + y0$
Weighting:
y No weighting
Chi²/DoF = 8.5842E-7
R² = 0.99747
y0 0.07245 0.00031
A1 0.14235 0.0006
t1 2544.85057 24.439
K1 3.93E-04

APPENDIX D
TABLES

Table D.1 Values of k_{obsd1} for C_{60} displacement from *fac*-($^2-C_{60}$)($^2\text{phen}$)Cr(CO) $_3$ by piperidine (pip) in chlorbenzene

Temp (K)	Concentration PIP (mol/L)	k_{obsd1} (10^{-3} s^{-1})	Average k_{obsd1} (10^{-3} s^{-1})
313.2	1.59	1.9(5)	2.24
	1.99	2.3(6)	
	0.107	3.5(1)	
	0.0552	1.27(3)	
323.2	0.254	9(3)	5.10
	0.591	0.18(2)	
	0.516	1.78(2)	
	1.03	7(1)	
	0.287	3.4(2)	
	0.0584	9.2(9)	
333.2	0.311	12(1)	13.3
	0.0434	8.6(1)	
	0.506	15(2)	
	0.614	13.0(2)	
	1.02	15(2)	
	2	7.9(6)	
	1.32	7.4(5)	
	1.58	13(3)	
	0.0287	11(2)	
	0.799	30(4)	

Table D.2 Values of $k_{\text{obsd}2}$ for C_{60} displacement from *fac*-($^2-C_{60}$)($^2\text{phen}$)Cr(CO) $_3$ by piperidine (pip) in chlorbenzene

Temp (K)	Concentration of pip (mol/L)	$k_{\text{obsd}2}$ (10^{-4} s^{-1})	Average $k_{\text{obsd}2}$ (10^{-4} s^{-1})
313.2	1.59	3.26(6)	3.86
	0.107	4.67(4)	
	0.0552	3.62(2)	
	1.99	3.87(8)	
323.2	0.254	4.86(6)	4.96
	0.591	4.3(7)	
	0.516	4.5(3)	
	1.03	4.1(3)	
	0.287	6.1(2)	
	0.0584	5.9(1)	
333.2	0.311	6.95(7)	5.77
	0.506	5.99(9)	
	1.02	4.50(6)	
	0.614	3.22(4)	
	2.00	6.53(9)	
	1.58	5.44(1)	
	1.32	6.70(9)	
	0.0434	8.96(1)	
	0.799	3.17(6)	
	0.0287	6.25(9)	

Table D.3 Values of k_{obsd} for C_{60} displacement from $fac-(^2-C_{60})(^2\text{phen})Cr(CO)_3$ by tri-phenylphosphine (PPh_3) in chlorbenzene

Temp (K)	Concentration of PPh_3 (mol/L)	k_{obsd} ($10^{-4} s^{-1}$)	Average k_{obsd} ($10^{-4} s^{-1}$)
303.2	0.100	3.05(2)	3.69
	0.301	3.89(4)	
	0.879	4.12(1)	
313.2	3.51E-04	5.38(2)	4.39
	1.16E-03	5.22(3)	
	0.133	3.27(3)	
	0.146	5.1(1)	
	0.151	3.34(3)	
	0.272	4.47(5)	
	1.00	3.54(7)	
323.2	1.45E-02	4.79(2)	4.98
	0.0146	6.00(6)	
	0.0510	5.29(1)	
	0.155	5.04(6)	
	0.309	5.23(5)	
	0.519	4.04(6)	
333.2	0.720	4.28(4)	5.52
	0.0679	5.07(7)	
	0.231	5.81(7)	
	0.484	5.69(7)	

Table D.4 Values of k_{obsd} for C_{60} displacement from $fac-(^2-C_{60})(^2phen)Cr(CO)_3$ by tri-phenylphosphine (PPh_3) in benzene

Temp (K)	Concentration of PPh_3 (mol/L)	k_{obsd} ($10^{-4} s^{-1}$)	Average k_{obsd} ($10^{-4} s^{-1}$)
303.2	0.187	3.32(3)	3.32
313.2	0.0516	3.95(2)	4.06
	0.146	4.80(6)	
	0.548	3.44(3)	
323.2	0.531	4.50(3)	5.09
	0.0517	5.81(3)	
	0.147	4.95(3)	
333.2	0.207	5.22(4)	6.04
	0.478	6.86(4)	

Table 5 Values of k_{obsd} for C_{60} displacement from $fac-(^2-C_{60})(^2phen)Cr(CO)_3$ by tri-phenylphosphine (PPh_3) in toluene

Temp (K)	Concentration of PPh_3 (mol/L)	k_{obsd} ($10^{-4} s^{-1}$)	Average k_{obsd} ($10^{-4} s^{-1}$)
303.2	0.0569	3.04(2)	3.04
313.2	0.0519	4.65(4)	4.09
	0.552	3.03(4)	
	0.0966	4.59(4)	
323.2	0.0589	5.19(5)	4.95
	0.152	4.82(5)	
	0.632	4.67(6)	
	0.0461	5.10(5)	
333.2	0.0461	5.23(7)	5.72
	0.402	5.83(6)	
	0.611	6.10(7)	